UNIVERSITÀ DELLA CALABRIA

UNIVERSITA' DELLA CALABRIA

Dipartimento di Fisica

Dottorato di Ricerca in

Scienze e Tecnologie Fisiche, Chimiche e dei Materiali
Convenzione Università della Calabria-Consiglio Nazionale delle Ricerche

CICLO

XXIX

TITOLO TESI

Innovative fluorinated membranes for water and organic solvent treatment application

Settore Scientifico Disciplinare CHIM/06 CHIMICA ORGANICA

Coordinatore: Ch.mo Prof. Vincenzo Carbone

Firma Vincenzo Carbone

Supervisore/Tutor: Ch.mo Prof. Bartolo Gabriele

Firma

Dott. Alberto Figoli

Firma

Dottorando: Dott.ssa Claudia Ursino

Firma Claudia Ursino

Alla mia Famiglia,

Contents

Abstract

The aim of this thesis was to study the use of different types of fluoropolymer in order to prepare membranes for chemical and pharmaceutical applications. In fact, the potential use of fluoropolymeric membranes respect to other materials, at industrial levels, has several advantages such as high mechanical strength, high efficiency and stability. However, the unique properties of these materials such as excellent chemical and thermal strength make them extremely versatile but at the same time very difficult to process. As example, Ethylene-Chlorotrifluoroethylene (ECTFE) is insoluble in common organic solvents, and it can only be processed at high temperature, depending on the solvent used.

In this work, three types of fluoropolymers have been studied, such as low-melting ECTFE (Halar®LMP-ECTFE), poly(vinylidene fluoride) (PVDF grade 1015) and perfluoropolyether (PFPEs) (Fluorolink®AD1700 and Fluorolink®MD700). Moreover, low-toxic solvents for humans and the environment have been appropriately selected and used for first time for solubilising the fluoropolymers of interest.

-The Halar®LMP-ECTFE polymer was studied and characterized in terms of solubility parameters, compared with the standard Halar® ECTFE 901 polymer. In fact, this new grade of Halar® shows comparable properties with standard Halar® (hydrophobicity and mechanical properties), but lower crystallinity and lower melting point. Porous membranes and dense film were produced by thermally induced phase separation (TIPs). Two solvents, Diethyl Adipate (DEA) and Dibutyl Itaconate (DBI), never tested before, were selected. The chemical stability of the dense film was evaluated over time (192h) by swelling tests with aggressive organic solvents. Porous Halar®LMP-ECTFE membranes have been tested for organic solvents ultra- (UF) and nano-filtration (NF), such as methanol, ethanol and dimethylformamide. The results show that Halar®LMP ECTFE membranes are promising candidates to be used in separation processes under harsh conditions, such as chemicals production, purification and processing of food, nutraceuticals products and solvents recycling.

- The influence of three different solvents in the membrane formation, using PVDF 1015 as polymer, was studied. Plasticizers from to Citroflex family, such as acetyl tributylcitrate (ATBC), acetyl triethylcitrate (ATEC) and triethylcitrate (TEC) have been selected and used. In particular ATEC and TEC as solvents, were used for the first time. Membranes were produced by thermally induced phase separation (TIPs) technique. The flat sheet membranes produced have been tested in microfiltration process (MF). These membranes can be used in several industrial applications such as sterilisation and clarification of pharmaceuticals or applied to separate contaminants from the water.

- Perfluoropolyethers (PFPE) (Fluorolink®AD100 and Fluorolink®MD700) studied are new types of PFPE, UV cross-linkable. These PFPE photo-reticulated, have been used for coating commercial hydrophilic membrane, such as polyamide (PA) and polyethersulfone (PES) membranes. The aim of this work was to produce hydrophilic/hydrophobic coated membranes, keeping the morphology of the started membrane, unchanged. The study focused on morphological analysis, and on the influence of coating on the support membrane. The membranes produced, hydrophilic/hydrophobic, were characterized and the coating resistance was evaluated over time by direct contact with several chemical agents. The membranes were then tested, in membrane distillation process for direct contact (DCMD), using both deionized water and 0.6M saline. The results show that these coated membranes can be applied to desalination of seawater and wastewater treatment.

Riassunto

L'elaborato di tesi ha come obbiettivo lo studio di fluoropolimeri per la produzione di membrane adatte ad applicazioni in campo chimico e farmaceutico. L'uso di membrane fluoropolimeriche a livello industriale, presenterebbe diversi vantaggi quali l'elevata resistenza meccanica, l'alta efficienza e stabilità. Le proprietà uniche di questi materiali, quali l'inerzia, l'eccellente resistenza chimica e termica li rendono estremamente versatili ma nello stesso tempo molto difficili da processare. Molti di loro come l'etilenclorotrifluro etilene (ECTFE), sono infatti insolubili nei comuni solventi organici, e sono lavorabili solo ad alte temperature.

Sono stati studiati tre diversi tipi di fluoropolimeri, quali l'ECTFE a basso punto di fusione (Halar® LMP-ECTFE), il polivinilidenfluoruro (PVDF grado 1015) e i perfluoropolieteri (PFPE) (Flurolink®AD1700 e Fluorolink®MD700). Inoltre, per la preparazione delle membrane sono stati selezionati e impiegati solventi, mai testati precedentemente, a ridotta tossicità per l'uomo e per l'ambiente.

-Lo studio sul nuovo polimero Halar® LMP-ECTFE, con basso punto di fusione, ha previsto un'attenta analisi dei parametri di solubilità e un confronto con il polimero standard Halar® ECTFE 901. Infatti la particolarità del nuovo grado di Halar®, LMP-ECTFE, è la capacità di mantenere inalterate le medesime proprietà dello standard Halar® ECTFE 901, quali l'idrofobicità e le proprietà meccaniche, ma essendo meno cristallino presenta un punto di fusione più basso, consentendo di solubilizzarlo a temperature più basse. Le membrane porose e il film denso, sono state prodotte mediante la separazione di fase indotta termicamente (TIPs). Sono stati selezionati e confrontati due nuovi solventi quali il Dietil Adipato (DEA) e Dibutil Itaconato (DBI). La stabilità chimica della membrana è stata valutata nel tempo (192h) attraverso il contatto diretto con solventi aggressivi. Le membrane porose di Halar®LMP-ECTFE sono state testate per la filtrazione di solventi organici, quali metanolo, etanolo e dimetil formammide, comunemente usati nell'industria chimica e farmaceutica. I risultati ottenuti hanno dimostrato che le membrane prodotte con l'Halar®LMP ECTFE, potrebbero essere impiegate nella separazione di composti organici, ad esempio durante la produzione di composti chimici e farmaceutici, nel settore petrolchimico e nel riciclo dei solventi.

-Lo studio effettuato con il polimero PVDF 1015, è stato incentrato sull'influenza di tre diversi solventi nella formazione della membrana. Sono stati utilizzati plasticizzanti appartenenti alla famiglia dei Citroflex, quali acetil tributilcitrato (ATBC), acetil trietilcitrato (ATEC) e il trietilcitrato (TEC). In particolare l'ATEC e il TEC non mai stati usati precedentemente nella produzione di membrane mediante la separazione di fase indotta termicamente (TIPs). Le membrane piane prodotte

sono da microfiltrazione (MF) e sono state testate per la purificazione dell'acqua. A livello industriale troverebbero una facile applicazione per la sterilizzazione dei farmaci o per separare i contaminanti dall'acqua.

- I perfluoropolieteri (PFPE) (Fluorolink®AD100 e Fluorolink®MD700) studiati in questo lavoro di tesi, appartengono ad una nuova classe attivabile mediante raggi UV. Questi PFPE foto-reticolabili, sono stati utilizzati per il rivestimento di membrane commerciali, idrofile, come membrane in poliammide (PA) e in polietersulfone (PES). Lo scopo di questo lavoro, è stato quello di conferire a queste membrane di supporto, le proprietà dei PFPE quali l'idrofobicità, lasciando però inalterata la loro morfologia. Lo studio è stato incentrato sull'analisi morfologica, ovvero sull'influenza del rivestimento nella membrana commerciale di supporto. Le membrane prodotte, idrofiliche/idrofobiche sono state caratterizzate e la resistenza del rivestimento è stata valutata nel tempo attraverso il contatto diretto con diversi agenti chimici. Le membrane sono state quindi testate nel processo di distillazione a membrana per contatto diretto (DCMD), usando sia acqua deionizzata che soluzione salina 0.6M per la produzione di acqua ultra-pura. I risultati ottenuti confermano che le membrane prodotte potrebbero essere applicate per la dissalazione dell'acqua marina o per il trattamento di acque reflue o di scarico potenzialmente riutilizzabili in processi industriali

Introduction

Work objectives

With technological advancement, membrane technology is steadily growing in various industries due to competitive energy prices and environmental concerns. In fact, membrane processes, lead to several advantages comparing with traditional processes: ease of use, low energy use, the possibility to operate without the addition of chemicals or additives, high ability to separate thermolabile compounds, excellent selectivity of specific components and environmental friendliness. One of the most important aspects of membranes preparation is the starting materials. Several polymers have been used and studied in order to prepare tailored membranes. Consequently, a strong motivation for improving established membrane materials and processes is driving the current research. Near to the research of new materials and techniques, also the attention of the impact of the solvents employed is ingrown. Alternative solvents suitable for green chemistry are those that have low toxicity, are easy to recycle, are inert and do not contaminate the product [1]. The combination of the use innovative materials for membrane preparation, such as fluoropolymers, and the non-toxic solvents are the main research studies of this PhD Thesis.

The aim of the present work is the study of fluoropolymer materials in order to produce several membranes that could be applied in the major area of membranes technology.

The research carried out in the present thesis can be summarized as follows:

- Fluoropolymers membranes preparation via phase inversion or coating procedures using non-toxic solvents.
- Characterization tests were carried out in order to study membranes structure and properties.
- Fluoropolymers membranes have been applied in different processes in order to evaluate their potentiality in terms of performance such as flux and selectivity towards the species of interest.

The different activity conducted in the present work are schematically presented in Figure 1.

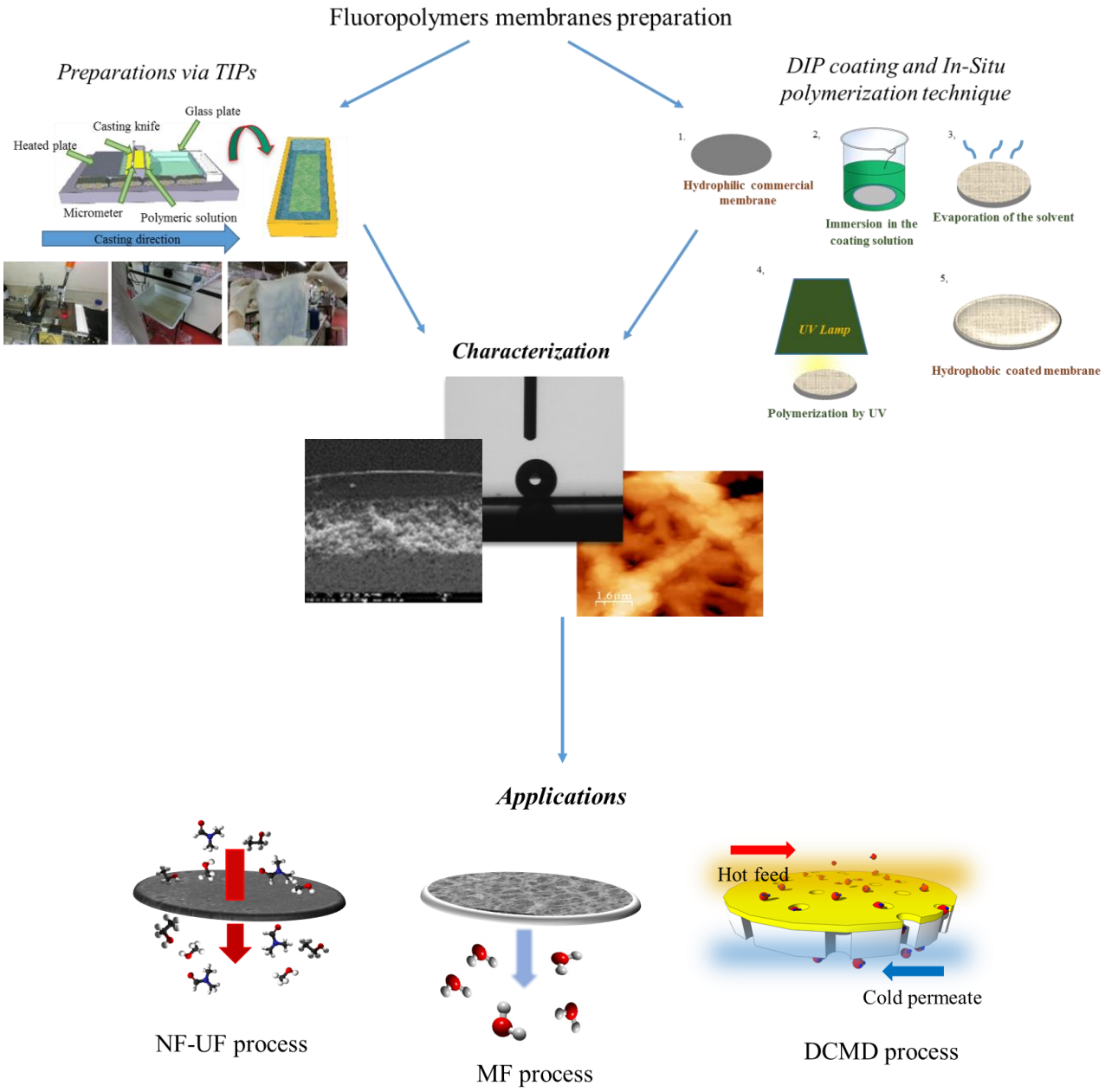

Figure 1. Schematic illustration of the research carried out in the present PhD Thesis

Fluoropolymers

Fluorinated polymers are produced from alkenes in which some or all hydrogen atoms have been replaced by fluorine (F). These polymers constitute an interesting and unique class of material thanks to the presence of the strong and stable C-F bond (490 kJ/mol; for comparison: C–H 420 kJ/mol, C-C 340 kJ/mol) [2] on the polymeric backbone. In fact, fluorine is the most abundant halogen, and is the most electronegative and least polarisable element. The influences of the C–F bond, make fluorinated polymers extremely hydrophobic with very low surface tensions, that making them liquid

repellent and useful as surfactants. Generally, these polymers have high thermal stability (at high and cryogenic temperatures), photostability, chemical and solvent resistance, properties that increases increasing the fluorine content. However, polymers solubility in solvents usually decreases by increasing the fluorine content of the molecule [3]. Based on the presence or absence of hydrogen atoms (-H) on the structure, fluoropolymers can be divided in perfluorinated (e.g., PTFE, PFA, FEP, etc.) and partially fluorinated (e.g., ECTFE, ETFE, PVDF, etc.) [2,4], Figure 2.

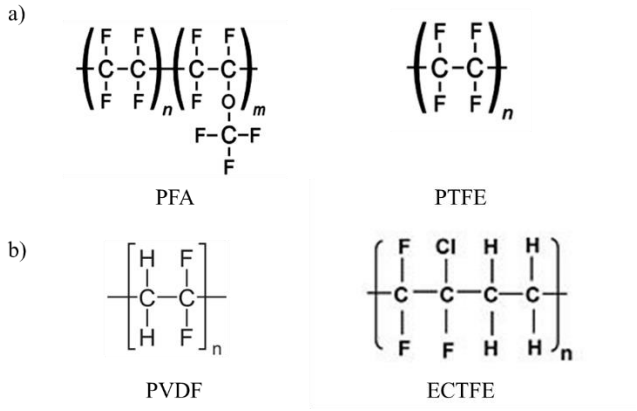

Figure 2. E.g. of chemical structure of *a)* perfluorinated and *b)* partially fluorinated fluoropolymers

It is possible to divide the fluoroplastics and amorphous fluoropolymers into four categories [2]:

1. High-crystalline, non melt-processable PTFEs
2. Semicrystalline (mp > 80°C), melt-processable fluorothermoplastics
3. Amorphous fluoropolymers with Tg > 70°C
4. Amorphous, curable fluoroelastomers

These important physical and chemical features, including excellent chemical resistance, good mechanical properties, good thermal stability, and ferroelectric, piezoelectric, and dielectric properties, which originated from the low polarity, strong electronegativity and small van der Waals radius, (1.32 A˚) of the fluorine atoms, have made fluoropolymers a material of choice for many industrial and commercial applications.

Fluoropolymers in membranes science

Membranes production is one of the several areas where fluoropolymers have found widespread application. In fact membranes applications have been used in a large variety of processes such as separation of industrial chemicals, water desalination, waste water treatment, removal of micropollutents, pharmaceutical (enzymes, antibiotics, pyrogens), removal of VOC's, gas separation,

etc.. Membranes were simply defined as a selective barrier between two phases. Thanks to their versatility can be applied in separation, fractionation and concentration applications [5]. For all these processes, the performance limits are clearly determined by the membrane itself and the choice of the polymer play a crucial role. Fluoropolymers, as reported above, exhibit many desirable properties for a much wider range of applications in membrane processes, some examples are listed in table 1.

Table 1. Examples of typical fluoropolymer used in membrane processes

POLYMER	MEMBRANE PROCESS
PVDF poly(vinylidene fluoride) Homo- and copolymer	MF, UF, MD, PV, fuel cell, Lithium ion battery, tissue regeneration
ECTFE poly(ethylene chlorotrifluoroethylene)	PV, MF, UF, NF
PTFE poly(tetrafluoroethylene) Homo- and copolymer	MD, PV, MGA, Fuel cell

*MF: Microfiltration; UF: Ultrafiltration; MD: Membrane Distillation; PV: Pervaporation; NF: Nanofiltration; MGA: Membrane Gas Absorption;

Depending of the polymer workability, phase inversion, electro-spinning, sintering, stretching, track etching, as techniques can be applied in order to produce fluoropolymer membranes. Phase inversion methods is the most commonly technique used, thanks to their simplicity and flexible production scales [6]. The concept of phase inversion or phase separation covers a range of different techniques, such as vapor induced phase separation (VIP_S), evaporation induced phase separation (EIPs), non-solvent induced phase separation (NIPs) and thermally induced phase separation (TIPs) [7]. Among these techniques, TIPs and NIPs are the two most commonly employed methods in order to prepare polymeric membranes including fluoropolymer membranes. The major difference between NIPs and TIPS is that TIPs processes requires thermal energy to convert the solution into a two-phase mixture, while the one involves an exchange between solvent and non-solvent for membrane formation. However, the phase-separation behavior of a fluoropolymer is often complicated by its semi-crystalline nature, in fact its show two types of phase separation processes: liquid-liquid and solid-liquid demixing [8,9]. Furthermore, as a result of their chemical and physical stability, many fluoropolymers, e.g. ECTFE, show difficult processability and are insoluble in many solvents at room temperature. The problem of solubility has been solved increasing the temperatures of work, so is possible prepare membrane via TIPS process.

Besides these preparation techniques, the development of coated membranes represents an important approach to functionalise the membranes with tailored properties.

In the present work TIPs, Dip-coating and In situ polymerization as preparation membrane techniques are used and below illustrated.

The synthesis of novel fluoropolymers more processable, the choice of solvent less toxic, the functionalization of membranes via coating technique, represents the new way to prepare tailored fluoropolymers membranes.

- *TIPs*

Thermally induced phase separation technique provide that a homogeneous solution is prepared by dissolving the polymer in a high-boiling-point, low-molecular-weight diluent at high temperature (T_1) and then the homogeneous solution is cooled slowly (T_2) to induce phase separation [7,10]. The solution separates in two phases, one rich of polymer and the other poor in polymer. The polymer-rich phase solidifies by crystallization, gelation or on passing the glass transition temperature. Generally, solvents used in TIPs processes are called "latent solvent", because they can work to compound as a solvent only at high temperatures, namely, close to the polymer melting point [11]. After demixing is induced, the solvent is removed by extraction using alcohol, evaporation or freeze-drying. Polymer concentration, the selection of solvents, the cooling rate and the quenching conditions are important factors influencing the phase separation process and resulting morphology [9].

- *Solvents*

As mentioned before, fluoropolymers solubility decreases by increasing the fluorine content of the molecule, and usually were dissolved in a high-boiling organic solvents. Traditionally solvents used, are in general phthalates (dimethyl phthalate DMP, dibutyl phthalate DBP, etc.)[11,13], or N-methyl pyrrolidone [11], toxic, teratogenic and reprotoxic solvents. Recently, the attention of industries, from food and agricultural to chemical and pharmaceutical, focused towards the concepts of sustainable development, harmless solvents, eco-friendly production [13]. Despite membranes processes is described as a clean and environmentally friendly technology, often membranes, were produced using toxic solvents. Fortunately, the studied and the publications related to the membranes preparation using harmless solvents, were in exponential growth [14], table 2.

Table 2. List of recently publication about fluoropolymers membranes preparation *via* TIPs method, using less toxic solvents

POLYMER	SOLVENT	HAZARD STATEMENTS*	RELEVANT TOXICOLOGICAL INFORMATION*	YEAR OF PUBBLICATION
ECTFE	Di-ethyl Phthalate (DEP)	Not a hazardous substance or mixture according to Regulation (EC) No. 1272/2008. This substance is not classified as dangerous according to Directive 67/548/EEC	No component of this product present at levels greater than or equal to 0.1% is identified as probable or confirmed human carcinogen by IARC	2016 [15]
	Glycerol tri-acetate (GTA)			
ECTFE	Di-butyl Sebacate (DBS)	H315 - Causes skin irritation H319 - Causes serious eye irritation H335 - Causes respiratory irritation	No component of this product present at levels greater than or equal to 0.1% is identified as probable or confirmed human carcinogen by IARC	2016 [16]
ECTFE	Tri-phenyl Phosphite (TPP)	H302 - Harmful if swallowed H315 - Causes skin irritation H317 - Cause an allergic skin reaction. H319 - Causes serious eye irritation H410 - Very toxic to aquatic life with long lasting effects	Group 3: The agent (mixture or exposure circumstance) is not classifiable as to its carcinogenicity to humans	
ECTFE	Di-ethyl Adipate (DEA)	Not a hazardous substance or mixture according to Regulation (EC) No. 1272/2008. This substance is not classified as dangerous according to Directive 67/548/EEC	No component of this product present at levels greater than or equal to 0.1% is identified as probable or confirmed human carcinogen by IARC	2016 [17]
ECTFE	Glycerol tri-acetate (GTA)	Not a hazardous substance or mixture according to Regulation (EC) No. 1272/2008. This substance is not classified as dangerous according to Directive 67/548/EEC	No component of this product present at levels greater than or equal to 0.1% is identified as probable or confirmed human carcinogen by IARC	2014 [18]
ECTFE	Di-ethyl Phthalate (DEP)	Not a hazardous substance or mixture according to Regulation (EC) No. 1272/2008. This substance is not classified as dangerous according to Directive 67/548/EEC	No component of this product present at levels greater than or equal to 0.1% is identified as probable or confirmed human carcinogen by IARC	2012 [19]
PVDF	Acetyl tri-Butyl Citrate (ATBC)	Not a hazardous substance or mixture according to Regulation (EC) No. 1272/2008. This substance is not classified as dangerous according to Directive 67/548/EEC	No component of this product present at levels greater than or equal to 0.1% is identified as probable or confirmed human carcinogen by IARC	2016 [20]

PVDF	Rhodiasolv PolarClean®	H319 – Causes serious eye irritation	-	2016 [21]
PVDF	γ-Butyrolactone (GBL)	H302 - Harmful if swallowed H318 - Causes serious eye damage H336 - May cause drowsiness or dizziness	No component of this product present at levels greater than or equal to 0.1% is identified as probable or confirmed human carcinogen by IARC	2015 [22]
	N-methyl Pyrrolidone (NMP)	H315 – Causes skin irritation H319 – Causes serious eye irritation H335 – Causes respiratory irritation H360D – May damage the unborn child	Damage to fetus possible	
PVDF	Acetyl tri-Butyl Citrate(ATBC)	Not a hazardous substance or mixture according to Regulation (EC) No. 1272/2008. This substance is not classified as dangerous according to Directive 67/548/EEC	No component of this product present at levels greater than or equal to 0.1% is identified as probable or confirmed human carcinogen by IARC	2015 [23]
	Acetyl tri-Ethyl Citrate (ATEC)			
	Tri-Ethyl Citrate (TEC)	H332-Harmful if inhaled		
PVDF	Glycol monoethyl Ether Acetate (DCAC)	H319 – Causes serious eye irritation	No component of this product present at levels greater than or equal to 0.1% is identified as probable or confirmed human carcinogen by IARC	2015 [24]
	Tri-ethyl Phosphate (TEP)	H302 - Harmful if swallowed H319 – Causes serious eye irritation		
PVDF	Tri-Ethylene Glycol di-Acetate	Not a hazardous substance or mixture according to Regulation (EC) No. 1272/2008. This substance is not classified as dangerous according to Directive 67/548/EEC	No component of this product present at levels greater than or equal to 0.1% is identified as probable or confirmed human carcinogen by IARC	2015 [25]
PVDF	Di-Phenyl Carbonate (DPC)	H302 - Harmful if swallowed	No component of this product present at levels greater than or equal to 0.1% is identified as probable or confirmed human carcinogen by IARC	2014 [26]
	Di-Methyl Acetamide (DMAc)	H360D – May damage the unborn child H312 + H332 – Harmful in contact with skin or if inhaled H319 – Causes serious eye	May cause congenital malformation to the fetus, Presumed human reproductive toxicant Overexposure may cause reproductive	

			disorder(s) based on tests with laboratory animals	
PVDF	Acetyl tri-Butyl Citrate (ATBC)	Not a hazardous substance or mixture according to Regulation (EC) No. 1272/2008. This substance is not classified as dangerous according to Directive 67/548/EEC	No component of this product present at levels greater than or equal to 0.1% is identified as probable or confirmed human carcinogen by IARC	2014 [27] 2013 [28]
PVDF	Tri-ethyl Phosphate (TEP)	H302 - Harmful if swallowed H319 – Causes serious eye irritation	No component of this product present at levels greater than or equal to 0.1% is identified as probable or confirmed human carcinogen by IARC	2013 [29]
PVDF	Di-Methyl Sulfone ($DMSO_2$)	Not a hazardous substance or mixture according to Regulation (EC) No. 1272/2008. This substance is not classified as dangerous according to Directive 67/548/EEC	No component of this product present at levels greater than or equal to 0.1% is identified as probable or confirmed human carcinogen by IARC	2013 [30]

* Classification according to regulation (EC) no 1272/2008- http://www.sigmaaldrich.com/italy.html (accessed February 2017)

- *Functionalization of membranes*

During the last decades, membrane processes have been widely used for water treatment in different applications, such as desalination, micro- and -ultrafiltration, reverse osmosis, pervaporation, etc. In order to achieve high-performance membranes and overcome problems, several methods have been developed and studied for modifying and tailoring the membrane surfaces. In fact, membrane functionalization could be the way to minimize undesired interactions, which reduce the membranes performance, or for introducing additional functional groups for improving the selectivity, creating an entirely novel separation functional layer [31], improving chemical and thermal stability. In particular, coated membranes are prepared combining two or more different materials with different properties and they are also named (thin film-) (nano-) composite membranes. In order to produce hydrophobic coating on porous membranes of different configuration (flat and hollow-fiber), fluoropolymers can be used. In general, the preparation of these coatings can be summarized in two basic steps using (i) non-woven or porous membrane polymer support and (ii) deposition/coating of one of more functionalized materials [32]. One important advantage is that each layer can be optimized independently modifying the thickness, the type polymer employed both as the porous support and the selective barrier layer. Several techniques can be applied for preparing these tailor coated membranes and two main coating categories can be identified (Table 3): 1) solution coatings; 2) polymerisation reactions.

COATING METHODS	
Solution coating	***Polymerization reactions***
Dip - coating	Interfacial polymerization
Spin - coating	In situ polymerization
Spray - coating	Plasma polymerization
Casting - coating	Grafting

Table 3. Principal coating methods

Dip-coating

Dip-coating technique is widely used in making composite membranes thanks to its simplicity. In general, the membrane is immersed in a precursor solution. After a fixed time, the membrane is recovered and the excesses of solution is removed and dried. It possible that after immersion the membrane can be exposed at UV or IR radiation if the precursor solution contained a reactive pre-polymer (or monomer) [32]. Membranes obtained by this method present a very thin layer but often dense. The technique is shown schematically in Figure 3.

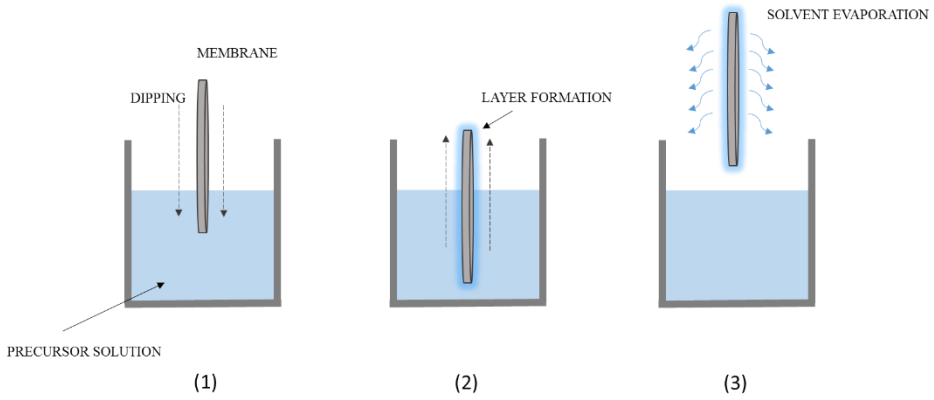

Figure 3. Simplified scheme of solution coating by dip-coating;

The final thickness of the coated layer can be controlled by the withdrawal speed (immersion time) and the polymer concentration (or pre-polymer or monomer) [33].

*Parts of this paragraph will be published in Figoli A., Ursino C., Galiano F, chap.10 "Innovative coating membranes for water treatment" in "Nanostructured Materials Membranes"-Pan Stanford Publishing

An equation, derived by Navier-Stokes equation, can be utilized for calculating the final thickness of the coating layer:

$$T_{equ.} = \frac{2}{3}\sqrt{\frac{\eta v}{\rho g}} \quad (1)$$

Where, $T_{equ.}$ is the equilibrium thickness, η dynamic viscosity, v the withdrawal speed, ρ the solution density and g represents the gravity.

In situ polymerization

In-situ polymerization process is an easy technique where the reactive monomer (or oligomer, or reactive particles), is placed in direct contact on membrane, by casting or immersion, in order to make the polymerization directly on its surface, Figure 4. Polymerization can occur by irradiation, heating, organic initiator or by a catalyst presents in the initial solution.

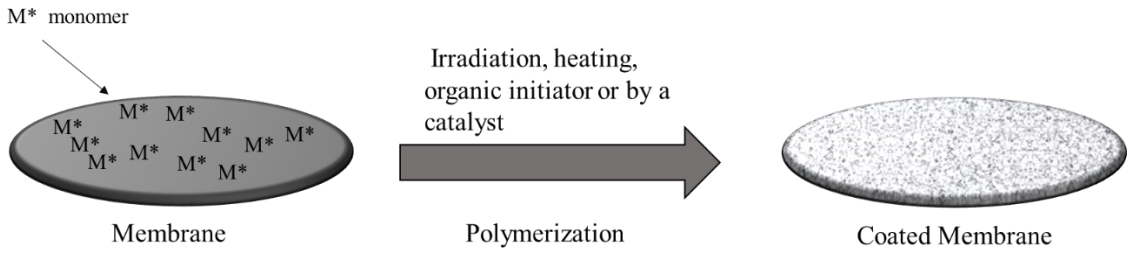

Figure 4. In-situ polymerization procedure

Hydrophobic coating application

Membrane materials determine the interactions of the membrane with water or other chemical species, thus affecting its wettability. While hydrophilic membranes are characterized by the presence of active groups on their surface that have the ability to form "hydrogen-bonds" with water, hydrophobic membranes presents the opposite response to water interaction (water repellent). The hydrophobic polymer/monomer can be used as coating material to improve membrane properties such as membrane hydrophobicity, mechanical strength and liquid entry pressure (LEP), and in case of fluoropolymers, to improve the chemical resistance as well [17].

Thesis outline

Within the scenario offered by the unique properties of fluoropolymer materials, this work focused in particular on their applications for membranes preparation and functionalization. Membranes have been prepared, characterized and tested in different membranes processes, such as nanofiltration NF, microfiltration MF and direct contact membrane distillation DCMD.
Consequently, this thesis is split in 4 chapter:

- ✓ **Chapter 1 and 2** is focused on fluoropolymers membranes preparation via TIPs, using solvents less toxic that ones;

Chapter 1 describes as a new grade of Ethylene-Chlorotrifluoroethylene, low melting point Halar® ECTFE (LMP ECTFE), was studied and used as polymer, for the preparation of resistant solvent flat-sheet membranes *via* thermally induced phase separation (TIPs). This new grade of Halar® was compared with the standard Halar® ECTFE 901 polymer. Di-ethyl Adipate (DEA) and Di-butyl Itaconate (DBI) were selected as non-toxic solvents, on the basis of their environmental impact, high boiling point and solubility towards the polymer used. Morphology of the membranes has been analyzed by scanning electron microscopy (SEM) and atomic force microscopy (AFM). Dense and porous membranes have been obtained and characterized by contact angle, pore size and porosity tests, too. Porous membranes shown asymmetric structure made of denser top-side and a spherulitic porous structure on bottom side. Membrane resistance was studied using dense membrane in contact with most aggressive organic solvents, such as polar protic, polar aprotic and non-polar solvents. The results suggest that the newly developed Halar® LMP ECTFE membranes are very promising candidates for organic solvents separation. Ultrafiltration (UF) and Nanofiltration (NF) tests with alcohols and di-methylformamide (DMF) demonstrated their solvent separation potentialities.
Chapter 2 treated about poly(vinylidene fluoride) (PVDF) flat membranes were prepared via TIPS by using three kinds of citroflex as solvents: acetyl tributyl citrate (ATBC); acetyl triethyl citrate (ATEC); and triethyl citrate (TEC). In particular, ATEC and TEC were reported in literature for the first time. While PVDF is one of the most attractive polymers for membrane preparation, this family of solvents is retrieving much interest thanks to its non-toxic properties. The prepared PVDF membranes were characterized in terms of morphology, porosity, pore-size, contact angle, tensile properties, and water permeability. The effect of the used solvent on the structures, properties and performance of the membranes was investigated. Membranes were tested in water MF process for potential application in sterilisation and clarification of pharmaceutical in the pharmaceutical industry or applied to separate contaminants from the water.

- ✓ **Chapter 3 and 4** are focused on the preparation of innovative composite hydrophilic/hydrophobic membranes, using perfluoropolyether compounds (PFPEs).

Innovative hydrophobic coated membranes have been prepared and characterised in Direct Contact Membrane Distillation (DCMD) for potential water treatment applications. A UV-curable perfluoropolyether (PFPE) hydrophobic compounds (Fluorolink® AD 1700 and Fluorolink® MD 700) were used as coating material to tailor the surface of commercial microfiltration hydrophilic polyamide (PA), and polyethersulfone (PES) membranes with different pore sizes (0.1-0.22-0.45μm).

The coated membranes consisted of a top thin hydrophobic porous layer overlying the hydrophilic commercial membrane support. Produced membranes were fully characterised in terms of surface and cross-section morphology, water contact angle, porosity, pore size, mechanical test and liquid entry pressure. The innovative coated hydrophobic membranes were tested in DCMD configuration, using deionized water and salty solution 0.6 M (NaCl) as feed. In particular, the effect of the coating concentration, and the starting materials, on the permeate fluxes was investigated. The coating resistance was evaluated over time by direct contact with several chemical agents. The measured permeate fluxes ranged between 4.56-22.81 kg/m2 h at different feed temperatures (40-50-60°C) keeping constant the permeate temperature at 14°C, for deionized water, whereas an average value of 11 kg/m2 h, at 50°C was found in case of the salty solution.

Reference

[1] F.M. Kerton, Alternative Solvents for Green Chemistry, RSC Publishing, Cambridge UK, 2009. doi:10.1039/9781849736824.

[2] K.L.H. Intzer, T.I.Z. Ipplies, Fluoropolymers , Organic, (2013).

[3] S. Ebnesajjad, Introduction to Fluoropolymers, Elsevier, 2011. doi:10.1016/B978-1-4377-3514-7.10004-2.

[4] J. Gardiner, Fluoropolymers: Origin, Production, and Industrial and Commercial Applications, Australian Journal of Chemistry. 68 (2015) 13–22. doi:10.1071/CH14165.

[5] R.W. Baker, Membrane Technology and Applications, 2004. doi:10.1002/0470020393.

[6] Z. Cui, E. Drioli, Y.M. Lee, Recent progress in fluoropolymers for membranes, Progress in Polymer Science. 39 (2014). doi:10.1016/j.progpolymsci.2013.07.008.

[7] H. Strathmann, L. Giorno, E. Drioli, Basic Aspects in Polymeric Membrane Preparation, Comprehensive Membrane Science and Engineering Volume 1. (2010) 1570.

[8] I.M. Wienk, R.M. Boom, M.A.M. Beerlage, A.M.W. Bulte, C.A. Smolders, H. Strathmann, Recent advances in the formation of phase inversion membranes made from amorphous or semi-crystalline polymers, 113 (1996) 361–371.

[9] P. van de Witte, P.J.J. Dijkstra, J.W. a. W. a van den Berg, J. Feijen, Phase separation processes in polymer solutions in relation to membrane formation, Journal of Membrane Science. 117 (1996) 1–31. doi:10.1016/0376-7388(96)00088-9.

[10] M. Gu, J. Zhang, X. Wang, H. Tao, L. Ge, Formation of poly(vinylidene fluoride) (PVDF) membranes via thermally induced phase separation, Desalination. 192 (2006) 160–167. doi:10.1016/j.desal.2005.10.015.

[11] S. Simone, A. Figoli, S. Santoro, F. Galiano, S.M. Alfadul, O.A. Al-Harbi, E. Drioli, Preparation and characterization of ECTFE solvent resistant membranes and their application in pervaporation of toluene/water mixtures, Separation and Purification Technology. 90 (2012) 147–161. doi:10.1016/j.seppur.2012.02.022.

[12] M. Gu, J. Zhang, X. Wang, W. Ma, Crystallization behavior of PVDF in PVDF-DMP system via thermally induced phase separation, Journal of Applied Polymer Science. 102 (2006)

3714–3719. doi:10.1002/app.24531.

[13] K. Alfonsi, J. Colberg, P.J. Dunn, T. Fevig, S. Jennings, T.A. Johnson, H.P. Kleine, C. Knight, M.A. Nagy, A. Perry, M. Stefaniak, Green chemistry tools to influence a medicinal chemistry and research chemistry based organisation {, Green Chemistry. 10 (2008) 31–36. doi:10.1039/b711717e.

[14] A. Figoli, T. Marino, S. Simone, E. Di Nicolò, X. Li, T. He, S. Tornaghi, Towards non-toxic solvents for membrane preparation : a review, Green Chemistry. 16 (2014) 4034–4059. doi:10.1039/c4gc00613e.

[15] H. Karkhanechi, S. Rajabzadeh, E. Di Nicolò, H. Usuda, A.R. Shaikh, H. Matsuyama, Preparation and characterization of ECTFE hollow fiber membranes via thermally induced phase separation (TIPS), Polymer. 97 (2016) 515–524. doi:10.1016/j.polymer.2016.05.067.

[16] B. Zhou, Q. Li, Y. Tang, Y. Lin, X. Wang, Preparation of ECTFE membranes with bicontinuous structure via TIPS method by a binary diluent, Desalination and Water Treatment. 57 (2016) 17646–17657. doi:10.1080/19443994.2015.1086898.

[17] C. Ursino, S. Simone, L. Donato, S. Santoro, M.P. De Santo, E. Drioli, E. Di Nicol?, A. Figoli, ECTFE membranes produced by non-toxic diluents for organic solvent filtration separation, RSC Advances. 6 (2016). doi:10.1039/c6ra13343f.

[18] E. Drioli, S. Santoro, S. Simone, G. Barbieri, A. Brunetti, F. Macedonio, A. Figoli, ECTFE membrane preparation for recovery of humidified gas streams using membrane condenser, REACTIVE AND FUNCTIONAL POLYMERS. 79 (2014) 1–7. doi:10.1016/j.reactfunctpolym.2014.03.003.

[19] B. Zhou, Y.K. Lin, W.Z. Ma, Y.H. Tang, Y. Tian, X.L. Wang, Preparation of ethylene chlorotrifluoroethylene co-polymer membranes via thermally induced phase separation, Gaodeng Xuexiao Huaxue Xuebao/Chemical Journal of Chinese Universities. 33 (2012) 2585–2590. doi:10.7503/cjcu20120033.

[20] J.F. Kim, J.T. Jung, H.H. Wang, S.Y. Lee, T. Moore, A. Sanguineti, E. Drioli, Y.M. Lee, Microporous PVDF membranes via thermally induced phase separation (TIPS) and stretching methods, Journal of Membrane Science. 509 (2016) 94–104. doi:10.1016/j.memsci.2016.02.050.

[21] J.T. Jung, J.F. Kim, H.H. Wang, E. di Nicolo, E. Drioli, Y.M. Lee, Understanding the non-solvent induced phase separation (NIPS) effect during the fabrication of microporous PVDF

membranes via thermally induced phase separation (TIPS), Journal of Membrane Science. 514 (2016) 250–263. doi:10.1016/j.memsci.2016.04.069.

[22] J. Lee, B. Park, J. Kim, S. Bin Park, Effect of PVP, lithium chloride, and glycerol additives on PVDF dual-layer hollow fiber membranes fabricated using simultaneous spinning of TIPS and NIPS, Macromolecular Research. 23 (2015) 291–299. doi:10.1007/s13233-015-3037-x.

[23] S.-I. Sawada, C. Ursino, F. Galiano, S. Simone, E. Drioli, A. Figoli, Effect of citrate-based non-toxic solvents on poly(vinylidene fluoride) membrane preparation via thermally induced phase separation, Journal of Membrane Science. 493 (2015). doi:10.1016/j.memsci.2015.07.003.

[24] L. Wang, D. Huang, X. Wang, X. Meng, Y. Lv, X. Wang, R. Miao, Preparation of PVDF membranes via the low-temperature TIPS method with diluent mixtures: The role of coagulation conditions and cooling rate, Desalination. 361 (2015) 25–37. doi:10.1016/j.desal.2015.01.039.

[25] Z. Cui, N.T. Hassankiadeh, S.Y. Lee, K.T. Woo, J.M. Lee, A. Sanguineti, V. Arcella, Y.M. Lee, E. Drioli, Tailoring novel fibrillar morphologies in poly(vinylidene fluoride) membranes using a low toxic triethylene glycol diacetate (TEGDA) diluent, Journal of Membrane Science. 473 (2015) 128–136. doi:10.1016/j.memsci.2014.09.019.

[26] L. Wu, J. Sun, Structure and properties of PVDF membrane with PES-C addition via thermally induced phase separation process, Applied Surface Science. 322 (2014) 101–110. doi:10.1016/j.apsusc.2014.10.083.

[27] N.T. Hassankiadeh, Z. Cui, J.H. Kim, D.W. Shin, A. Sanguineti, V. Arcella, Y.M. Lee, E. Drioli, PVDF hollow fiber membranes prepared from green diluent via thermally induced phase separation: Effect of PVDF molecular weight, Journal of Membrane Science. 471 (2014) 237–246. doi:10.1016/j.memsci.2014.07.060.

[28] Z. Cui, N.T. Hassankiadeh, S.Y. Lee, J.M. Lee, K.T. Woo, A. Sanguineti, V. Arcella, Y.M. Lee, E. Drioli, Poly(vinylidene fluoride) membrane preparation with an environmental diluent via thermally induced phase separation, Journal of Membrane Science. 444 (2013) 223–236. doi:10.1016/j.memsci.2013.05.031.

[29] Z.C. Zhang, C.G. Guo, X.M. Li, G.C. Liu, J.L. Lv, Effects of PVDF Crystallization on Polymer Gelation Behavior and Membrane Structure from PVDF/TEP System via Modified TIPS Process, Polymer-Plastics Technology and Engineering. 52 (2013) 564–570.

doi:10.1080/03602559.2012.762521.

[30] H.-Q. Liang, Q.-Y. Wu, L.-S. Wan, X.-J. Huang, Z.-K. Xu, Polar polymer membranes via thermally induced phase separation using a universal crystallizable diluent, Journal of Membrane Science. 446 (2013) 482–491. doi:10.1016/j.memsci.2013.07.008.

[31] M. Ulbricht, Advanced functional polymer membranes, Polymer. 47 (2006) 2217–2262. doi:10.1016/j.polymer.2006.01.084.

[32] Drioli E. and Giorno L., Membrane Operations Innovative Separations and Transformations, WILEY-VCH, 2009.

[33] S. Santoro, E. Drioli, A. Figoli, Development of Novel ECTFE Coated PP Composite Hollow-Fiber Membranes, Coatings. 6 (2016) 40–52. doi:10.3390/coatings6030040.

Chapter 1.

ECTFE membranes produced by non-toxic diluents for organic solvent filtration separation

1.1 Introduction

Organic solvents are usually employed in different production processes, such as chemicals production, pharmaceutical industries, petrochemical sector, cosmetic, purification and processing of food, nutraceuticals and natural products. Therefore, solvent recycling is one of the main issues of the chemical and pharmaceutical industries, in fact, industrial wastes may be toxic, corrosive or reactive, that can lead to environmental and human health consequences. The traditional practices of solvent recycling rely on pre-treatments (addition of additives), evaporation and distillation. However, these processes are costly, require high temperatures or use of other type of chemicals. With respect to these techniques, membranes allow the facile, safe and low-cost recovery, concentration or purification of the target molecules (non-thermal separation)[1]. In particular, ultrafiltration (UF) and nanofiltration (NF) pressure-driven membrane processes are of particular interest for the organic solvent separation. The first publications concerning their application were reported by Nguyen [2] for UF and Eriksson[3] for NF, respectively. Main examples of UF process include the fractionation and purification of peptide or impurities from protein solution [4] and the extraction polyphenols from seeds [5]. Organic solvent nanofiltration (OSN) has gained popularity as membrane process for different applications, such as purification of pharmaceutically active ingredients [6], specific recognition of genotoxins [7] recovery of catalyst in chemical synthesis [8], separation of ionic liquids [9], and solvent exchange [10]. Both UF and NF processes were used in pharmaceutical and biotechnological applications to extract, isolated and concentrated compounds of interest [5,11–14]from organic solvent media. For both types of membranes it is of primary importance the membranes stability in the presence of harsh solvents.

New generation of NF membranes is more stable towards organic solvents, but full-scale applications are still limited, because of the low number of available commercial solvent-resistant membranes. Nowadays, the typical polymers used for preparing NF membranes are Polyimide (PI) including co-Polyimidies (co-PIs), Polydimethylsiloxane (PDMS), Polyacrilonitrile (PAN) [15], Polyamide (PA) [16], Polysulfone (PS) [17]. Table 1 reports examples of typical polymers used in UF and NF membranes preparation and applications.

*Chapter based on the manuscript : C. Ursino, S. Simone, L. Donato, S. Santoro, M. P. De Santo, E. Drioli, E. Di Nicolò, A. Figoli "ECTFE membranes produced by non-toxic diluents for organic solvent filtration separation, *RSC Adv*., 6 (2016), 81001-81012, DOI: 10.1039/C6RA13343F

Table 1. Examples of typical polymers used in organic solvent UF and NF membranes preparation and applications

Authors	Polymer type	Solvents tested	Permeability (l/m^2 h bar)	Application of Organic Solvent Resistant Membranes
S. Darvishmanesha et al.[18]	PPS	Methyl ethyl ketone, diethyl ether, ethyl acetate, methanol, ethanol, 2-propanol, n-hexane, n-heptane, acetone and toluene	0.02 - 3.21	OSN Membranes permeation performance in pure solvents at lab scale
S. Darvishmanesha et al.[19]	PPS	Methanol	0.8 - 9	OSN Membranes permeation performance in pure solvents at lab scale
M.G. Buonomenna et al.[20]	PEEKWC	Water, Methanol, Ethanol, 2-Propanol and n-Butanol	0.27 - 3.63	OSN Membrane performance in pure solvents at lab scale
I. Soroko et al.[21]	PI	DMF	0.23 - 11	OSN Membrane performance in pure solvents at lab scale
M. Peyravi et al.[22]	thin film composite (TFC) membrane of PA and PS	Methanol, ethyl Acetate and n-Hexane	1.4 - 7.4	OSN Membrane performance in pure solvents at lab scale
D. Fritsch et al.[23]	TFC membrane of polymers of intrinsic microporosity (PIMs) and PAN	N-heptane, Toluene, Chloroform, Tetrahydrofuran, Methanol and Ethanol	0.1 - 7.3	OSN Membrane performance in pure solvents at lab scale
Jansen et al.[24]	PPS and PI	Methanol, Ethanol, 2-Propanol, Pentane, Hexane, Heptane, Acetone, Methyl ethyl ketone, Methylacetate, Ethylacetate, isopropyl Acetate	0.5 (NF) – 2000 (MF)	OSN Membrane performance in pure solvents at lab scale
K. Hendrix et al.[25]	TBPEEK	Alcohol, Alkanes, Alkylacetate and Ketone	0.09 - 0.77	OSN Membrane performance in pure solvents at lab scale

M. F. J. Solomon et al.[26]	PI TFC	THF, Toluene and ethyl Acetate	0. 3 - 3.83	OSN Membrane performance in pure solvents at lab scale
L. Liu et al.[27]	PASS	Water, Ethanol, Methanol, n-Butanol	0.5 – 1.24	OSN Membrane performance in pure solvents at lab scale
F. M. Penha et al.[28]	PES and Hydrophilic PES	Water, Ethanol, 2-Propanol and n-Hexane	0.3 (NF) – 250.3 (UF)	UF-NF Membrane performance in pure solvents at lab scale
F. M. Penha et al.[29]	PES and Hydrophilic PES	Oil and Hexane	0.1 – 2.5	NF Permeation of oil/hexane mixture at lab scale
M. Saxena et al.[30]	PS	Hexane	79- 364	UF Membrane performance in pure solvents at lab scale
M. V. Tres et al.[31]	PES/PVP	Oil and Hexane	2 (NF) - 27.5 (UF)	UF-NF Separation of soybean oil/n-butane at lab scale
M. Eliza et al.[11]	PAN-based	Aqueous solutions of Ethanol	0.45 - 2.34	NF Treatment of ethanol extracts of corn at lab scale
H. Nawaz et al.[5]	Cellulose acetate/cellulose nitrate mixed esters	Aqueous solutions of Ethanol	-	Extraction and concentration of polyphenols at lab scale

*PDMS: Polydimethylsiloxane; PEEKWC: Polyetheretherkeetone; PI: Polyimide, TFC: Thin-film composite membrane; DMF: Di-methyl Formamide; THF: Tetrahydrofuran; NMP: N-methyl Pyrrolidone; PAN: Polyacrylonitrile; PPS: Polyphenylsulfone, PES: Polyethersulfone, PS: Polysulfone, PVP: Poly(vinylpyrrolidone), PASS: Polyarylene sulfide sulfone, PA: Polyamide.

The influence of the polymeric materials, in terms of separation performance, was well summarized in the paper of Cheng et al.[32]. Other authors showed that, beside the polymer type, also the selected solvent and eventual additives influence the performance of the solvent resistant nanofiltration (SRNF) membranes [33]. A suitable solvent-resistant materials, as Halar® ECTFE (Ethylene-Chlorotrifluoroethylene), a perfectly alternating copolymer of ethylene and chlorotrifluoroethylene, could be used in the chemical process industry due to its properties such as excellent chemical resistance and mechanical properties [34,35]. However, due to its chemical-physical stability, ECTFE is difficult to be processed with the conventional membrane manufacturing techniques. In fact, ECTFE membranes are usually prepared *via* thermally induced phase separation (TIPS) technique and the polymer is solubilized in organic solvents at high temperature. The patent of Mutoh and Miura

was the first one reporting successful TIPS casting of ECTFE [36]. Several studies were performed to identify high-boiling organic solvents able to dissolve ECTFE [37]. Among them, Tri-ethyl Citrate (CTF), Glycerol Triacetate (GTA) and Di-octyl Adipate (DOA) have been used in the ECTFE membrane formation thanks to their low toxicity in comparison than phthalates, such as Di-butyl Phthalate (DBP) or Di-ethyl Phathalate (DEP)[38–42]. However, in all these cases, the ECTFE polymer was solubilised at temperature over 180°C. Solvay Specialty Polymers has recently developed a lower melting point grade of Halar® ECTFE, named here LMP ECTFE, which still offers the above quoted outstanding chemical resistance in caustic environments. Moreover, it shows comparable properties with standard Halar® (hydrophobicity and mechanical properties), but lower crystallinity and lower melting point [43]. ECTFE Halar® 901 and LMP ECTFE properties are summarized in Table 2. Molecular weight (MW) of ECTFE polymers cannot be directly determined by GPC. However, since the Melt Flow Index (MFI) can be provided and it is proportional to the molecular weight, information on their MW could be indirectly obtained [44]. For Halar 901, the Average Melt Flow Index (MFI) at 275 °C (527 °F), under a Load of 2.16 Kg, is 1 g/10 min; for LMP ECTFE, the MFI, at 225°C following ASTM D1238, is 1.5 g/10 min. On the basis of this parameter, it can be concluded that LMP ECTFE has lower MW and lower viscosity with respect to Halar 901. The same issue is related to the ethylene content, which is also not given by the supplier but it can be identified by other polymer properties. In fact, it is possible to obtain information on the Melting point and the Heat of fusion. For Halar 901 the Melting point is 242 °C, while the Heat of fusion is 42 J/g. For LMP ECTFE the Melting point is 175-185 °C, while the Heat of fusion is 18 J/g. These parameters are connected to the ethylene content. Since they are lower with respect to the standard Halar, in which the ethylene/cloro-trifluoroethylene ratio is 1:1; it could be concluded that, for LMP ECTFE, the ethylene content is less than 50 molar%.

Table 2. ECTFE Halar® 901 and LMP ECTFE properties

	Melting Point Tm (°C)	**Heat of Fusion (J/g)**	**Tensile Modulus (Mpa)**	**Contact Angle (°)**	**Melt flow index (g/10 min, @ 2.16 kg**
ECTFE Halar® 901	242	42	1650	90-95	1 (*)
LMP ECTFE	175-185	18	1100	90-95	1.5 (**)

(*) At 275°C following ASTM D 1238 “Standard Test Method for Melt Flow Rates of thermoplastics by Extrusion Plastometer”.
(**) At 225°C following ASTM D1238.

In this work, LMP ECTFE flat-sheet membranes were prepared by means of TIPS. In this perspective, solvents with low toxicity were employed. In particular, the first part of this investigation focused on the study of different non-toxic solvents as possible diluents selected on the basis of their environmental impact, high boiling point and solubility towards the polymer used. Then, LMP ECTFE flat membranes were prepared and characterized in terms of morphology, contact angle, mechanical test, porosity and pore size. In particular, swelling tests in pure organic solvents as Methanol, Ethanol, 2-Propanol, Hexane, Cyclohexane, Tetrahydrofuran, Toluene, N-methyl Pyrrolidone, Di-methyl Acetamide , Di-methyl Formamide were carried out for evaluating the LMP ECTFE dense film resistance. Finally, organic solvent permeation tests on selected solvents were performed using the novel LMP ECTFE membranes produced.

1.2 Experimental

1.2.1 Materials

The ECTFE based polymers (experimental ECTFE Halar® 901 and LMP ECTFE) were kindly supplied by Solvay Specialty Polymers and used without any further purification. Di-ethyl Adipate (DEA), Ethanol (EtOH), 2-Propanol (IPA), Methanol (MetOH), Acetone, Tetrahydrofuran (THF), Toluene (Tol), N-methyl Pyrrolidone (NMP), Di-ethylene Glycol (DEG), Di-butyl Itaconate (DBI), Glycerol, Chloroform, Di-methyl Acetamide (DMA), Di-methyl Formamide (DMF), Cyclohexane (C6H12), Hexane, Fluorinert® FC-40, Kerosene oil, were all purchased from Sigma–Aldrich and used without any further purification. Liquid nitrogen was purchased from Pirossigeno (Cosenza, Italy).

1.2.2 LMP ECTFE solubility tests

The solubility tests were carried out using different types of solvents: DBI and DEA. Their chemical structure is reported in Figure 1.

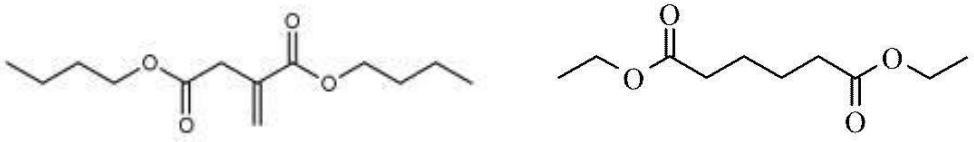

DBI **DEA**

Figure 1. Chemical structure of solvents of interest

Solvents were selected on the basis of their high boiling point, solubility parameters, lower toxicity and environmental impact, compared with the phthalates, 1,3,5-Trichlorobenzene (TCB), Di-butyl Phthalate (DBP) and Di-octyl Phthalate (DOP)[36], which are the solvents usually used for the preparation of ECTFE-based membrane by TIPS (Table 3). Similar solubility parameters indicate good affinity between solvent and polymer. In this case would be expected the completely dissolution of the polymer, whilst those with dissimilar values would not.

Table 3. Solvents properties

Solvent	**Molecular Formula**	**Molar Mass (g mol^{-1})**	**Density (g cm^{-3})**	**Boiling point (°C)**	**δ_d (MPa)$^{1/2}$**	**δ_p (MPa)$^{1/2}$**	**δ_h (MPa)$^{1/2}$**
DEA	$C_{10}H_{18}O_4$	202	1.01	251	16.4	6.2	7.5
DBI	$C_{13}H_{22}O_4$	242	0.98	284	16.9	10	22
ECTFE Halar® 901					16.8	8.4	7.8

- δd δp and δh, are the solubility parameters related to, dispersion parameters, polar forces and hydrogen bonding, respectively

Solubility tests were carried out heating and magnetically stirring (50 rpm) the polymeric solution (15wt% LMP ECTFE – 85wt% solvent) in an oil bath. The polymer solubilisation was evaluated by increasing the temperature of 10°C each 30min, from room to a maximum temperature value, close to the boiling point of the solvent employed.

In particular, an homogeneous solution (15wt% LMP ECTFE/ 85wt% solvent) was observed at 140°C for DEA and 170°C for DBI. The possibility of decreasing drastically the temperature of polymer solution makes easier the polymer processability. Based on these results and considering also the low toxicity, DEA was selected as solvent for the preparation of LMP ECTFE flat sheet membranes.

1.2.3 Polymeric dope solution preparation

Polymeric dopes were prepared by dissolving the polymer in DEA at different concentrations (15-20-25% w/w). Each solution was stirred for 1h at temperature of 193°C until complete dissolution of the components was achieved. The polymeric dope was allowed to degas, keeping the temperature, for 6h before casting.

1.2.4 Preparation of LMP ECTFE membranes and dense films

Membranes were prepared by casting the polymeric solution over a suitable smooth glass support by means of an automatized casting knife (DeltaE srl, Italy) Figure 2.

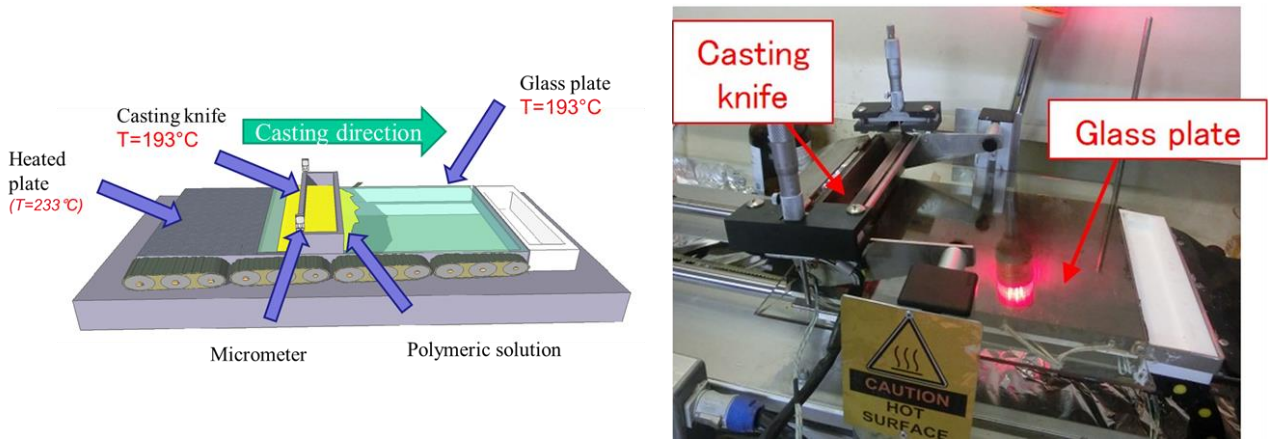

Figure 2. Automatized casting knife.

The dope solution, having a polymer concentration in the range of 15-25 wt.%, was cast by keeping both the casting knife and the support to the temperature of 193°C, to prevent premature precipitation of the polymer.

After casting and evaporation, polymeric membranes were cooled down by immersing them in the coagulation bath of pure Di-ethylene Glycol (DEG) at 5°C. This value of temperature, among the others used (25°C and 60°C), has been found optimal for the preparation of reproducible polymeric porous membranes. After coagulation, the membranes were washed overnight in 2-Propanol. In case of preparation of dense film, specifically made for evaluating the solvent resistant of the LMP ECTFE, no coagulation bath was used and the cast dope solutions were cool down overnight slowly. In the dense film (D), DEA was extract by washing in ethanol (typical step in a TIPS process), three times and drying in an oven for 6 h.

All the membrane conditions are resumed in Table 4.

Table 4. Summary of the main preparation conditions for LMP ECTFE membranes

Membrane type	Polymer conc. (wt%)	Casting knife (µm)	Air exposure time (sec)	Coagulation bath type	Coagulation bath Temperature (°C)	Drying procedure
L2	15	300	0			

M2	20	300	0	DEG	5	isopropanol over night and after drying at air
N2	25	300	0			
Dense Film (D)	20	250	over night	-	-	direct drying

1.2.5 Determination of the binary phase diagram

ECTFE Halar® 901 and LMP ECTFE solubility in DEA was evaluated by monitoring the cloud point (CP) of solutions containing different weight percentages of polymer. In each case, the polymer was added to the solvent at room temperature and solubilised by magnetically stirring the solution (50 rpm) increasing the temperature by using the oil bath. Once the polymeric solution was completely solubilised, the dope solution was cooled (rate of cooling was 0.1°C min-1) until the cloud point (Solid-Liquid Demixing) occurred. The tests were performed varying the polymer concentration from 5wt% to 35wt%.

1.3 Membrane characterization

1.3.1 Scanning electron microscopy *(SEM)*

Membranes morphology (cross section, top and bottom side) was observed by using a scanning electron microscope (Zeiss EVO MA 100, Assing, Italy). The sample for the evaluation of the membrane cross-section was fractured in liquid nitrogen. Samples were sputter-coated with a thin gold film prior to SEM observation.

1.3.2 Atomic force microscopy *(AFM)*

Atomic force microscopy was used to study the top and bottom surface morphology and roughness of the prepared membranes. The AFM device was a Bruker Multimode 8 with Nanoscope V controller. Data were acquired in tapping mode, using silicon cantilevers (model TAP150, Bruker). The membrane surfaces were imaged in a scan size of 10 μm x 10 μm.

1.3.3 Contact angle measurements

Contact angle measurements were performed with ultrapure water using the sessile drop method by a CAM100 instrument. For all membranes, at least five measurements were taken both on the air and the glass sides; the average values and the corresponding standard deviation were then calculated.

1.3.4 Swelling tests

According to Standard Practices for Evaluating the Resistance of Plastics to Chemical Reagents [45], to measure the swelling degree, dense film samples (A= 4cm^2) were weighted and placed in suitable solvent resistant containers. The quantity of reagent shall be approximately 12.5 mL/cm^2 of specimen surface area. Samples were kept totally immersed, for 72h-120h-172h at standard laboratory atmosphere (25°C), in one of the following pure organic solvents: EtOH, MetOH, Acetone, THF, Tol, NMP, EtOAc, DMA and DMF. The swelling degree (Sw) was calculated as follows:

$$Sw = \left(\frac{WW - WD}{WD}\right) * 100\%$$

Where W_W is the weight of the dense film after 72h-96h-172h of immersion and W_D is the initial weight of the dry dense film.

1.3.5 Mechanical tests

The Young's or elastic modulus (Emod), the tensile stress at break (Rm) and breaking elongation or stress at break (eBreak) were measured by means of a ZWICK/ROELL Z 2.5 test unit. Each sample was stretched unidirectionally at a constant rate of 5 mm/min; the initial distance between the clamps was of 50 mm. Five specimens were tested for each sample.

1.3.6 Porosity

Membrane porosity (Ɛm) was determined according to the gravimetric method, described in literature[47]. Porosity was defined as the ratio between the volume of the membrane and the volume of voids present within it. Dry membrane pieces were weighted and impregnated in kerosene for 24h; after this time, the excess of liquid was removed with tissue paper, and membranes weight was measured again. Finally, porosity was calculated applying the following formula:

$$Ɛ(\%) = \frac{\left(\frac{Ww - WD}{\rho K}\right)}{\left(\frac{(Ww - WD)}{\rho K} + \left(\frac{WD}{\rho P}\right)\right)} * 100$$

Where W_W is the weight of the wet membrane, W_D is the weight of the dry membrane, ρ_K is the kerosene density (0.82 g/cm^3) and ρ_P is the polymer density (1.71 g/cm^3). For all membranes types, three measurements were performed; then, the average values and corresponding standard deviation were calculated.

1.3.7 Bubble point and pore size distribution

Membrane bubble points, largest pore size and pore size distribution were determined using a PMI Capillary Flow Porometer (CFP1500 AEXL, Porous Materials Inc., USA). For each test, membranes samples were initially fully wetted using Fluorinert FC-40 (16 dyne/cm), for 24h and placed in the sample holder. Bubble point, gas pressure and flow rates through the dry membranes were measured. This operating mode, named wet-up/dry-up, was selected using the software Capwin. The measurement of bubble point, largest pore size and pore size distribution is based on the Laplace's equation:

$$d_P = \frac{4\,\tau\cos\theta}{P}$$

where d_P is the pore diameter, τ is the surface tension of the liquid, θ is the contact angle of the liquid (assumed to be 0 in case of full wetting, which means $\cos\theta = 1$) and P is the external pressure. The results of each test were exported as an excel file using the software Caprep for further processing.

1.3.8 Solvent Filtration experiments

Filtration tests were performed in a high pressure crossflow filtration cell (model HP4750) supplied from Sterlitech corporation (USA). The volume was 300 mL and the diameter 5.1 cm. The effective membrane area was 20.4 cm^2.

Experiments were performed using the solvents at room temperature, as indicated in Table 5.

Table 5. Characteristics of the organic solvents used in the filtration experiments [46]

Solvent	Molecular Weight (g/mol)	Density (g/mL)	Surface tension ϒ (mN/m)	Viscosity (cP)	Polarity
Methanol	32.04	0.791	22.1	0.60	Protic polar
Ethanol	46.10	0.789	21.9	1.20	Protic polar
DMF	73.09	0.944	37.1	0.82	Aprotic polar

The cell was filled with one of the following solvents: Methanol, Ethanol, and DMF. Before the tests, each membrane was conditioned by immersing in the target pure solvent for 24 h, and then placed in the cell. Experiments were carried out by applying different N_2 gas pressures (trans-membrane pressure (TMP)) from 2 to 10 bar. The permeate was collected at atmospheric pressure. Each membrane filtration test was conducted three times. Solvent flux (J) through each membrane, at a

given pressure, was defined as the volume permeated per unit area and per unit time. J was calculated by the following equation:

$$J = \frac{V}{(A\,\Delta t)}$$

where V (L) is the volume of permeate, A (m^2) is the membrane area, and Δt (h) is the operation time. The average and relative standard deviation were calculated.

From the slope of the J vs. P linear relationship, the membrane permeability was calculated according to a least-square fitting method.

1.4 Results and discussion

1.4.1 Determination of the binary phase diagram

The cloud point (CP) of LMP ECTFE/DEA and ECTFE Halar® 901 system, as a function of polymer concentration, was determined. The initial thermodynamically stable homogeneous solution, made of polymer and solvent, separates into two phases decreasing the temperature. The polymer-rich phase forms the membrane structure, and the polymer-lean phase forms the pores [47]. The binary phase diagram indicates the miscibility gap of the solution, at different polymer concentration. In general, the CP of a polymer/solvent system depends on its stability, which in turn is influenced by the solubility of the polymer in the same solvent. This depends on the Hansen's solubility parameters, but also on the polymer degree of crystallinity. Since, usually, a crystalline polymer is more stable, the interactions between the chains are stronger and, therefore, it is more difficult to dissolve. As reported in Figure 3, LMP ECTFE CP was lower that the ECTFE Halar® 901. In this case, the two polymers' solubility parameters are very close. However, LMP ECTFE is easier to dissolve because of its lower crystallinity (Table 2) and therefore, the compatibility of polymer/solvent is higher for LMP ECTFE/DEA. Moreover, it was observed that the CP increased at higher polymer concentration. Phase separation mechanism usually influences the membrane morphology. In fact, the liquid-liquid (L/L) demixing is favoured at low temperature and low polymer concentration, leading to cellular morphologies, while solid-liquid (S/L) demixing generally occurred at high polymer concentration and high temperature and brings to the formation of spherulites and axialites structures[47]. In particular, both our systems, LMP ECTFE/DEA and ECTFE Halar 901/DEA, did not become cloudy, until they began to form gels at the sol–gel transition temperature. Similar results were observed for PVDF/Citroflex system reported by Sawada et al.[48]. This result is in agreement with TIPS processes, where the higher temperature is necessary to keep the polymer/solvent system

homogeneous (latent solvent). According to literature [37,40], and SEM observation, S/L phase separation, typical in a TIPS process, is observed in our experiments. The obtained membranes morphology is discussed more in details in Section 3.2.

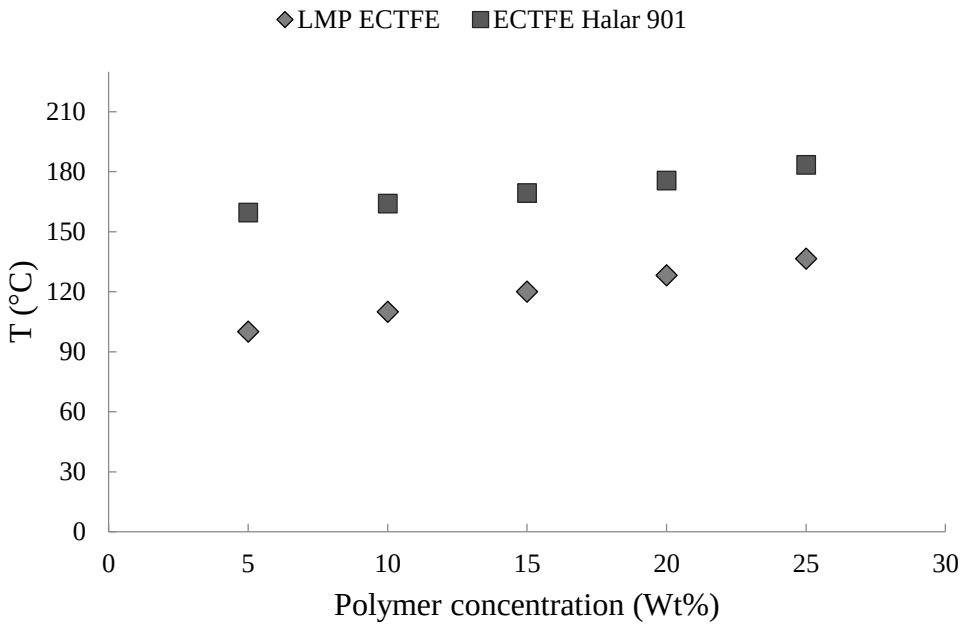

Figure 3. Sol-gel transition temperature of ECTFE Halar® 901 and LMP ECTFE solutions as a function of polymer concentration

1.4.2 SEM, AFM and Contact Angle Analyses

The SEM pictures of the produced LMP ECTFE membranes are shown in Figure 4. Membrane D shows a fully dense structure, whilst L2, M2, and N2 membranes are asymmetric. In the latter, the top-side (airside during casting) is dense while the bottom side (glass side) is porous. This is in agreement with previous literature work. Moreover, it can be clearly seen that spherulitic structures are well defined in all the prepared membranes. This morphology is due to S/L demixing, which takes place during film cooling, as reported in Section 3.1. As described in literature [47], when membranes are prepared via TIPS, S-L phase separation can take place only if, during solution cooling, the crystallization temperature of the polymer is reached. Semi-crystalline and crystalline polymers can give, then, rise to chain folded lamellae and supramolecular architectures as axialites and spherulites.

D (DENSE) MEMBRANE

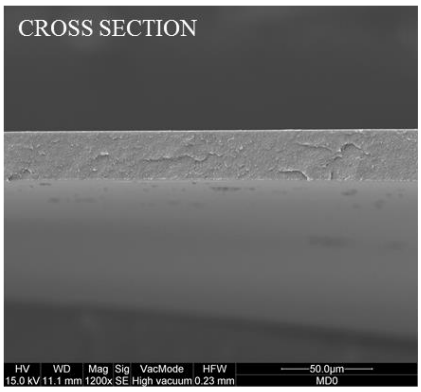

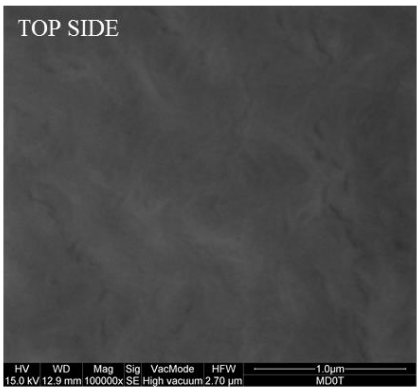

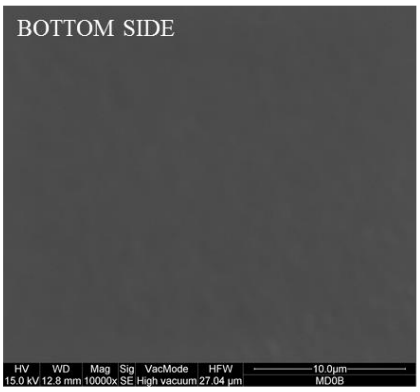

L2 (15wt%) MEMBRANE

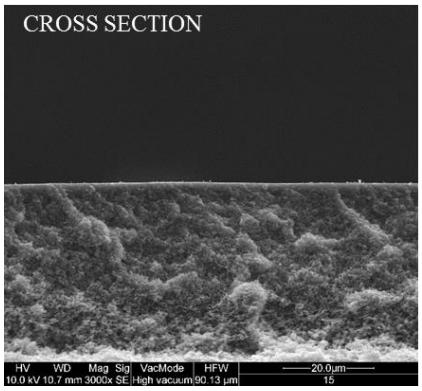

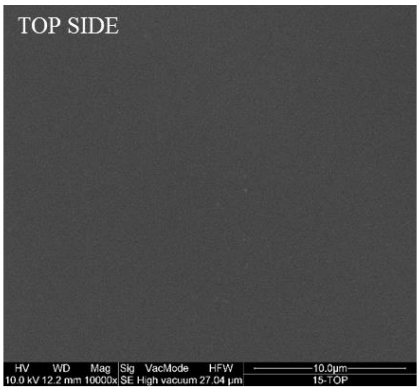

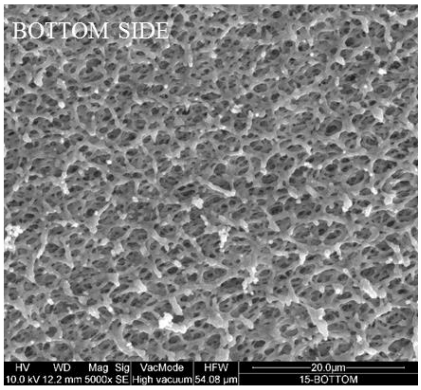

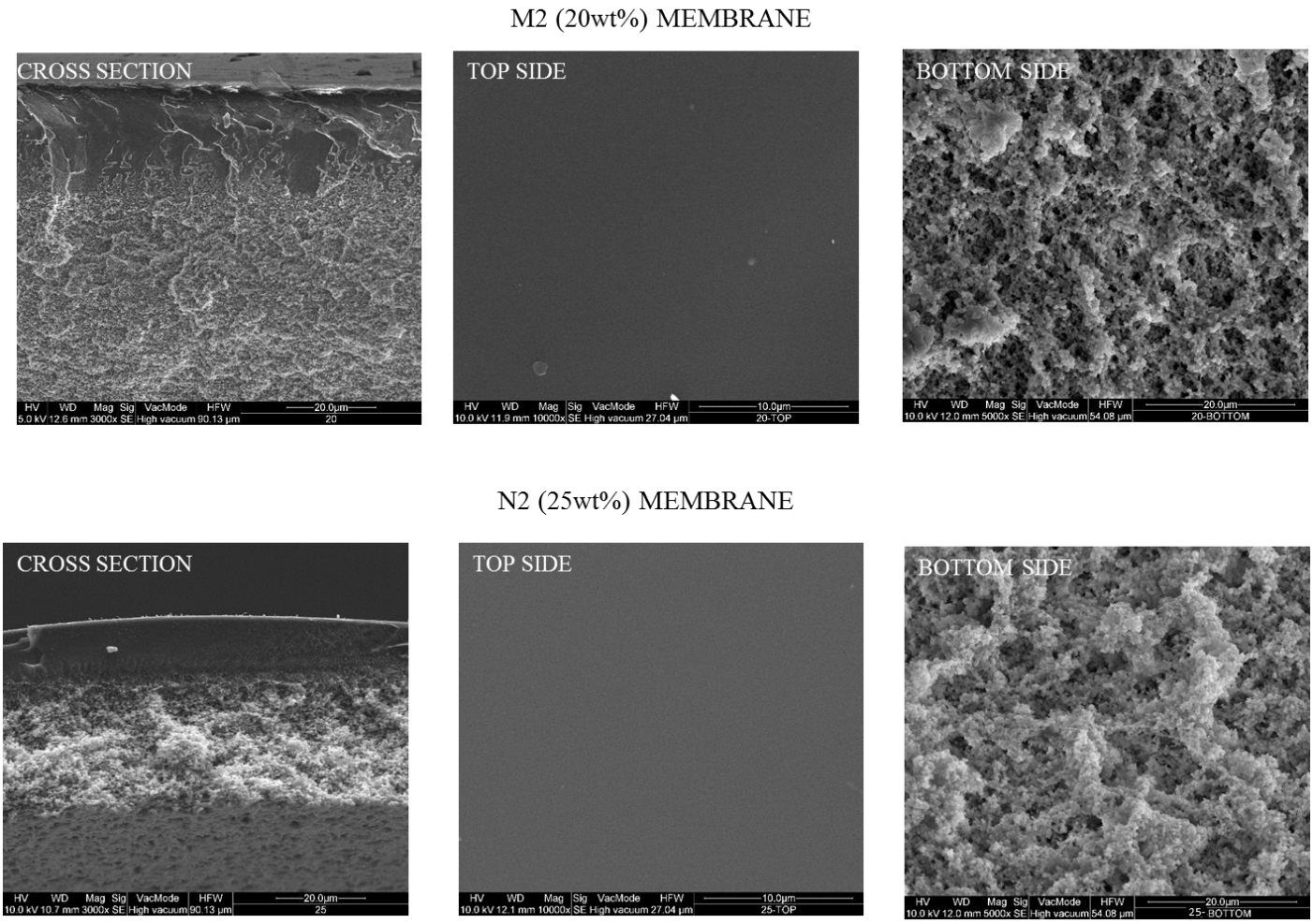

Figure 4. SEM pictures of membranes D, L2, M2 and N2.

The roughness of the top and bottom surfaces was investigated using AFM and only for the membranes having the intermediate polymer concentration and the best drying procedure. AFM, with respect to SEM imaging, provides quantitative information on the sample topography. Figures 5a and 5b show respectively the top and bottom surfaces topography of the membrane M2, while Figures 5c and 5d show the correspondent 3D views.

Topography was measured on five different areas on the sample surface and the RMS roughness (with its standard deviation) was calculated. The RMS roughness for the top-side of the membrane is found to be 2.79 ± 1.01 nm while the RMS roughness for the bottom part is 590 ± 160 nm. The obtained results indicate that the bottom surface has a much higher roughness with respect to the top surface in agreement with SEM analysis. In fact, the bottom side of the membrane presents a porous structure that contributes to the higher roughness.

These values are useful for the interpretation of the contact angle measurements which

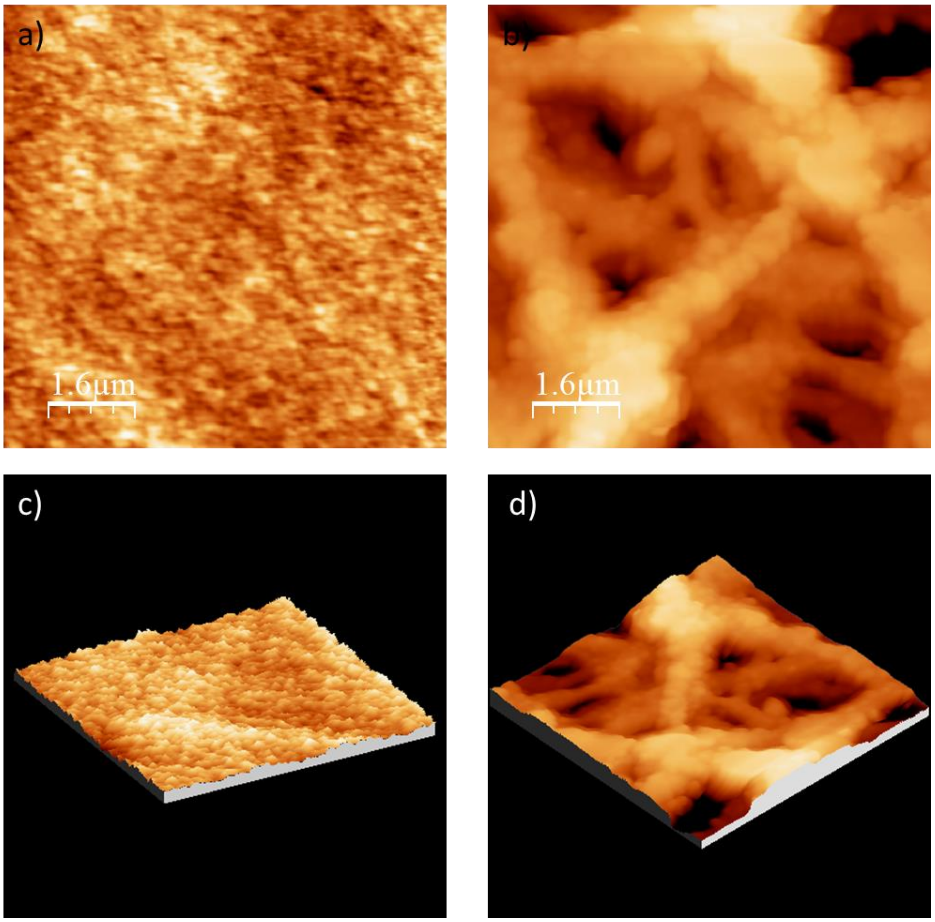

Figure 5. AFM pictures of membranes M2 where a) and b) show respectively the top and bottom surfaces topography of the membrane, while c) and d) show the correspondent 3D views.

are performed to quantify the membranes hydrophobic properties, on both membrane surfaces. The average values are reported in Table 7. The relative standard error is less than 5% in all cases. Contact angle measurements also confirmed that the produced membranes are, in general, asymmetric with top-side more hydrophilic than bottom side; due to surface smoothness (denser skin layer) as shown in AFM and SEM results. In fact, the apparent contact angle of a sessile droplet changes not only with the chemical texture, determined by the composition of the polymeric solution, but also with the roughness. Wenzel et al.[49] suggested a phenomenological model for understanding how roughness affects wetting:

$$\cos\theta^* = \cos\theta \times r$$

Where θ is the Young's angle and r the surface roughness.

Smooth surfaces reduce the absolute value of Cos θ and for this reason the corresponding contact angle is lower.

1.4.3 Membrane properties

Swelling tests on the dense film (membrane D) were carried out in order to evaluate the membrane resistance to the most used solvents in chemical and pharmaceutical industries. According to the procedure, reported in the materials and method section 2.2.6.4, membrane stability plays a crucial role in organic solvent separation, and the swelling test could be an important criteria to understand, predict, and describe the membrane performance. Swelling is a thermodynamic phenomenon which takes place in three different steps: solvent absorption on membrane surface, penetration/diffusion into the polymer free volume and, finally, polymer expansion.

Membrane swelling depends on the affinity between solvent and polymer. Indeed, if mutual affinity between them is higher, swelling will be enhanced. This may lead to an increase in the free volume (polymer expansion), which will affect membrane's morphology. In case of porous membranes, the solvent uptake is much more pronounced than swelling in dense membranes. This is because the solvent also filled their porous structure. Membrane swelling could reduce selectivity, increase solvent flux and reduce membrane cut-off. Figure 6 indicates that swelling takes 120 hours to reach equilibrium.

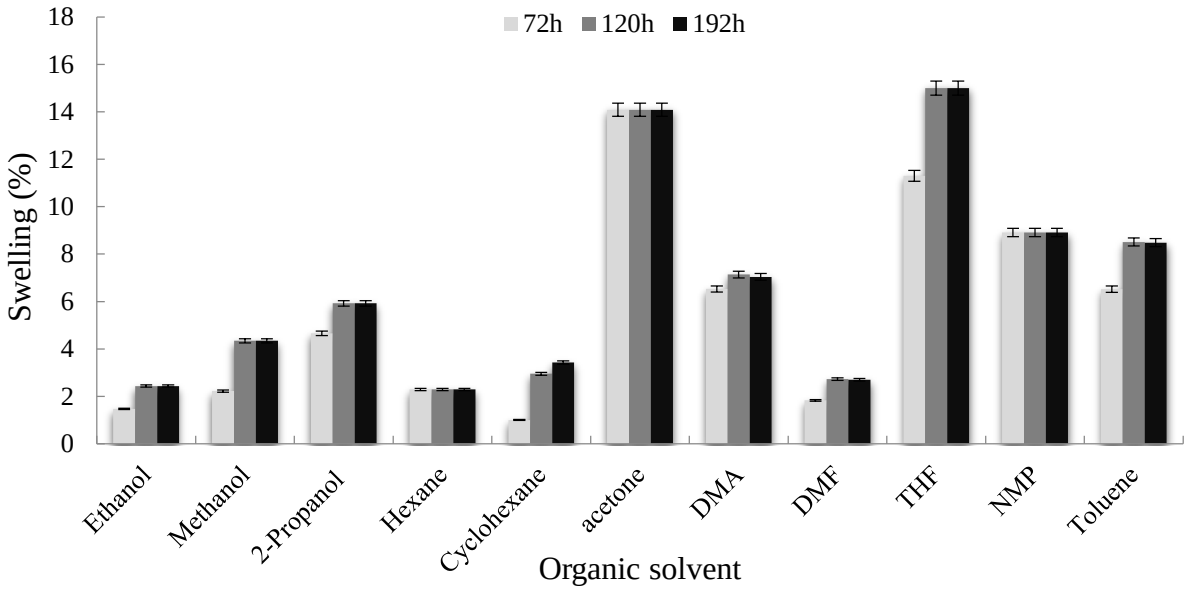

Figure 6. Swelling tests for membrane D (dense membrane)

Moreover, depending on the type of solvent employed (Table 6) a different behaviour is observed:

- polar protic solvents, the swelling increases in function of the surface tension (Ethanol>Methanol>Propanol).

- non-polar solvents, swelling increases with the Hansen solubility parameter (THF>Toluene>Cyclohexane>Hexane).
- polar aprotic solvents, the results indicate that the total degree of swelling is influenced by both superficial tension NMP>DMA>DMF and hydrogen bonding parameters Acetone>NMP>DMA>DMF.

Table 6. Hansen solubility parameters and surface tension of the solvents used for swelling test

Solvent	**Solubility parameters (Mpa)$^{1/2}$**				**Surface tension @ 20 °C in mN/m**
	δ_h (MPa)$^{1/2}$	δ_d (MPa)$^{1/2}$	δ_p (MPa)$^{1/2}$	δ (MPa)$^{1/2}$	
Ethanol	9.5	7.73	4.3	12.92	22.1
Methanol	10.9	7.42	6	14.28	22.7
2-Propanol	8.5	7.75	3.3	11.97	23
Hexane	0	7.24	0	7.24	18.43
Cyclohexane	0	8.18	0	8.18	24.95
Acetone	6.9	15.5	10.4	19.9	25.2
DMA	11.8	17.8	14.1	22.7	36.7
DMF	11.3	17.4	13.7	24.8	37.1
THF	3.7	19.0	10.2	22.5	26.4
NMP	7.2	18.4	12.3	22.9	40.79
Toluene	2.0	18.0	1.4	18.2	28.4

- δh, δd and δp are the solubility parameters related to hydrogen bonding, dispersion parameters, and polar forces, respectively

Comparing the swelling tests results to what observed by S. Simone et al. [40] it can be noticed that: *a)* the swelling percentages are, in general, lower, since the pure ECTFE Halar® 901 membranes prepared in that work were asymmetric dense, and, hence, solvent uptake by the porous polymer matrix was observed, *b)* The pure ECTFE Halar® 901 membranes solvent uptake percentages increased in the following order: DMF<DMA<Acetone<Toluene<NMP<EtOH<MetOH<THF. In the case of LMP ECTFE, DMF presented the lowest swelling degree; while, Acetone, THF and

Toluene produced the highest one swelling, *c)* The swelling degree observed of DMF using LMP ECTFE dense film, was lower than that observed with DMA, and this is in agreement with the ECTFE Halar® 901 solvent-uptake reported in literature [40]. A possible explanation could be that despite these two solvents are similar, some differences in their chemical structure and physical properties may lead to a different behaviour. In fact, DMA is polar, possess an electron lone pair and thanks to the presence of three $–CH_3$ groups that promote the hydrogen bonds, which makes it more reactive than DMF. Moreover, DMF readily interacts by hydrogen bonding with the polymer backbone enhancing the decreasing of swelling, while DMA forms H-bonds only at high temperature, as observed in literature for sulfonated polymers [50].

1.4.5 Mechanical tests, porosity and pore size characterisation

The tensile strength of the prepared membranes was measured in order to study how polymer concentration affected the mechanical properties and the results are summarised in Table 7. The elongation at break (eBreak) increases from 35.15% for membrane L2 (15wt.%), to 155.45% for membrane N2 (25wt.%). In addition, the elastic modulus and the tensile stress at break both increased when raising the polymer concentration. These results were in agreement with the porosity measurements. In fact, porosity decreased whilst all tensile properties (strength, modulus and extension at break) increased at higher concentration of LMP ECTFE as also reported in table 7.

The mean pore size of the membranes is in the range 0.01-0.03 μm and it decreased at higher polymer concentration. Moreover, the bubble point was increased from 2.08 bar, for the membrane with 15wt.% of polymer (L2), to 2.43 bar, for the membrane with 25wt.% of polymer (N2) as shown in Table 5. This is in agreement with the corresponding largest pore size of 0.22 and 0.18 μm of the membranes L2 and N2, respectively.

Table 7. Properties of the LMP ECTFE membranes

Membrane	Contact angle (°)		Mechanical tests			Porosity (%)	Pore size measurements			
	Top side	Bottom side	EMod (N/mm^2)	Tensile-strength (N/mm2)	eBreak (%)		Bubble point (Bar)	Largest pore size (µm)	Mean flow pore diameter (µm)	Diameter at maximum pore size distribution (µm)
L2	98	137	40.2	1.3	35.1	69.5	2.08	0.22	0.03	0.03
M2	98	108	277.5	4.6	141.7	56	2.11	0.21	0.01	0.02
N2	105	114	370	17.1	155.4	42.3	2.43	0.18	0.01	0.01

Note: The relative standard error is less than 5% in all cases

1.4.6 Membrane filtration performance in organic solvents

The low degree of swelling for dense membranes in different solvents, as MetOH, EtOH, and DMF, suggested the possible use of the novel LMP ECTFE membranes for organic solvent filtration separation. The permeability of the membranes L2, M2 and N2 prepared using 15-20-25wt.% of polymer, respectively, was measured using the dead-end filtration cell described in section 2.6.8. The trans-membrane flux was measured at different pressure values and the permeability was calculated as described in the materials and methods section. The results are shown in Figure 7.

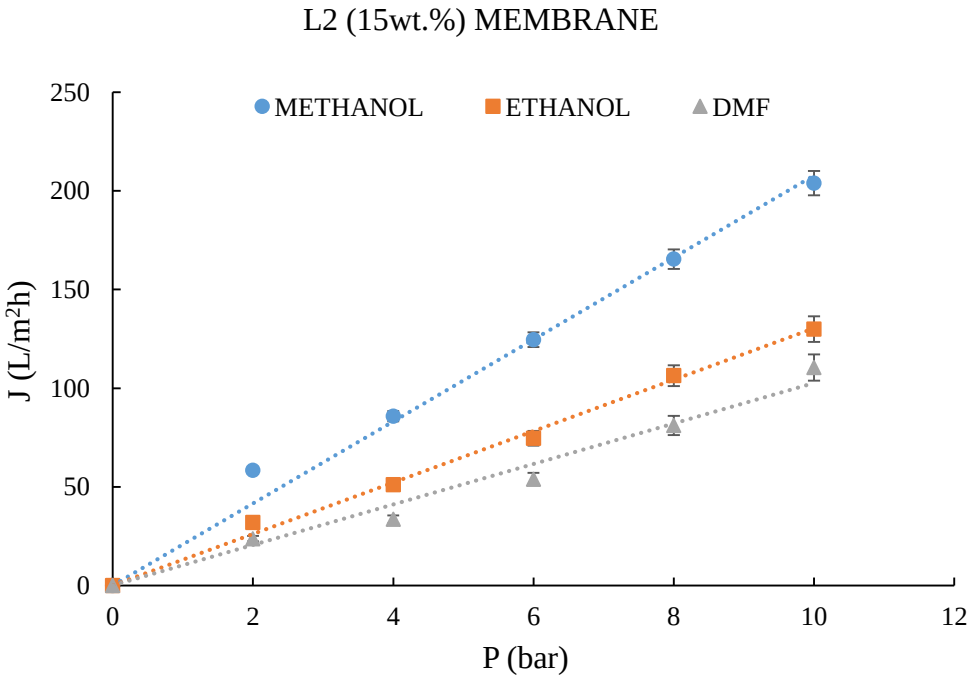

M2 (20wt.%) MEMBRANE

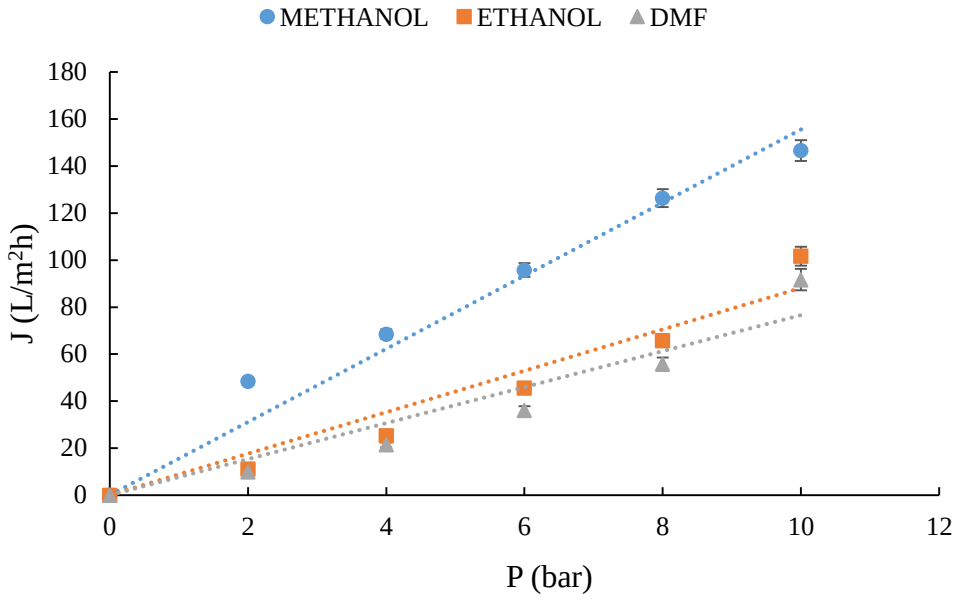

N2 (25wt.%) MEMBRANE

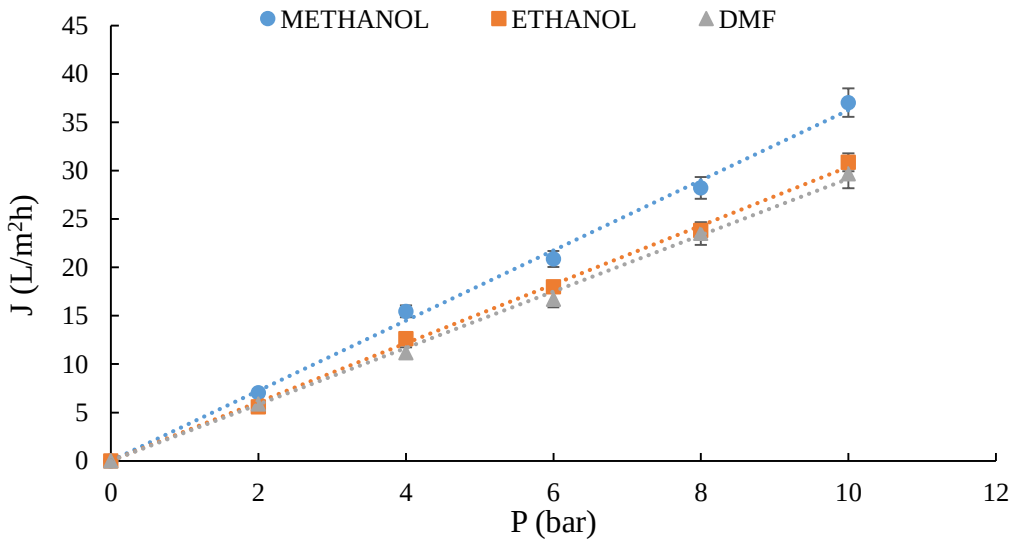

Figure 7. Solvent permeability trends with three different organic solvents and the membranes L2 (a), M2 (b) and N2 (c)

In all the cases, the permeate flux increased linearly when increasing the pressure. In particular, ethanol flux was lower with respect to methanol flux. In agreement with literature [51], this result can be justified considering the molecular weight and the viscosity of the two solvents (Table 5). In fact, the viscosity of the ethanol is twice of that one of methanol. Moreover, the molecular weight of Ethanol is 46.10 gr/mol while the one of Methanol is 32.09 gr/mol.

A lower DMF flux was observed and it is due by the combination of different factors such as molecular weight (73.09 gr/mol), the density (0.94 gr/mL) and the superficial tension (37.1 mN/m). In fact, the higher molecular weight of DMF is responsible of an increase of the steric hindrance, while the higher superficial tension (37.1 mN/m), is responsible of the decrease of the organic solvent diffusion through the membranes. Moreover, the increase of the polymer content (from 15wt% to 25wt%) determines a decrease of the solvent permeability, as expected. This allows tailoring the produced membranes depending on the type of application. In fact, the permeability values were between UF and NF range for the membranes L2 (MetOH: 20 L/m^{2}h*bar; EtOH: 13 L/m^{2}h*bar; DMF: 10 L/m^{2}h*bar), and M2 (MetOH: 15.5 L/m^{2}h*bar; EtOH: 8.81 L/m^{2}h*bar; DMF: 7.66 L/m^{2}h*bar), and in the NF range for the membrane N2 (MetOH: 3.6 L/m^{2}h*bar; EtOH: 3 L/m^{2}h*bar; DMF: 2.9 L/m^{2}h*bar), as reported in literature [52].

1.5 Conclusions

Novel LMP ECTFE dense and porous asymmetric flat membranes were prepared using a suitable non-toxic solvent as the Di-ethyl Adipate *via* TIPS technique. Polymeric membranes with different concentrations (from 15 wt.% to 25 wt.%) were successfully cast *via* TIPS technique. All the produced porous asymmetric membranes showed a spherulitic structure, with a top-side more hydrophilic than the bottom side, this result was confirmed by SEM and AFM analysis. Dense membrane shows good resistance to most aggressive organic solvents, as confirmed by the swelling tests carried out for 192h. Porous asymmetric membranes were tested for organic solvent filtration using pure Methanol, Ethanol and DMF. Varying polymer concentration in dope solution, it is possible to tailor the produced membranes in the NF and UF range. The results obtained show that LMP ECTFE membranes are promising candidates to be use in separation filtration processes under harsh conditions. Moreover, this polymer can be used as alternative of Halar® 901, thanks to its property, which makes it easy processable at lower temperature keeping the material properties unchanged.

References

[1] J.P. Sheth, Y. Qin, K.K. Sirkar, B.C. Baltzis, Nanofiltration-based diafiltration process for solvent exchange in pharmaceutical manufacturing, Journal of Membrane Science. 211 (2003) 251–261.

[2] Q.T. Nguyen, P. Aptel, J. Neel, Characterization of ultrafiltration membranes : Part I . Water and organic-solvent permeabilities, Journal of Membrane Science. 5 (1979) 235–251. doi:10.1016/S0376-7388(00)80451-2.

[3] P. Eriksson, Nanofiltration extends the range of membrane filtration, Environmental Progress. 7 (1988) 58–62. doi:10.1002/ep.3300070116.

[4] N.N. Li, A.G. Fane, W.S.W. Ho, T. Matsuura, Advanced Membrane Technology and Applications, John Wiley, John Wiley & Sons, Inc., Hoboken, New Jersey, 2008.

[5] H. Nawaz, J. Shi, G.S. Mittal, Y. Kakuda, Extraction of polyphenols from grape seeds and concentration by ultrafiltration, Separation and Purification Technology. 65 (2009) iii. doi:10.1016/S1383-5866(08)00514-5.

[6] D. Ormerod, B. Sledsens, G. Vercammen, D. Van Gool, T. Linsen, A. Buekenhoudt, B. Bongers, Demonstration of purification of a pharmaceutical intermediate via organic solvent nanofiltration in the presence of acid, Separation and Purification Technology. 115 (2013) 158–162. doi:10.1016/j.seppur.2013.05.007.

[7] S.G. Del Blanco, L. Donato, E. Drioli, Development of molecularly imprinted membranes for selective recognition of primary amines in organic medium, Separation and Purification Technology. 87 (2012) 40–46. doi:10.1016/j.seppur.2011.11.018.

[8] D. Nair, S.S. Luthra, J.T. Scarpello, L.S. White, L.M. Freitas dos Santos, A.G. Livingston, Homogeneous catalyst separation and re-use through nanofiltration of organic solvents, Desalination. 147 (2002) 301–306. doi:10.1016/S0011-9164(02)00556-8.

[9] S. Han, H.-T. Wong, A.G. Livingston, Application of Organic Solvent Nanofiltration to Separation of Ionic Liquids and Products from Ionic Liquid Mediated Reactions, Chemical Engineering Research and Design. 83 (2005) 309–316. doi:10.1205/cherd.04247.

[10] E.M. Rundquist, J. Pink, A.G. Livingston, Organic solvent nanofiltration: a potential alternative to distillation for solvent recovery from crystallisation mother liquors, Green Chemistry. 14 (2012) 2197–2205. doi:10.1039/c2gc35216h.

[11] E.M. Tsui, M. Cheryan, Membrane processing of xanthophylls in ethanol extracts of corn, Journal of Food Engineering. 83 (2007) 590–595. doi:10.1016/j.jfoodeng.2007.03.041.

[12] M. Cissé, F. Vaillant, D. Pallet, M. Dornier, Selecting ultra fi ltration and nano fi ltration membranes to concentrate anthocyanins from roselle extract (Hibiscus sabdariffa L .), Food Research International. 44 (2011) 2607–2614. doi:10.1016/j.foodres.2011.04.046.

[13] B. Díaz-Reinoso, A. Moure, H. Domínguez, J.C. Parajó, Ultra- and nanofiltration of aqueous extracts from distilled fermented grape pomace, Journal of Food Engineering. 91 (2009) 587–593. doi:10.1016/j.jfoodeng.2008.10.007.

[14] Y.H. See Toh, X.X. Loh, K. Li, A. Bismarck, A.G. Livingston, In search of a standard method for the characterisation of organic solvent nanofiltration membranes, Journal of Membrane Science. 291 (2007) 120–125. doi:10.1016/j.memsci.2006.12.053.

[15] F.P. Cuperus, K. Ebert, Nanofiltration : Principles and Applications, Elsevier, Amsterdam, 2005.

[16] P.B. Kosaraju, K.K. Sirkar, Interfacially polymerized thin film composite membranes on microporous polypropylene supports for solvent-resistant nanofiltration, Journal of Membrane Science. 321 (2008) 155–161. doi:10.1016/j.memsci.2008.04.057.

[17] A.K. Ho, B. Aernouts, W. Saeys, I.F.J. Vankelecom, Study of polymer concentration and evaporation time as phase inversion parameters for polysulfone-based SRNF membranes, Journal of Membrane Science. 442 (2013) 196–205. doi:10.1016/j.memsci.2013.04.017.

[18] S. Darvishmanesh, J. Degre, B. Van Der Bruggen, Performance of Solvent-Pretreated Polyimide Nanofiltration Membranes for Separation of Dissolved Dyes from Toluene, Industrial & Engineering Chemistry Research. 49 (2010) 9330–9338.

[19] S. Darvishmanesh, J.C. Jansen, F. Tasselli, E. Tocci, P. Luis, J. Degrève, E. Drioli, B. Van der Bruggen, Novel polyphenylsulfone membrane for potential use in solvent nanofiltration, Journal of Membrane Science. 379 (2011) 60–68. doi:10.1016/j.memsci.2011.05.045.

[20] M.G. Buonomenna, G. Golemme, J.C. Jansen, S.H. Choi, Asymmetric PEEKWC membranes for treatment of organic solvent solutions, Journal of Membrane Science. 368 (2011) 144–149. doi:10.1016/j.memsci.2010.11.036.

[21] I. Soroko, Y. Bhole, A.G. Livingston, Environmentally friendly route for the preparation of solvent resistant polyimide nanofiltration membranes, Green Chemistry. (2011) 162–168.

doi:10.1039/c0gc00155d.

[22] M. Peyravi, A. Rahimpour, M. Jahanshahi, Thin film composite membranes with modified polysulfone supports for organic solvent nanofiltration, Journal of Membrane Science. 423–424 (2012) 225–237. doi:10.1016/j.memsci.2012.08.019.

[23] D. Fritsch, P. Merten, K. Heinrich, M. Lazar, M. Priske, High performance organic solvent nanofiltration membranes : Development and thorough testing of thin film composite membranes made of polymers of intrinsic microporosity (PIMs), Journal of Membrane Science. 401–402 (2012) 222–231. doi:10.1016/j.memsci.2012.02.008.

[24] J.C. Jansen, S. Darvishmanesh, F. Tasselli, F. Bazzarelli, P. Bernardo, E. Tocci, K. Friess, A. Randova, E. Drioli, B. Van der Bruggen, Influence of the blend composition on the properties and separation performance of novel solvent resistant polyphenylsulfone/polyimide nanofiltration membranes, Journal of Membrane Science. 447 (2013) 107–118. doi:10.1016/j.memsci.2013.07.009.

[25] K. Hendrix, M. Vaneynde, G. Koeckelberghs, I.F.J. Vankelecom, Synthesis of modified poly(ether ether ketone) polymer for the preparation of ultrafiltration and nanofiltration membranes via phase inversion, Journal of Membrane Science. 447 (2013) 96–106. doi:10.1016/j.memsci.2013.07.006.

[26] M.F.J. Solomon, Y. Bhole, A.G. Livingston, High flux hydrophobic membranes for organic solvent nanofiltration (OSN) — Interfacial polymerization , surface modification and solvent activation, Journal of Membrane Science. 434 (2013) 193–203. doi:10.1016/j.memsci.2013.01.055.

[27] L. Liu, X. Wang, Y. Wang, L. Li, K. Pan, J. Yang, B. Cao, Preparation and characterization of asymmetric polyarylene sulfide sulfone (PASS) solvent-resistant nanofi ltration membranes, Materials Letters. 132 (2014) 11–14. doi:10.1016/j.matlet.2014.05.154.

[28] M.F. Penha, K. Rezzadori, M. Carolina, V. Zanatta, G. Zin, D. Walker, J.V. De Oliveira, J. Carlos, C. Petrus, M. Di, Influence of different solvent and time of pre-treatment on commercial polymeric ultrafiltration membranes applied to non-aqueous solvent permeation, EUROPEAN POLYMER JOURNAL. 66 (2015) 492–501. doi:10.1016/j.eurpolymj.2015.03.010.

[29] F.M. Penha, K. Rezzadori, M.C. Proner, G. Zin, L.A. Fogaça, J. Carlos, C. Petrus, J.V. De Oliveira, M. Di Luccio, Evaluation of permeation of macauba oil and n -hexane mixtures

through polymeric commercial membranes subjected to different pre-treatments, Journal OF Food Engineering. 155 (2015) 79–86. doi:10.1016/j.jfoodeng.2015.01.020.

[30] M. Saxena, P. Ray, P.S. Singh, Studies towards understanding the effect of hexane on polysulfone membranes, Polymer Bulletin. 72 (2015) 2157–2169. doi:10.1007/s00289-015-1395-3.

[31] M. V Tres, J.C. Racoski, R. Nobrega, R.B. Carvalho, Solvent recovery from soybean oil / n-butane mixtures using a hollow fiber ultrafiltration membrane, Brazilian Journal of Chemical Engineering.31 (2014) 243–249.

[32] X. Cheng, Y. Zhang, Z.Wang, Z. Guo, Y. Bai, Y. Shao, Recent Advances in Polymeric Solvent-Resistant Nanofiltration Membranes, Advances in Polymer Tecnhnology. 33 (2014) 1–24. doi:10.1002/adv.21455.

[33] I. Soroko, M.P. Lopes, A. Livingston, The effect of membrane formation parameters on performance of polyimide membranes for organic solvent nanofiltration (OSN): Part A. Effect of polymer/solvent/non-solvent system choice, Journal of Membrane Science. 381 (2011) 152–162. doi:10.1016/j.memsci.2011.07.027.

[34] J.P. Sibillia, J.P. Roldan, S. Chandrasekaran, Structure of Ethylene –Clorotrifluoroethylene copolymers, Journal of Polymer Science Part A: Polymer Chemistry. 10 (1972) 249–563. doi:10.1002/pola.25925.

[35] Solvay technical sheets, Halar® ECTFE ethylene-chlorotrifluoroethylene Design and Processing Guide, Downloaded from www.solvaysolexis.com.

[36] M.M. Y. Mutoh, Porous fluorine resin membrane and process for preparing the same, U.S. Patent N. 4.702.836, 1987.

[37] S. Ramaswamy, A.R. Greenberg, W.B. Krantz, Fabrication of poly (ECTFE) membranes via thermally induced phase separation, Journal of Membrane Science. 210 (2002) 175–180. doi:10.1016/S0376-7388(02)00383-6.

[38] I. Juhn, S. Ramaswamy, W.B. Krantz, A.R. Greenberg, Poly (ethylene chlorotrifluoroethylene) membrane formation via thermally induced phase separation (TIPS), Journal of Membrane Science. 362 (2010) 211–220. doi:10.1016/j.memsci.2010.06.042.

[39] H.J. Müller, A new solvent resistant membrane based on ECTFE, Desalination. 199 (2006) 191–192. doi:10.1016/j.desal.2006.0.

[40] S. Simone, A. Figoli, S. Santoro, F. Galiano, S.M. Alfadul, O.A. Al-Harbi, E. Drioli, Preparation and characterization of ECTFE solvent resistant membranes and their application in pervaporation of toluene/water mixtures, Separation and Purification Technology. 90 (2012) 147–161. doi:10.1016/j.seppur.2012.02.022.

[41] E. Drioli, S. Santoro, S. Simone, G. Barbieri, A. Brunetti, F. Macedonio, A. Figoli, ECTFE membrane preparation for recovery of humidified gas streams using membrane condenser, Reactive and Functional Polymers. 79 (2014) 1–7. doi:10.1016/j.reactfunctpolym.2014.03.003.

[42] J. Pan, C. Xiao, Q. Huang, C. Wang, H. Liu, Fabrication and properties of poly(ethylene chlorotrifluoroethylene) membranes via thermally induced phase separation (TIPS), RSC Advances. 5 (2015) 45249–45257. doi:10.1039/c5ra05675f.

[43] Solvay Specialty Polymers, HALAR®ECTFE XPH-793, Technical Presentation March 2012.

[44] Standard Practices for Evaluating the Resistance of Plastics to Chemical Reagents Copyright by ASTM Int'l (all rights reserved) for licensee's use only. A00390972 19 Dec 06.

[45] C.W. Macosko, Rheology, principles, measurements and Applications, Wiley VCH, 1994.

[46] I. Smallwood, Handbook of Organic Solvent Properties, Arnold, london, 2000.

[47] G. Ji, L. Zhu, B. Zhu, C. Zhang, Y. Xu, Structure formation and characterization of PVDF hollow fiber membrane prepared via TIPS with diluent mixture, Journal of Membrane Science. 319 (2008) 2008.

[48] S.-I. Sawada, C. Ursino, F. Galiano, S. Simone, E. Drioli, A. Figoli, Effect of citrate-based non-toxic solvents on poly(vinylidene fluoride) membrane preparation via thermally induced phase separation, Journal of Membrane Science. 493 (2015). doi:10.1016/j.memsci.2015.07.003.

[49] R.N. Wenzel, Resistance of Solid Surfaces To Wetting By Water, Industrial & Engineering Chemistry. 28 (1936) 988–994. doi:10.1021/ie50320a024.

[50] G.P. Robertson, S.D. Mikhailenko, K. Wang, P. Xing, M.D. Guiver, S. Kaliaguine, Casting solvent interactions with sulfonated poly(ether ether ketone) during proton exchange membrane fabrication, Journal of Membrane Science. 219 (2003) 113–121. doi:10.1016/S0376-7388(03)00193-5.

[51] D.R. Machado, D. Hasson, R. Semiat, Effect of solvent properties on permeate flow through nanofiltration membranes. Part I: Investigation of parameters affecting solvent flux, Journal of Membrane Science. 163 (1999) 93–102. doi:10.1016/S0376-7388(99)00158-1.

[52] M. Mulder, Basic Principles of Membrane Technology. Kluwer Academic Publishers, (1997) 2003.

Chapter 2.

Effect of citrate-based non-toxic solvents on poly(vinylidene fluoride) membrane preparation *via* thermally induced phase separation

2.1 Introduction

Membrane processes are currently used extensively in a number of areas of water treatment, thanks to their relatively low energy consumption, ease of operation, and lack of requirement for the addition of further chemicals to the process [1,2]. In particular, they represent one of the most attractive solutions to the problem of water shortage, which is an ongoing global issue because of population growth and economic expansion particularly in developing countries. Membrane processes are considered to be promising techniques for achieving a sustainable society; however the membrane preparation process itself remains problematic due to the use of substances that are hazardous to humans and environment. Microfiltration (MF) is a liquid-phase pressure-driven membrane process that is widely applied to separate contaminants such as bacteria, algae, colloids, and macromolecules, from the feed water. Together with other pressure-driven membrane processes (*e.g.* ultrafiltration, nanofiltration, and reverse osmosis) and membrane distillation processes (especially coupled with crystallization), MF could become a useful tool in addressing the increasing worldwide demand for clean water [3,4]. The porous MF membranes play the role of a size exclusion barrier, through which only water and other substances smaller than the pore size can permeate from the feed side to the other side. The pore size of MF membranes tends to range from 0.05 to 10 □m [2], depending on the size of the contaminants to be separated. MF membranes are required to have not only suitable porous structures, but also sufficient mechanical strength and chemical resistance for long term stability and use. Poly(vinylidene fluoride) (PVDF), a polymer with repeating units of (CF_2CH_2), is one of the most widely used polymers for membrane preparation, due to its outstanding chemical and physical stability [5-7]. PVDF is soluble at room temperature in polar aprotic solvents, and in addition, a range of chemicals can work as solvents at high temperatures [6]. PVDF membranes can therefore either be prepared *via* non-solvent induced phase separation (NIPS) or thermally induced phase separation (TIPS) methods [5,7]. In the NIPS process, the immersion of a polymer solution in a non-solvent causes the precipitation of a polymer-rich phase that turns into a membrane by exchange of a solvent with the non-solvent.

---

*Chapter based on the manuscript: S. Sawada, C. Ursino, F. Galiano, S. Simone, E. Drioli, A. Figoli, "Effect of citrate-based non-toxic solvents on poly(vinylidene fluoride) membrane preparation via thermally induced phase separation"- *Journal of Membrane Science*- Volume 493, 1 November 2015, Pages 232–242. DOI: 10.1016/j.memsci.2015.07.003.

In the TIPS process, the polymer solution is cooled from high temperature, and the polymer phase is expelled from the solvent to form a membrane due to the polymer/solvent immiscibility at low temperatures. Compared to the NIPS method, the TIPS method is capable of producing PVDF membranes with better mechanical strength, higher porosity and narrower pore-size distribution [7], which are appropriate properties for use in MF applications.

Traditionally, solvents such as dimethyl phthalate (DMP) [8,9], diethyl phthalate (DEP) [10], dibutyl phthalate (DBP) [11,12], and dioctyl phthalate (DOP) [12], have been used in the preparation of PVDF. However, these phthalate esters are extremely toxic and have a negative effect on human health [13]. As highlighted by Figoli *et al* [14]., one of the most urgent issues for membrane scientists is the discovery and development of less toxic alternatives to such solvents. However, this is not an easy task, and is complicated further by the fact that the structures of membranes prepared *via* the TIPS process are greatly influenced by the type of solvent used. Therefore, it is of paramount importance to select an appropriate solvent of low or non-toxicity, which is still capable of dissolving PVDF at high temperatures. In recent years, alternative solvents such as diphenyl ketone (DPK) [15] and diphenyl carbonate (DPC) [16] have been tested for PVDF membrane preparation *via* TIPS.

Citric acid esters, commercially known as "Citroflex", represent a non-toxic family of plasticizers used in food contact polymer applications. The toxicological safety of Citroflex is demonstrated by satisfactory results in numerous long-term tests conducted in animals [17], and therefore Citroflex is expected to be an environmental-friendly reagent for use in a range of chemical processes. To date, there have been few reports regarding the TIPS membrane preparation employing Citroflex as a solvent. The citroflex used in these studies are tributyl citrate (TBC), acetyl tributyl citrate (ATBC), and triethyl citrate (TEC). Liu *et al.* reported the preparation of flat PVDF membranes using a ternary system comprising the polymer, TBC as the solvent, and di-(2-ethylhexyl) phthalate (DEHP) as the non-solvent. They examined the effect of the PVDF / TBC / DEHP composition on the structures and properties of the resulting PVDF membranes [18]. Cui *et al.* prepared both flat and hollow fiber PVDF membranes using ATBC, and reported that the membrane structures were significantly affected by the experimental conditions, including the polymer concentration, quenching temperatures, air gap, and bore fluid temperature [19]. Hassankiadeh *et al.* also reported the preparation of PVDF hollow fiber membranes using ATBC, and examined the effect of polymer molecular weight on the membrane structures [20]. Besides PVDF, Mullette *et al.* also successfully prepared both poly(ethylene chlorotrifluoroethylene) (ECTFE) flat and hollow fiber membranes using TEC [21]. These previous studies clearly demonstrate that Citroflex appears to be an extremely useful solvent for application in the TIPS membrane preparation process.

Therefore, in the study reported herein, in addition to the use of the previously reported ATBC [19,20], we employed for the first time two additional Citroflex solvents, namely acetyl triethyl citrate (ATEC) and TEC, for the preparation of flat PVDF membranes *via* TIPS. The effect of the different solvents, together with that of the gap between the casting knife and plate, on the structures and properties of the resulting PVDF membranes was investigated. As mentioned in section 2.3.1, the solubility for PVDF of the used Citroflex (ATBC, ATEC, and TEC) is closely similar but clearly different from each other. Accordingly, the selection of these three Citroflex allowed us to in detail examine how the polymer / solvent affinity influenced the membrane formation during the TIPS process, which is of importance from the viewpoint of fundamental polymer science.

2.2. Experimental

2.2.1 Materials

PVDF (Solef 1015, purity: 100%) was kindly provided by Solvay Specialty Polymers (Bollate, Italy). ATBC (purity: 99%), ATEC (purity: 99%), TEC (purity: 99%), kerosene (purity: 100%) and ethanol (purity: 99.8%) were purchased from Sigma-Aldrich. The chemical formulae, properties and safety data information of the Citroflex solvents used in this study are shown in Table 1. Liquid nitrogen was purchased from Pirossigeno (Cosenza, Italy). Deionized water was obtained from a water purification system (Zeneer RO 180), and was used for the water permeability test.

Table 1. Properties of three kinds of Citroflex: ATBC, ATEC and TEC

Classification according to regulation (EC) n° 1272/2008	**SOLVENT**		
	ATBC 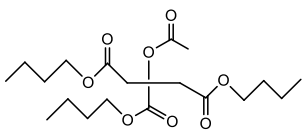	ATEC 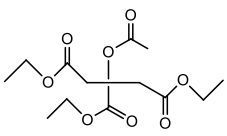	TEC 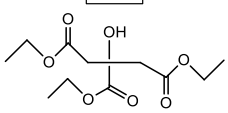
Molecular weight (g/mol)	402.5	318.3	276.3
Hazard statements	Not a hazardous substance or mixture according to Regulation (EC) No. 1272/2008. This substance is not classified as dangerous according to Directive 67/548/EEC.		H332- Harmful if inhaled.
Precautionary statements			–
Other hazards			–
Relevant toxicological information	No component of this product present at levels greater than or equal to 0.1% is identified as probable or confirmed human carcinogen by IARC.		
Density at 25 °C (g/mL) [22]	1.05	1.14	1.14
Boiling point at 1 mm Hg (°C) [22]	173	132	127

2.2.2 Sol-gel transition temperature

PVDF solubility in ATBC, ATEC, and TEC was evaluated by monitoring the sol-gel transition of solutions with variation of the PVDF polymer concentration. A vessel containing the PVDF / solvent

solution was heated in an oil bath at 200 °C for 2 hours to give a homogeneous solution. Then, the temperature of the oil bath was dropped to the planned value in the range of 100-170 °C, causing the solution in the vessel to be gradually cooled and reach the equilibrium state after 3 hours. The vessel was removed from the oil bath, and tilted for observation of the state of the PVDF / solvent mixture at this temperature. If the mixture was homogeneous and can smoothly flow (at higher temperature), it was recorded as a "solution". If the mixture was viscous and partially solidified (at lower temperature), it was recorded as a "gel". In this way, the following procedures were repeatedly conducted: heating of the vessel to 200 °C again to revert the mixture to a homogeneous solution; cooling of the vessel to another temperature; and record of the mixture state (solution or gel). The sol-gel transition temperature was defined as the lowest temperature at which the PVDF / solvent mixture was a smooth-flowing liquid.

2.2.3 Preparation of PVDF flat membranes

The PVDF polymer and Citroflex (ATBC or ATEC or TEC) were mixed in a closed vessel, and heated at 190 °C in an oil bath. The polymer concentration was 16wt% in all cases (When the polymer concentration was more than 16%, the solution was a bit viscous, thereby failing to prepare the homogeneous membrane). The resulting solutions were stirred for 3 hours at 190 °C until complete dissolution of the polymers was achieved. After the stirring was stopped, the solution was kept exposed to the air for 2 hours in order to get rid of airbubbles.

The flat PVDF membranes were prepared by using the casting knife containing a narrow rectangular opening at the bottom and a smooth glass support plate set below the casting knife. The polymer solution poured into the casting knife at 190 °C passed through the opening, and then was accumulated on the plate at 30 °C. Just after that, the glass plate started moving at the fixed velocity of 22 cm/min, spreading the polymer solution onto the glass plate. The gap between the casting knife and the glass plate for membrane casting was varied between 200 and 400 μm, allowing the thickness of the final membrane to be varied. After being kept under the ambient atmospheric condition for 2 hours, the nascent membrane with a glass plate was immersed in an ethanol bath (purity: 99.8%) for 24 hours to extract solvents from the membrane. Finally, the membrane was dried in an oven at 40 °C for 24 hours. The membrane side exposed to air during the casting is referred to as the "top side" surface, whereas the side contact with the glass plate is referred to as the "bottom side" surface. The membranes prepared using ATBC, ATEC and TEC are referred to as the "PVDF/ATBC membrane", "PVDF/ATEC membrane" and "PVDF/TEC membrane", respectively.

2.3 Characterization of PVDF membranes

2.3.1 FT-IR analysis

The crystalline phase of PVDF membranes was studied by Fourier-transform infrared (FT-IR) spectroscopy. Spectral data were recorded on a Nicolet^{TM} iS^{TM} 10 FT-IR ATR spectrometer over the range of 400-1000 cm^{-1} with a resolution of 2 cm^{-1}.

2.3.2 Crystallinity

The thermal properties of the PVDF membranes were examined by differential scanning calorimetry (DSC) using a Rigaku Thermo plus DSC 8230 under N_2. Thermograms of the heat flow *vs.* temperature of the specimens (around 5 mg) were obtained in the range of 100-200 °C at a heating rate of 5 °C/min. The heat of the fusion of the specimens, H_s, was calculated from the peak area of the thermograms. The degree of crystallinity, X_c, was calculated by:

$$X_c = 100 \times H_s / H_{100} \quad (1)$$

where H_{100} is the heat of fusion for the 100% crystalline PVDF sample (104.7 J/g) [23].

2.3.3 SEM morphology

The morphology of the top-side and bottom-side of the prepared membranes was observed using a scanning electron microscope (SEM) (Carl Zeiss Microscopy EVO Ma 10). The cross-section morphology of the membranes was also observed using an SEM (JSM-5600, JEOL). Cross-section samples were prepared by freeze fracture in liquid nitrogen. Before analysis by SEM, all samples were sputter-coated with a thin gold film to improve the imaging resolution, and to avoid electrical charging during the SEM observation.

2.3.4 Porosity

The overall porosity of the membrane, which is defined as the volumetric ratio of the voids to the entire membrane, was determined by the gravimetric method as described elsewhere [24-26]. The membrane weight in a dry state, M_d, was measured, and then the membrane was immersed in kerosene for 24 hours. After the excess kerosene was wiped off from the surface, the membrane weight in a fully-wet state, M_w, was measured. The porosity was calculated by:

$$\text{Porosity} = \frac{\dfrac{M_w - M_d}{\rho_k}}{\dfrac{M_w - M_d}{\rho_k} + \dfrac{M_d X_c}{100 \rho^{C}_{p}} + \dfrac{M_d (100 - X_c)}{100 \rho^{A}_{p}}} \times 100 \quad (2)$$

where ρ^{C}_{p} is the density of crystalline PVDF (1.92 g/cm^3) [23], ρ^{A}_{p} is the density of amorphous PVDF (1.68 g/cm^3) [23], and ρ_k is the density of kerosene (0.82 g/cm^3). The ρ^{C}_{p} is the value for α-phase crystals, because all membranes had α-phase crystals as mentioned in section 2.4.1.

2.3.5 Pore size

The pore size of the membranes was determined by using a PMI Capillary Flow Porometer (CFP 1500 AXEL, Porous Materials Inc., USA) as described elsewhere [25,26]. Membrane samples were immersed in a Porewick solution (its surface tension is 16 dyne/cm) for 24 hours to achieve full wetting, and were placed in the sealed chamber. Nitrogen gas (with increasing pressure over time) was supplied to one side of the sample in order to record the gas pressure and gas flow rate through the sample. The so-called "bubble point" corresponds to the pressure at which the first gas flow is detected. After the bubble point, the gas pressure increased until all pores were empty and the sample was considered to be dry. Gas pressure and flow rate for the dry samples were also recorded. This "wet-up/dry-up" mode was selected using the CapWIN software. Information relating to pore size and pore size distribution was determined based on Laplace's equation as follows:

$$d_P = 4 \sigma \cos \theta / P \quad (3)$$

where d_P is the pore diameter, σ is the surface tension of the liquid, θ is the contact angle of the liquid (assumed to be 0 in the case of fully wetting), and P is the external pressure.

2.3.6 Static contact angle

The static contact angle of water is defined as the angle between the membrane surface and the tangent line at the contact point of the water droplet on the membrane surface. The contact angles at room temperature were measured using an optical contact angle meter (CAM100, KSV Instruments) as described elsewhere [27]. A water droplet of 5 μL was placed on the top- or bottom-side surface of the membrane sample. The measurements were repeated in quintuplicate for each membrane, and the average value was reported.

2.3.7 Tensile properties

The mechanical properties of the membranes were measured using a ZWICK/ROELL Z 2.5 test unit at room temperature. Rectangular samples (1 × 5 cm) were extended at a constant elongation speed of 5 mm / min. Young's modulus (Emod), the tensile stress and elongation at breaking point were determined. The measurements were repeated in quintuplicate for each membrane, and the average value was reported.

2.3.8 Water flux

Water permeation experiments were conducted at room temperature using a stainless dead-end filtration cell (Model HP4750, supplied from Sterlitech Co.) with an effective permeation area of 20.4 cm^2. The membrane sample was submerged in purified water for 24 hours by putting it under a metallic stick to ensure complete wetting prior to measurement. The membrane was placed at the bottom of the cell, and the reservoir (300 mL) behind the membrane was filled with purified water. Transmembrane water flux was driven by applying pressure with nitrogen gas. The gas pressure was varied in the order of 1.0, 0.7 and 0.4 bar. Permeated water was collected, and its mass was recorded on a balance at the desired time intervals. Water flux, J_W, was calculated using the following equation:

$$J_W = W / \rho_w A t, \quad (4)$$

where W is the weight of permeated water (g), ρ_w is the density of water (1 g/cm^3), A is the permeation area (20.4 cm^2), and t is the permeation time (sec).

2.4 Results and discussion

2.4.1 Phase diagrams of PVDF/Citroflex systems

Several number of previous studies [15-16,18] have focused on the phase diagrams of PVDF solutions with relation to the cloud point temperature, at which a transparent polymer solution becomes more viscous and turbid. Cloudiness can occur in a solution of polymer due to separation between the polymer-lean and polymer-rich phases, and this process is known as liquid-liquid (L-L) phase separation. In our PVDF / Citroflex systems, no solutions became turbid until they began to form gels at the sol-gel transition temperature. Figure 1 shows the measured sol-gel transition temperatures for the three chosen Citroflex solvents as a function of PVDF concentration.

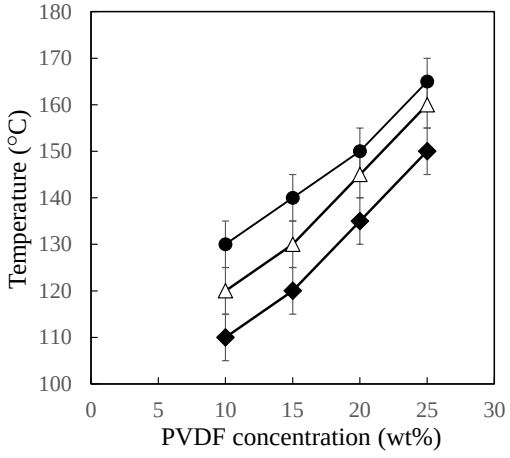

Figure 1. Sol-gel transition temperature of PVDF solutions with (●) ATBC, (△) ATEC, and (◆) TEC

For all solvents used in these studies, the sol-gel transition temperature increased with the PVDF concentration. This can be easily explained by the fact that a higher temperature is required to keep the polymer/solvent system homogeneous with increasing polymer concentration. At the same PVDF concentration, the sol-gel transition temperature decreased in the following solvent order of ATBC (130–165 °C) > ATEC (120–160 °C) > TEC (110–150 °C). It follows that the solvent miscibility with PVDF increases in the opposite order of ATBC < ATEC < TEC. The theory of Hansen solubility parameters [28] is often used to predict the solubility of a selected polymer in a range of solvents. In this theory, each molecule (polymer or solvent) is assumed to have three Hansen parameters, namely an atomic dispersive interaction (δ_d), a polar interaction (δ_p), and a hydrogen-bonding interaction (δ_h). The miscibility between the polymer and the solvent is related to the solubility parameter distance, R_a, calculated by the following equation [28]:

$$R_a = \left\{4\left(\delta_{d1} - \delta_{d2}\right)^2 + \left(\delta_{p1} - \delta_{p2}\right)^2 + \left(\delta_{h1} - \delta_{h2}\right)^2\right\}^{0.5} \quad (5)$$

where subscripts 1 and 2 denote the polymer and solvent, respectively. According to equation (5), the lower the value of R_a, the more soluble the polymer is in the selected solvent system. Table 2 shows the δ_d, δ_p, and δ_h values for PVDF and the three Citroflex solvents. Although the chosen Citroflex solvents have similar molecular structures, their Hansen parameters show a degree of variation.

Table 2. Hansen solubility parameters of PVDF and citroflex

Polymer or solvent	**δ_d (MPa$^{1/2}$)**	**δ_p (MPa$^{1/2}$)**	**δ_h (MPa$^{1/2}$)**	**R_a (MPa$^{1/2}$)**
PVDF	17.2[a]	12.5[a]	9.2[a]	–
ATBC	15.4[b]	4.1[b]	6.2[b]	9.6
ATEC	16.6[b]	3.5[b]	8.6[b]	9.1
TEC	16.5[b]	4.9[b]	12[b]	8.2

[a]REF. 29, [b]REF. 30.

For example, TEC shows the highest δ_h of 12 as it contains polar hydroxyl groups (–OH). The R_a between PVDF and Citroflex was calculated by equation (5), and also shown in Table 2. It can be seen that the R_a value decreased in the order of ATBC > ATEC > TEC, and it could therefore be predicted that the solubility of PVDF in each solvent was enhanced in the order of ATBC < ATEC < TEC, which agrees with the miscibility trend expected from the sol-gel transition temperature. Based on these results, it was worth examining how the structure and properties of the membranes were affected by the solvents with such different miscibility values.

2.4.2 Membrane morphology studies

- Crystal structure

As reported in literature [31], PVDF possesses at least four different crystalline phases, named α, β, γ and δ. Among these, the two most common polymorphs are the α (*trans*-gauche, TGTG') and β (all-*trans*, TTTT) phases. The α phase is a kinetically stable non-polar crystalline form with a monolithic lattice structure, whereas the β phase is a thermodynamically favoured polar form with an orthorhombic lattice structure [32]. The type of PVDF crystalline phase depends on the temperature of the solution before casting. The α phase usually forms at high temperature (>110 °C), while the β phase is formed exclusively at lower temperature (<70 °C) [33].

Figure 2 shows the FT-IR spectra of the PVDF / ATBC, PVDF / ATEC and PVDF / TEC membranes prepared in this study. For all membranes, characteristic peaks were observed at 409, 532, 764, 795, and 972 cm^{-1}, which are indicative of the α-phase of PVDF [19]. Accordingly, it was found that all the three kinds of Citroflex, *i.e.*, ATBC, ATEC, and TEC, induced the formation of α-phase PVDF.

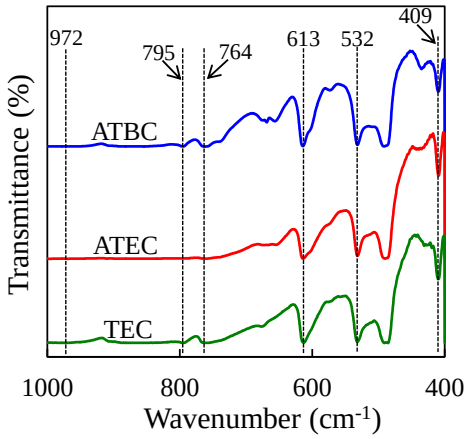

Figure 2. FT-IR spectra of PVDF membranes

Fig. 3 shows the DSC thermograms of the prepared PVDF membranes.

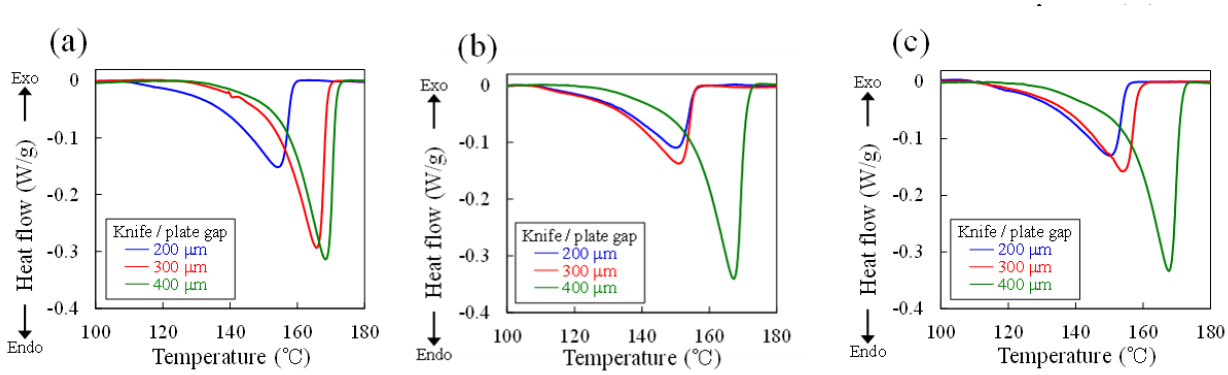

Figure 3. DSC thermograms of (a) PVDF/ATBC, (b) PVDF/ATBC, and (c) PVDF/TEC membranes

The endothermic peak temperature, H_s and X_c are listed in Table 3. For all solvent cases, the peak temperature and X_c increased as the gap between the casting knife and plate became wider. This means that the size of each crystal and the total amount of crystalline regions increased with the gap widening.

Table 3. The peak temperature, H_s, and X_c for the PVDF membranes

Solvent	Knife / plate gap (μm)	Peak temp. (°C)	H_s (J/g)	X_c (%)
ATBC	200	154	32.2	30.8
ATBC	300	166	44.3	42.3
ATBC	400	168	45.2	43.2
ATEC	200	150	24.9	23.8
ATEC	300	151	30.4	29.0
ATEC	400	167	54.2	51.8
TEC	200	150	27.4	26.1
TEC	300	154	32.1	30.7
TEC	400	167	53.6	51.2

- SEM morphology

The SEM analyses of the membranes prepared under a range of conditions are shown in Figs 4-6. The first comparison was made for the membranes prepared at the knife / plate gap of 400 μm (Figure 4(c), Figure 5(c), and Figure 6(c)) to examine the effect of solvents on the morphology.

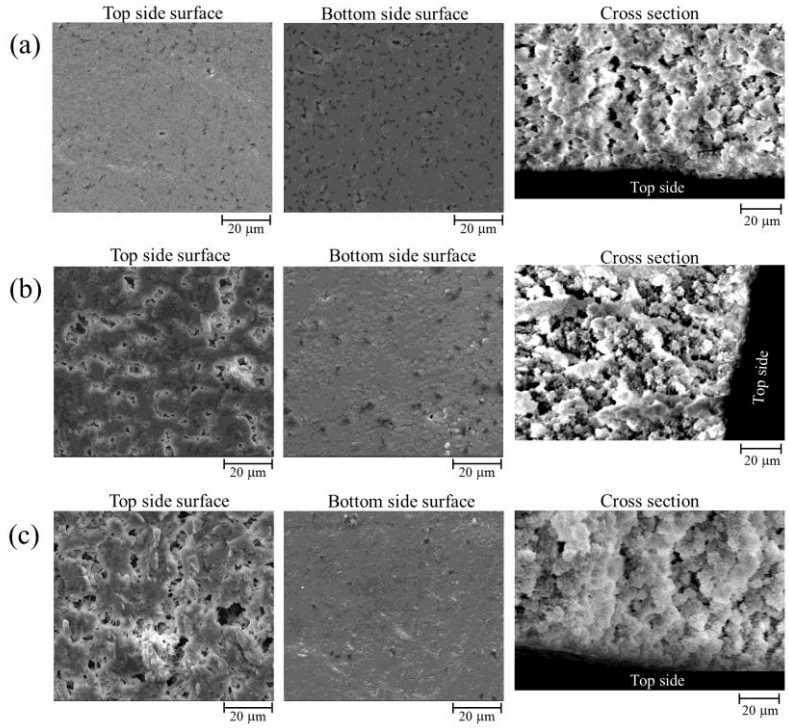

Figure 4. SEM photographs of membranes prepared from PVDF / ATBC solutions at the different knife / plate gap of (a) 200, (b) 300, and (c) 400 μm

For the PVDF / ATEC and PVDF / TEC membranes, it can be seen that spherulites are formed at both the top and bottom sides of the membranes, indicating the occurrence of the solid-liquid (S-L) phase separation. During the casting process, the polymer solution on the glass plate was cooled to 30 °C, which is significantly lower than the crystallization temperature of PVDF. The polymer chains aggregated each other to form a primary nucleus, to which further polymer chains moved by thermal diffusion to initiate crystallization. These polymer aggregations grew over time to become spherulites, composed of lamellar stacks of alternating crystalline and amorphous layers radiating from the nucleic center. On the other hand, in the case of PVDF / ATBC membranes, only fibrillar structures were observed instead of spherulites, suggesting that the system underwent an L-L phase separation and subsequent crystallization [34]. Cui *et al.* also observed that this L-L phase separation took place in PVDF / ATBC systems at PVDF concentration lower than 24wt% [19]. According to the TIPS mechanism [35], S-L phase separation occurs if the compatibility between the polymer and the solvent is high, whereas L-L phase separation occurs if this compatibility is low. Since ATBC has lower affinity with PVDF compared to ATEC and TEC, as shown by the sol-gel transition temperature (section 3.1), it should cause L-L phase separation in the solution system.

For the PVDF / ATBC membranes prepared at the knife / plate gap of 400 μm, it can be seen that the top-side and bottom-side surfaces are porous and considerably dense, respectively. The observed asymmetric structure can be explained by taking into account the difference in the cooling speed of

the polymeric solution during the casting process. The bottom side of the nascent membrane was in direct contact with the glass plate at 30 °C and underwent fast cooling. Polymer chains were thought to be immediately phase separated from solvent molecules to gather with each other. Additional polymer chains that happened to approach the bottom side by thermal diffusion presumably lost the molecular mobility due to low temperature, and then began to be aggregated together, excluding solvent molecules. Such a fast phase separation behavior should increase the local polymer concentration to make the bottom surface dense. Solvent molecules rejected from the polymer phase were forced to vertically ascend to the upper regions. In contrast to the bottom side, the cooling speed of the top side was quite slow, since it was exposed to the air, whose thermal conductivity was far lower than that of the glass plate. Consequently, it is expected that solvent molecules were accumulated in the top side to decrease the local polymer concentration, thereby producing the porous top surface. A similar morphology of a porous top surface and dense bottom surface has been previously reported in studies on the preparation of ECTFE membranes *via* the TIPS process [36,37].

It is seen from Figs. 4(a)-(c) that the top side surface of the PVDF / ATBC membranes became less porous as the knife / plate gap was reduced. As mentioned above, the formation of the porous top surface was related to the slower cooling speed in comparison with the bottom side. When the membrane was thinner, the cooling speed of the top side was faster and closer to that of the bottom side due to the enhanced transmembrane thermal conduction. In other words, the thinner membrane was more homogeneously cooled in whole, producing the less porous top surface. At the narrowest gap of 200 μm, the top side and bottom side surfaces looked alike each other, which may be caused by the almost same cooling speed at the both sides.

Unlike the PVDF / ATBC membranes, the PVDF / ATEC and PVDF / TEC ones prepared at the knife/plate gap of 400 μm did not have the dense skin surface at the bottom side (Figure 5(c) and Figure 6(c)).

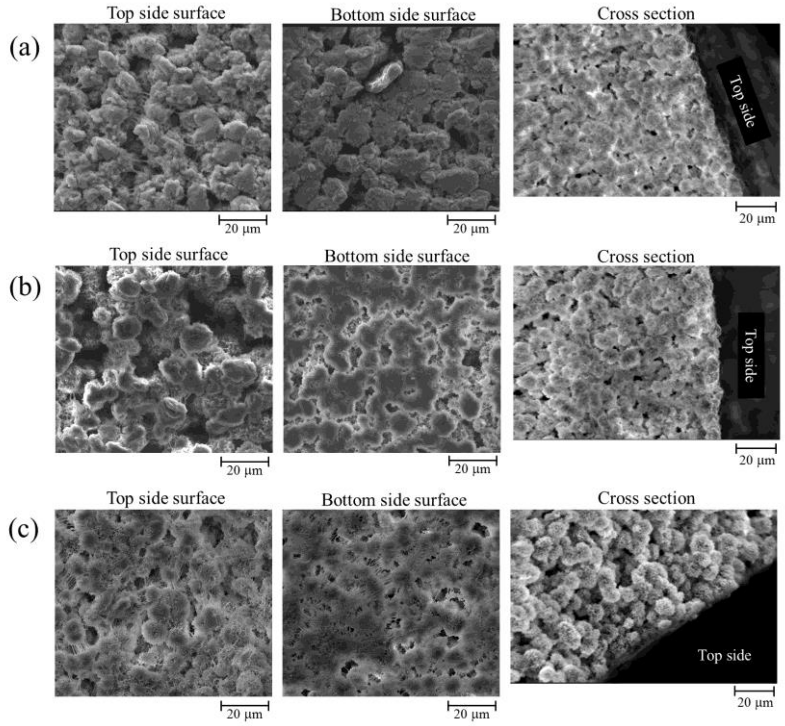

Figure 5. SEM photographs of membranes prepared from PVDF / ATEC solutions at the different knife / plate gap of (a) 200, (b) 300, and (c) 400 μm.

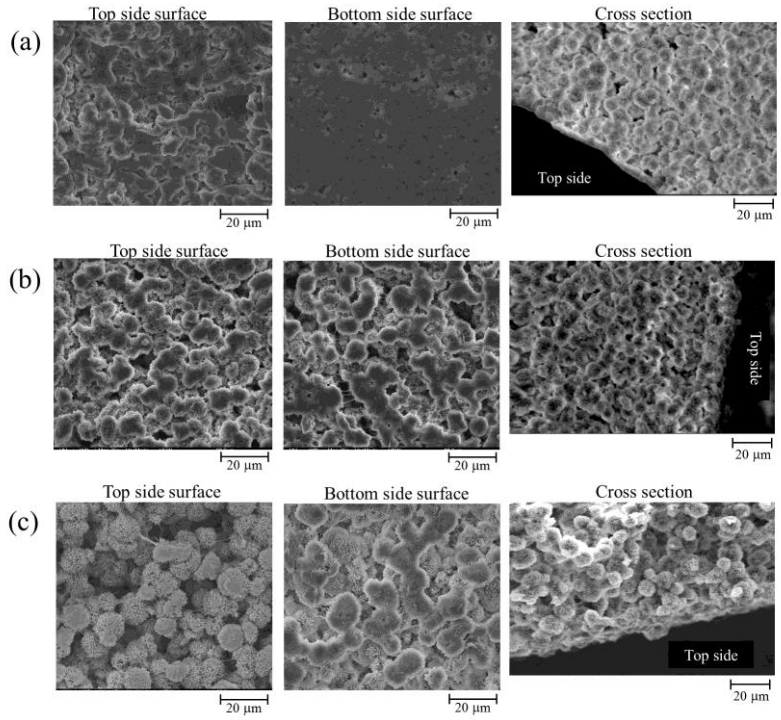

Figure 6. SEM photographs of membranes prepared from PVDF / TEC solutions at the different knife plate gap of (a) 200, (b) 300, and (c) 400 μm

This result can be related to the fact that ATEC and TEC were better solvents for PVDF than ATBC, as mentioned in section 3.1. In both the ATEC and TEC cases, even in the fast-cooled bottom side, polymer chains may keep their molecular mobility at a certain degree because of the high

polymer/solvent miscibility. As a consequence, the phase separation throughout the membrane probably occurred at the similar speed, making the both top- and bottom-side surfaces porous. The avoidance of formation of the dense skin layer is an advantage when using ATEC and TEC as solvents. When the gap was narrowed from 400 to 200 μm, the spherulites looked less prominent, and their size tended to be smaller (seen in the cross section images of Figs 5-6). The gap narrowing quickened the cooling of the whole membrane and gave a polymer solution shorter time for phase separation to form spherulites. This result was in consistent with the DSC data in Table 3 (*i.e.*, the membranes prepared at the narrower gap showed the lower X_c.). It was noted that the PVDF/TEC membrane prepared at 200-μm gap seemed to have almost no spherulites (especially in the bottom side). This membrane with the lowest thickness of only 90 μm (see Table 4) was cooled at the fastest speed, and so the phase separation would be significantly restricted.

2.4.3 Membrane properties

- Pore structure

Table 4 shows the thickness, porosity, mean pore size, and contact angle of the prepared PVDF membranes.

Table 4. Properties of prepared PVDF membranes

SOLVENT	KNIFE/PLATE GAP (μm)	THICKNESS (μm)	POROSITY (%)	MEAN PORE SIZE (μm)	CONTACT ANGLE (Top side)	CONTACT ANGLE (Bottom side)
ATBC	200	97 ± 5	57.7 ± 0.3	0.86	102 ± 2	89 ± 6
ATBC	300	116 ± 6	58.9 ± 0.2	0.82	106 ± 8	82 ± 3
ATBC	400	137 ± 8	65.9 ± 0.3	0.93	123 ± 7	98 ± 8
ATEC	200	94 ± 10	53.2 ± 0.2	2.44	112 ± 5	104 ± 5
ATEC	300	112 ± 5	56.9 ± 0.3	2.88	116 ± 4	104 ± 3
ATEC	400	149 ± 4	76.0 ± 0.7	2.98	123 ± 3	112 ± 3
TEC	200	90 ± 6	52.3 ± 0.4	3.90	123 ± 5	99 ± 4
TEC	300	125 ± 3	56.1 ± 3.0	4.29	120 ± 2	104 ± 5
TEC	400	157 ± 9	75.5 ± 1.2	7.24	125 ± 6	111 ± 5

For all the cases, the thickness was significantly lower than the knife / plate gap due to evaporation of solvent from the nascent membrane cast on the plate. The pore size obviously increased in the following order of solvent: ATBC < ATEC < TEC. For example, at the gap of 400 μm, the pore sizes were 0.93 μm (ATBC), 2.98 μm (ATEC) and 7.24 μm (TEC), respectively. This pore size trend is in consistent with the order of the PVDF / solvent miscibility shown in Figure 1, and can be explained based on the TIPS mechanism [38,39]. For the TEC case, as discussed in section 3.2, a high PVDF / TEC miscibility resulted in remarkable S-L phase separation. Simultaneously with the spherulite

formation, TEC molecules gathered to form solvent-rich regions that turned into large pores after solvent extraction. For the ATEC case, a lower PVDF / ATEC miscibility resulted in a more viscous solution, retarding the molecular mobility of polymer and solvents. The formation of spherulites and solvent-rich regions was a little restricted, thereby producing smaller pores, as well as smaller spherulites. Moreover, for the ATBC case, the TIPS mechanism shifted to the L-L phase separation due to the lowest PVDF / ATBC miscibility. ATBC molecules had less time to aggregate with each other, leading to formation of very small pores. This pore-size trend is in agreement with the work of Su *et al* [40]., who prepared PVDF membranes *via* TIPS using four types of solvents: γ-butyrolactone (γ-BL); propylene carbonate (PC); DBP; and dibutyl sebacate (KD). The membrane pore size was reduced by changing the solvents from γ-BL and PC (higher miscibility with PVDF) to DBP and KD (lower miscibility with PVDF). In contrast to their qualitative discussion based on only SEM observation, we quantitatively reported the effect of solvent on the pore size, leading to a better understanding of pore formation *via* TIPS.

At the knife/plate gap of 400 μm, the PVDF/ATBC membrane showed the porosity of 65.9%, while the PVDF/ATEC and PVDF/TEC membranes showed the higher porosity of 76.0% and 75.5%, respectively. During the casting process, parts of the solvents can reach the top side surface and be expelled to the outside of the membrane. Accordingly, the porosity corresponds to the total amount of the remaining solvents inside the membrane. Since ATBC had the lowest miscibility with PVDF, ATBC were relatively easily expelled to the outside (low porosity). On the other hand, ATEC and TEC with higher miscibility likely remained inside the membrane (high porosity).

When the knife/plate gap was wider, an increase in both porosity and pore size was observed, especially for the ATEC and TEC cases. The enlargement in the knife/plate gap presumably caused the two effects. The first effect is that solvents were unable to easily reach the top side surface owing to the greater distance to move. The amount of solvents remaining inside the membrane increased, leading to an increase in porosity. The second effect is that the cooling speed throughout the membrane was slow due to low vertical thermal conduction. The polymer/solvent phase separation took place over a longer period of time, resulting in an increase in pore size. To the best of our knowledge, our study reported in detail for the first time that the pore structure was significantly influenced by the knife / plate gap in the TIPS membrane preparation.

- Contact angle

The measured contact angle of a sessile droplet, θ_m, is related to the roughness of the surface by the following equation [41]:

$$\cos\theta_m = r\cos\theta_y \quad (6)$$

where r is the ratio of the actual to projected surface area (r = 1 for a smooth surface and r > 1 for a rough surface), and θ_y is the Young contact angle, which is equal to θ_m if r = 1. From equation (6), we can determine that the greater the roughness of the surface, the higher the measured contact angle is. This relationship is useful for analyzing the contact angle data. As shown in Table 4, the contact angle measured on the top side surface was higher than that on the bottom side surface for all membranes. This suggests that the top side surface was somewhat more porous and rough than the bottom side surface as shown in Figs. 4-6. The PVDF / ATBC membranes showed the lowest contact angle of 82 – 98 ° at the bottom side surface, which is in agreement with the dense and flat surface observed by SEM (see Figure 4). The reason for formation of porous top and dense bottom sides is due to the different cooling speed of the two polymeric film surfaces after casting, as discussed in section 2.3.2.

- Tensile properties

Table 5 shows the tensile properties of the prepared membranes. One notable point is that the Emod of the PVDF / ATBC membranes are 2-times or more higher than that of the other two membranes. This can be explained by taking into account that the PVDF / ATBC membranes had the smallest pore sizes amongst all the prepared membranes.

Table 5. Tensile properties of PVDF membranes

SOLVENT	KNIFE/PLATE GAP (μm)	Emod (N/mm^2)	TENSILE STRENGTH (MPa)	ELONGATION AT BREAK (%)
ATBC	200	16,5 ± 1,3	0,58 ± 0,07	38,5 ± 5,2
ATBC	300	14,1 ± 1,4	0,39 ± 0,05	35,9 ± 3,2
ATBC	400	16,0 ± 1,4	0,36 ± 0,04	23,4 ± 3,9
ATEC	200	6,4 ± 0,5	0,47 ± 0,04	58,1 ± 9,6
ATEC	300	6,2 ± 0,6	0,46 ± 0,05	53,7 ± 5,3
ATEC	400	6,5 ± 0,6	0,31 ± 0,02	32,3 ± 3,6
TEC	200	6,9 ± 0,4	0,42 ± 0,02	52,4 ± 4,1
TEC	300	6,4 ± 1,3	0,44 ± 0,07	42,9 ± 8,9
TEC	400	6,0 ± 1.2	0,26 ± 0,02	26,7 ± 3,1

The tensile strength and elongation at breaking point did not strongly depend on the identity of the solvent used in the membrane preparation process, but decreased as the thickness of the membranes increased. This is consistent with the result that the porosity and mean pore size increased with the membrane thickness (see Table 4). For the thick membrane, highly porous structures would make the samples more fragile, reducing the tensile strength and elongation at breaking point.

- Water flux

For all the membranes, the amount of permeated water increased proportionally with time at every water supply pressure, indicating the continuous porous structure to transport water through the membrane. As shown in Figure 7, the J_W of the membranes was linearly raised with increasing the water supply pressure.

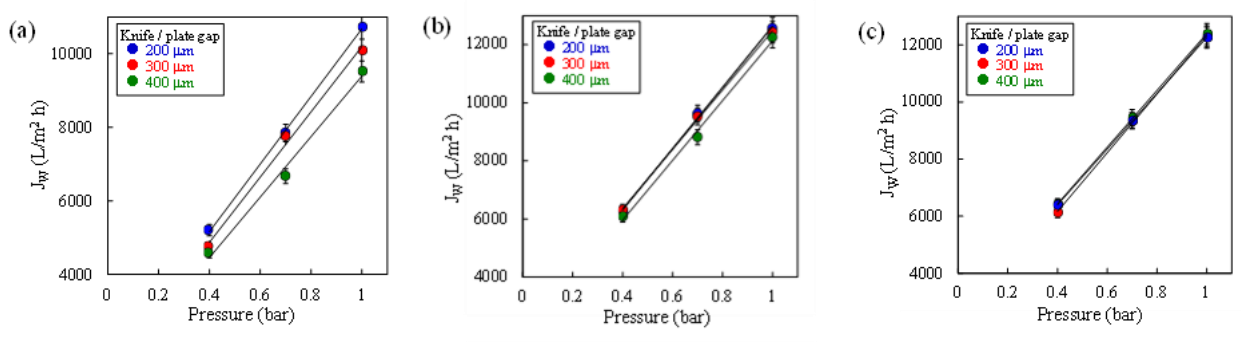

Figure 7. J_W of the PVDF membranes prepared from (a) PVDF / ATBC, (b) PVDF / ATEC, and (c) PVDF/TEC systems

This means that the pore structure is stable and unchanged regardless of the pressure, which should be due to enough mechanical strength of the membranes suggested in section 3.3.3. If the membranes had had poorer mechanical property, high pressure would have caused the collapse of the porous structures to merge plural inside pores into larger ones. If so, the J_W would have been abnormally high at the high pressure, deviating from the linear relationship (this is not the case with our membranes). The data plots shown in Figure 7 were fit to a straight line using the least squares regression method. The water permeability of the membrane, P_W, corresponding to the slope of the line, is listed in Table 6.

Table 6. Water permeation properties of PVDF membranes

SOLVENT	KNIFE/PLATE GAP (µm)	P_W ($\times 10^3$ L / m^2 h bar)	P_W^t (L m / m^2 h bar)
ATBC	200	9,20 ± 0,28	0,89 ± 0,03
ATBC	300	8,87 ± 0,27	1,03 ± 0,03
ATBC	400	8,23 ± 0,25	1,13 ± 0,03
ATEC	200	10,54 ± 0,32	0,99 ± 0,03
ATEC	300	10,20 ± 0,31	1,14 ± 0,03
ATEC	400	10,29 ± 0,31	1,53 ± 0,05
TEC	200	9,77 ± 0,29	0,88 ± 0,03
TEC	300	10,29 ± 0,31	1,29 ± 0,04
TEC	400	9,95 ± 0,30	1,56 ± 0,05

In order to fairly compare the water flux for all the membranes, the effect of the thickness should be obviated. Then, the thickness-normalized water permeability, P_W^t, was calculated by multiplying the P_W with the membrane thickness, and listed in Table 6.

Based on the Hagen-Poiseuille flow, the P_W^t through a material is expressed as follows:

$$P_W^t = \frac{\varepsilon r_p^{\,2}}{8\eta\tau} \qquad (7)$$

where ε is the porosity of the material, r_p is the pore radius, η is the dynamic viscosity of water, and τ is the tortuosity of the water transport pathways. The τ value represents the degree of geometrical complexity of the water transport pathways, which are not perfectly straight but curved and branched. The τ is defined as L / material thickness, where L is the actual average length travelled by water from the feed side to the permeate side. As expressed in Equation (7), the P_W^t is determined by the three factors, ε, r_p, and τ.

As shown in Table 6, the thicker membranes (prepared at a wider knife / plate gap) enhanced the P_W^t. This could be because the porosity and pore size increased with the membrane thickness, as already reported in Table 4. The results from these measurements were then compared with literature data reported by Cui *et al* [19], who performed the water flux test of the PVDF / ATBC membranes prepared at a knife / plate gap of 400 μm. At a polymer concentration of 15wt%, the J_W was reported to be 1550 $L/m^2 h$ (at 0.5 bar), 3200 $L/m^2 h$ (at 1.0 bar), 4700 $L/m^2 h$ (at 1.5 bar), respectively. Since the thickness was 186 μm, the P_W^t of Cui's membrane was calculated to be 0.59 $L\,m/m^2\,h\,bar$. This value is somewhat lower than the P_W^t for our PVDF / ATBC membrane, due to the smaller pore size of Cui's membrane.

Furthermore, at the same knife / plate gap, the P_W^t depended on the type of solvent used. With a gap of 300 μm, the P_W^t was 1.03 $L\,m/m^2\,h\,bar$ (ATBC), 1.14 $L\,m/m^2\,h\,bar$ (ATEC) and 1.29 $L\,m/m^2\,h\,bar$ (TEC), respectively. Since these three membranes have similar porosity (56.1 – 58.9%), the increase in P_W^t was mainly caused by the enlargement of the pore size: ATBC (0.82 μm) < ATEC (2.88 μm) < TEC (4.29 μm). However, it is noteworthy that the P_W^t of the PVDF / ATBC and PVDF / ATEC membranes did not differ to a great extent even though the latter membrane had about 3.5–times larger pores than the former one. According to Equation (7), the P_W^t increases twelvefold if the r_p increases by 3.5 times. Contrary to this estimation, the P_W^t of the PVDF / ATEC membrane was only 1.1–times higher than that of the PVDF / ATBC one. This result could be justified by considering the following two factors that relatively increased the P_W^t of the PVDF / ATBC membranes. The first

factor is the τ, the geometrical complexity of water transport pathways. Recall that ATBC induced L–L phase separation, while ATEC and TEC induced S–L phase separation. L–L phase separation was assumed to produce the bicontinuous porous structures [15,16,18] for smooth water transportation. This resulted in a lower τ for the PVDF / ATBC membranes, leading to the increase in the P_W^t. The second factor is the contact angle of the membranes. In this water flux test, the bottom side of the membrane was contacted to the supplied water. Namely, the bottom and top sides are the feed and permeate sides, respectively. The PVDF / ATBC membranes had the flattest surface with the lowest contact angle, compared with the PVDF / ATEC and PVDF / TEC ones. Accordingly, water can smoothly enter into the PVDF / ATBC membranes for permeation, thereby increasing the P_W^t. From the results of our study it was revealed that the type of Citroflex solvent used, as well as the knife / plate gap, significantly affected the porous structures of the prepared membranes, making it possible to widely control their P_W^t values.

2.5 Conclusions

In this study, we successfully prepared flat PVDF membranes *via* TIPS using three non-toxic Citroflex solvents, namely ATBC, ATEC, and TEC. From the results obtained during these studies we could conclude the following:

- Sol-gel transition temperature measurements revealed that the three solvents had different miscibility with PVDF, which increased in the order of ATBC < ATEC < TEC. This miscibility trend coincides with that predicted by Hansen solubility theory.

- SEM analysis showed that the formation of spherulites was observed in the PVDF / ATEC and PVDF / TEC membranes, indicating S-L phase separation during the casting process. In contrast, the PVDF / ATBC membranes formed only fibrillar structures, indicating L-L phase separation.

- Pore size of the membranes increased in the solvent order of ATBC < ATEC < TEC. Both pore size and porosity increased with a wider knife / plate gap. The dependence of the pore structures on the solvent and knife / plate gap was explained by taking into account the phase separation behavior during the membrane casting.

- For all the membranes prepared in this study, the P_W^t also varied with both the solvent type and the knife / plate gap. The result of P_W^t can be explained by taking into account the porosity, pore size, and the tortuosity of water transport pathways.

This work therefore demonstrates how a detailed analysis of membrane preparation using non-toxic solvents can lead to interesting and useful results, which proves the feasibility of the replacement of more toxic solvents in the membrane preparation. Finally, the application of the produced membranes in microfiltration has also the aim of increasing the sustainability and reducing the environmental impact of human activities.

References

[1] A. Bottino, G. Capannelli, A. Comite, F. Ferrari, R. Firpo, S. Venzano, Membrane technologies for water treatment and agroindustrial sectors, Comptes Rendus Chimie. 12 (2009) 882-888. doi.10.1016/j.crci.2008.06.021

[2] A.G. Fane, C.Y. Tang, R. Wang, Membrane Technology for Water: Microfiltration, Ultrafiltration, Nanofiltration, and Reverse Osmosis, Treatise on Water Science, Chapter 4.11 (2011) 301-335.

[3] G. Szekely, M. Jimenez-Solomon, P. Marchetti, J. Kim, A. Livingston, Sustainability assessment of organic solvent nanofiltration: from fabrication to application, Green Chemistry. 16 (2014) 4440-4473. doi.10.1039/C4GC00701H

[4] E. Drioli, F. Macedonio, Membrane Engineering for Water Engineering, Industrial & Engeneering Chemistry Research. 51 (2012) 10051-10056. doi.10.1021/ie2028188

[5] F. Liu, N. A. Hashim, Y. Liu, M. R. Moghareh Abed, K. Li, Progress in the production and modification of PVDF membranes, Journal of Membrane Science. 375 (2011) 1-27. doi. 10.1016/j.memsci.2011.03.014

[6] Z. Cui, E. Drioli, Y. M. Lee, Recent progress in fluoropolymers for membranes, Progress in Polymer Science. 39 (2014) 164-198. doi.org/10.1016/j.progpolymsci.2013.07.008

[7] G. D. Kang, Y. M. Cao, Application and modification of poly(vinylidene fluoride) (PVDF) membranes – A review, Journal of Membrane Science. 463 (2014) 145-165. doi.10.1016/j.memsci.2014.03.055

[8] M. Gu, J. Zhang, X. Wang, W. Ma, Crystallization Behavior of PVDF in PVDF-DMP System via Thermally Induced Phase Separation, Journal of Applied Polymer Science. 102 (2006) 3714-3719. doi.10.1002/app.24531

[9] M. Gu, J. Zhang, X. Wang, H. Tao, L. Ge, Formation of poly(vinylidene fluoride) (PVDF) membranes via thermally induced phase separation, Desalination. 192 (2006) 160-167. doi.10.1016/j.desal.2005.10.015

[10] S. Rajabzadeh, C. Liang, Y. Ohmukai, T. Maruyama, H. Matsuyama, Effect of additives on the morphology and properties of poly(vinylidene fluoride) blend hollow fiber membrane prepared by the thermally induced phase separation method, Journal of Membrane Science. 423-424 (2012) 189-194. doi.10.1016/j.memsci.2012.08.013

[11] Y. Su, C. Chen, Y. Li, J. Li, Preparation of PVDF Membranes via TIPS Method: The Effect of Mixed Diluents on Membrane Structure and Mechanical Property, Journal of Macromolecular Science, Part A: Pure and Applied Chemistry. 44 (2007) 305-313. doi.10.1080/10601320601077741

[12] X. Lu, X, Li, Preparation of Polyvinylidene Fluoride Membrane Via a Thermally Induced Phase Separation Using a Mixed Diluent, Journal of Applied Polymer Science. 114 (2009) 1213-1219. doi.10.1002/app.30184

[13] A. J. Martino Andrade, I. Chahoud, Reproductive toxicity of phthalate esters, Molecular Nutrition & Food Research. 54 (2010) 148-157. doi.10.1002/mnfr.200800312

[14] A. Figoli, T. Marino, S. Simone, E. Di Nicolò, X.M. Li, T. He, S. Tornaghi, E. Drioli, Towards non-toxic solvents for membrane preparation: a review, Green Chemistry. 16 (2014) 4034-4059. doi.10.1039/C4GC00613E

[15] J. Yang, D. W. Li, Y. K. Lin, X. L. Wang, F. Tian, Z. Wang, Formation of a Bicontinuous Structure Membrane of Polyvinylidene Fluoride in Diphenyl Ketone Diluent Via Thermally Induced Phase Separation, Journal of Applied Polymer Science. 110 (2008) 341-347. doi.10.1002/app.28606

[16] Y. Lin, Y. Tang, H. Ma, J. Yang, Y. Tian, W. Ma, X. Wang, Formation of a Bicontinuous Structure Membrane of Polyvinylidene Fluoride in Diphenyl Carbonate Diluent Via Thermally Induced Phase Separation, Journal of Applied Polymer Science. 114 (2009) 1523-1528. doi. 10.1002/app.30622

[17] P. Guiot, M. Ryan, S. Kennedy, Citrate plasticized resins in healthcare, Manufactoring Chemistry. 69 (1998) 27-34.

[18] M. Liu, Z. Xu, D. Chen, Y. Wei, Preparation and characterization of microporous PVDF membrane by thermally induced phase separation from a ternary polymer / solvent / non-solvent systems, Desalination Water Treatment. 17 (2010) 183-192. doi.10.5004/dwt.2010.1716

[19] Z. Cui, N. T. Hassankiadeh, S. Y. Lee, J. M. Lee, K. T. Woo, A. Sanguineti, V. Arcella, Y. M. Lee, E. Drioli, Poly(vinylidene fluoride) membrane preparation with an environmental diluent *via* thermally induced phase separation, Journal of Membrane Science. 444 (2013) 223-236. doi.10.1016/j.memsci.2013.05.031

[20] N. Hassankiadeh, Z. Cui, J. H. Kim, D. W. Shin, A. Sanguineti, V. Arcella, Y. M. Lee, E. Drioli, PVDF hollow fiber membranes prepared from green diluent via thermally induced phase separation: Effect of PVDF moleculr weight, Journal of Membrane Science. 471 (2014) 237-246. doi.10.1016/j.memsci.2014.07.060

[21] D. Mullette and H.J. Muller, Halar membranes, US Pat, 0098494 (2005).

[22] M. Finkelstein, H. Gold, Toxicology of the Citric Acid Esters: Tributyl Citrate, Acetyl Tributyl Citrate, Triethyl Citrate, and Acetyl Triethyl Citrate, Toxicology and Applied Pharmacology. 1 (1959) 283-298. doi.10.1016/0041-008X(59)90113-9

[23] Z. Zhudi, Y. Wenxue, C. Xinfang, Study on increase in crystallinity in γ-irradiated poly(vinylidene fluoride), Radiation Physics and Chemistry. 65 (2002) 173-176. doi.10.1016/S0969-806X(02)00194-9

[24] C. Feng, B. Shi, G. Li, Y. Wu, Preparation and properties of microporous membrane from poly(vinylidene fluoride-co-tetrafluoroethylene) (F2.4) for membrane distillation, Journal of Membrane Science. 237 (2004) 15-24. doi.10.1016/j.memsci.2004.02.007

[25] S. Simone, A. Figoli, A. Criscuoli, M.C. Carnevale, A. Rosselli, E. Drioli, Preparation of hollow fibre membranes from PVDF/PVP blends and their application in VMD, Journal of Membrane Science. 364 (2010) 219-232. doi.10.1016/j.memsci.2010.08.013

[26] E. Drioli, A. Ali, S. Simone, F. Macedonio, S.A. Al-Jlil, F.S. Shabonah, H.S. Al-Romaih, O. Al-Harbi, A. Figoli, A. Criscuoli, Novel PVDF hollow fiber membranes for vacuum and direct contact membrane distillation applications, Separation and Purification Technology. 115 (2013) 27-38. doi.10.1016/j.seppur.2013.04.040

[27] S. Simone, A. Figoli, S. Santoro, F. Galiano, S.M. Alfadul, O.A.Al-Harbi, E. Drioli, Preparation and characterization of ECTFE solvent resistant membranes and their application in pervaporation of toluene/water mixtures, Separation and Purification Technology. 90 (2012) 147-161. doi.10.1016/j.seppur.2012.02.022

[28] C. M. Hansen, The three dimensional solubility parameter and solvent diffusion coefficient, Ph. D. Thesis, Danish Technical Press 1967.

[29] J. Brandrup, E.H. Immergut, E.A. Grulke, Polymer Handbook, 4th Ed., Wiley, New York (1999).

[30] C. Hansen, Hansen Solubility Parameters: A User's Handbook, CRC Press, Boca Raton, FL, USA (2007).

[31] W. Ma, J. Zhang, S. Chen, X. Wang, Crystalline Phase Formation of Poly(vinylidene fluoride) from Tetrahydrofuran / N,N-dimethylformamide Mixed Solutions, Journal of Macromolecular Science, Part B: Physics. 47 (2008) 434-449.

[32] Y.K. Ong, N. Widjojo, T.S. Chung, Fundamentals of semi-crystalline poly(vinylidene fluoride) membrane formation and its prospects for biofuel (ethanol and acetone) separation via pervaporation, Journal of Membrane Science. 378 (2011) 149-162. doi.10.1016/j.memsci.2011.04.037

[33] R. Gregorio, Determination of the α, β, and γ Crystalline Phases of Poly(vinylidene fluoride) Films Prepared at Different Conditions, Journal of Applied Polymer Science. 100 (2006) 3272-3279. doi.10.1002/app.23137

[34] Z. Cui, N.T. Hassankiadeh, S.Y. Lee, K.T. Woo, J.M. Lee, A. Sanguineti, V. Arcella, Y.M. Lee, E. Drioli, Tailoring novel fibrillar morphologies in poly(vinylidene fluoride)

membranes using a low toxic triethylene glycol diacetate (TEGDA) diluent, Journal of Membrane Science. 473 (2015) 128-136.doi.10.1016/j.memsci.2014.09.019

[35] D.R. Lloyd, S.S. Kim, K.E. Kinzer, Microporous membrane formation via thermally-induced phase separation. II. Liquid-liquid phase separation, Journal of Membrane Science. 64 (1991) 1-11. doi.10.1016/0376-7388(91)80073-F

[36] S. Ramaswamy, A.R. Greenberg, W.B. Krantz, Fabrication of poly (ECTFE) membranes via thermally induced phase separation, Journal of Membrane Science. 210 (2002) 175-180.

[37] J. Roh, S. Ramaswamy, W.B. Krantz, A.R. Greenberg, Poly(ethylene chlorotrifluoroethylene) membrane formation via thermally induced phase separation (TIPS). Journal of Membrane Science. 362 (2010) 211-220. doi.10.1016/j.memsci.2010.06.042

[38] S.S. Kim, G.B.A Lim, A.A. Alwattari, Y.F. Wang, D.R. Lloyd, Microporous membrane formation via thermally-induced phase separation. V. Effect of diluent mobility and crystallization on the structure of isotactic polypropylene membranes, Journal of Membrane Science. 64 (1991) 41-53. doi.10.1016/0376-7388(91)80076-I

[39] K.S. Mcguire, D.R. Lloyd, G.B.A Lim, Microporous membrane formation via thermally-induced phase separation. VII. Effect of dilution, cooling rate, and nucleating agent addition on morphology, Journal of Membrane Science. 79 (1993) 27-34.doi.10.1016/0376-7388(93)85015-O

[40] Y. Su, C. Chen, Y. Li, J. Li, Preparation of PVDF membranes via TIPS method: The effect of mixed diluents on membrane structure and mechanical property, Journal of Macromolecular Science, Part A: Pure and Applied Chemistry. 44 (2007) 305-313. doi.10.1080/10601320601077419

[41] R.N. Wenzel, Resistance of solid surfaces to wetting by water, Industrial & Engineering Chemistry. 28 (1936) 988-994.

Chapter 3.

Innovative hydrophobic coating of perfluoropolyether (PFPE) on commercial hydrophilic membranes for DCMD application

3.1 Introduction

Fluoropolymers are defined as a class of polymers containing carbon (C) and fluoride (F) atoms. Partially fluorinated fluoropolymers contain hydrogen (H) or other atoms such as chlorine (Cl), other than C and F. The presence of F provides a wide number of properties such as high thermal and chemical stability, increased solvent resistance, photostability, high oxidation resistance and lower surface tension (as evidenced by the high repellence towards water) [1-2]. The outstanding properties exhibited by fluorinated polymers can be referred to the high electronegativity of the F atom, to the low polarizability and to the strong C-F bond induced by the small Van der Waals radius (1.32 Å).

The most common fluoropolymers available on the market derive from three main monomers: tetrafluoroethylene (TFE), vinylidene fluoride (VDF), and chlorotrifluoroethylene (CTFE) [3]. Polytetrafluoroethylene (PTFE) was the first fluoropolymer discovered in 1938 (marketed under the DuPont Teflon® trademark), and, from that time on, a wide number of fluoropolymers such as polyvinylidene fluoride (PVDF), ethylene chlorotrifluoroethylene (ECTFE) and perfluoroalkoxy (PFA) have been produced. Nowadays, fluoropolymers represent the preferred choice in a vast area of applications ranging from the building (paint and coatings) and the medical (diagnostic devices) industry, to the petrochemical, chemical (pumps, diaphragms), aerospace and automotive industry (O-rings, gaskets) [4]. Due to their excellent properties, fluorinated polymers, have found a large application, also, as membrane materials. In particular, PVDF, thanks to the combination of easy processability and superior properties (due to the high level of crystallinity) has been widely used in membrane preparation in numerous processes such as microfiltration (MF), ultrafiltration (UF), pervaporation (PV) and membrane distillation (MD) [5].

Among the family of fluoropolymers, ECTFE, due to its high resistance to corrosive chemicals, organic solvents and oxidizing agents, is considered as a very promising material for the preparation of membranes functioning under harsh conditions [6-7]. Moreover, thanks to its very hydrophobic behaviour, ECTFE porous membranes, have been applied in MD. As a consequence of the increasing demand for materials with outstanding properties in terms of resistance and durability, advances in polymer technology resulted in the production of novel materials able to overcome some of the limitations presented by the traditional fluoropolymers. In this direction, a new class of perfluoropolyethers (PFPEs) based compounds has been developed. PFPEs are a class of fluorinated

oligomers characterised by perfluorinated carbon units, as $–CF_2-$ and $-CF_2-CF_2-$, separated by oxygen atoms [8]. The use of PFPEs for coatings is considered a very attractive technology for the modification of surfaces. In fact, their peculiar characteristics such as high thermal and chemical stability, low friction coefficient in addition with their high degree of hydrophobicity, makes them highly appreciated when harsh and specific performances are requested. Moreover, PFPEs, are soluble in common organic solvents and curable at high or room temperature [9].

Bongiovanni et al. [10], for instance, explored the possibility of using two PFPEs bisurethane methacrylates as novel additives for the preparation of UV-cured acrylic films. In another recent work, Oldani et al. [11] performed a coating of functionalised PFPEs on a film of ceramic oxide nanoparticles for the improvement of surface anti-fouling properties.

During the last two decades, an increasing demand of fluorinated compounds (fluoropolymers, fluorinated fluids and fluoroelastomers) has been observed and it is expected to further grow in the coming years [12]. A new generation of UV-curable PFPE-(meth)acrylate resins (Fluorolink®) has been developed by Solvay Specialty Polymers and specifically designed for the modification of surfaces (paper, textile, membranes) and as additives for various polymers. Fluorolink® MD 700, for instance, was successfully used by Bertolotti et al. [13] in an interpenetrating polymer network for the production of anion exchange membranes to protect air electrodes functioning in aqueous lithium-air battery configuration. In a recent patent by Sanguineti et al. [14], a coated membrane was prepared using different types of Fluorolink® (AD 1700 and MD 700) for water treatment applications by membrane distillation. Hydrophobic porous membranes are, in fact, generally applied in DCMD configuration and they act as an interphase liquid-vapour at the pores generated by temperature difference between the hot feed and the cold permeate. The hydrophobic nature of the membranes prevents the wetting of the surface from the aqueous phase, while vapour molecules are allowed to migrate and diffuse through the membrane pores. The main membrane materials, used in DCMD have been described by Garcìa-Fernàndez et al. [15], and comprising polypropylene (PP), PVDF and PTFE. However, the aforementioned membranes are not specifically designed for MD applications [16]. The membranes, should meet, in fact, two contradictory requirements: being thick enough to provide the adequate mechanical resistance and also to function as a heat conduction barrier; but, on the other hand, being as thin as possible to maximize the membrane permeability. In order to overcome this controversy, the concept of hydrophobic/hydrophilic dual layer membranes has been widely described by M. Khayet et al. [17]. In practice, the advantages of these types of membranes are that a thinner hydrophobic layer combined with a hydrophilic sub-layer leads to an increase of the flux since the mass transfer resistance decreases. Khayet and Matsuura [18] and Khayet et al. [19], for instance, produced porous hydrophobic/hydrophilic composites by using fluorinated surface

modifying macromolecules (SMMs) blended with polyetherimide (PEI) polymer for potential applications in MD. The membrane formation occurred by phase inversion accompanied with the migration of SMMs towards the surface of the membrane and creating, thus, a hydrophobic layer.

The aim of this work was to produce hydrophobic/hydrophilic coated flat sheet membranes using an UV-curable PFPE compound (Fluorolink® AD 1700) by modifying the surface of microfiltration hydrophilic polyamide (PA) membranes. Using UV-curable PFPE compounds we can coat whatever microfiltration membrane (either hollow fibre or flat sheet) making it highly hydrophobic via UV curing while only slightly modifying the surface pores. In this way, membranes with the right morphology can be selected "a priori". An additional advantage of producing hydrophobic/hydrophilic coated membranes lies in the possibility of modifying the surface of cheaper hydrophilic commercial membranes (such as PA) in comparison to more expensive hydrophobic membranes normally applied in MD such as PTFE, ECTFE, PVDF and PP. These membranes are usually produced for applications different from MD, are difficult to manufacture and with characteristics difficult to optimize and tune [20]. In fact, for example, PTFE porous membranes are prepared with a process which involves several steps: first PTFE powder is mixed with a lubricant, then the resulting paste is pressed, extruded in the form of flat sheet and after drawn by uniaxial or biaxial stretching at 327°C or above [21]. Finally the items are sintered forming a microporous structure of nodes interconnected by small fibrils [3,22]. Usually these membranes are very thin and must be supported to guarantee the necessary mechanical strength. Actually, they are usually quite expensive due to the complexity of the manufacturing process. PP membranes instead are prepared via TIPs, stretching or leaching; also in this case the production is costly and it is difficult to control the morphology. ECTFE is difficult to process and it is insoluble in most of the solvents at room temperature; and therefore must be processed via TIPs [23]. Only PVDF membranes can be manufactured via phase inversion at room temperature allowing a certain flexibility in tuning the final morphology of the membranes but, on the other hand, PVDF possesses lower hydrophobicity than the other materials. The contact angle of the PVDF dense film was around 82° [24].

Three different PA membrane pore sizes (0.45, 0.22 and 0.1 μm) and three different Fluorolink® concentrations (5, 10 and 20 wt.%) were, then, used and their effect on membrane performances studied.

Prepared membranes were, characterised in terms of surface morphology (SEM and AFM), water contact angle, porosity, pore size and liquid entry pressure. Experiments in DCMD configuration have been carried out with deionized water for all prepared membranes, and with a salty solution 0.6M (NaCl) as feed, for one selected optimized membrane.

3.2. Experimental

3.2.1 Materials

Fluorolink® AD1700 (PFPE backbone Mw = 4000 g mol^{-1}) was supplied form Solvay Specialty Polymers S.p.A., Bollate (Italy). Its chemical structure is as follows, R_H-CF_2O-$(CF_2CF_2O)_m$-$(CF_2O)_n$-CF_2-R_H, where R_H are urethane (meth)acrylates blocks which, in the case of Fluorolink® AD 1700, are bifunctional. 2-Propanol (IPA), Butyl acetate, 2-Hydroxy-2-methylpropiophenone (Darocure 1173), Sodium chloride and Methoxy perfluro butane (HFE7100) were purchased from Sigma and used without any further purification. Liquid nitrogen was purchased from Pirossigeno (Italy). Polyamide membranes (0.45-0.22-0.1µm) were supplied from Sterlitech (USA).

3.2.2 Polymeric dope solution preparation

Fluorolink® AD1700 solution was prepared using different oligomer concentration (5-10-20wt.%). Butyl acetate and HFE7100 were used as solvents and Darocure 1173 was used as photo-initiator (1wt.%)**.** The solution was stirred for 2h at a room temperature until complete dissolution of the oligomers was achieved. This solution was allowed to degas for 30' before using it.

3.2.3 Coated membrane preparation by Dip-Coating

Commercial membranes, used as supporting material, were dipped into the oligomer solution for 10 min, and dried over-night. The coated membranes were exposed for 5 min at UV lamp (500Watt – Purchased from Helios Italquarz s.r.l.). In order to remove the un-polymerized oligomer, the coated membrane was washed using a solution of butyl acetate/HFE700 for 10 min. The membrane was then dried in air, and put in an oven, at 40°C, over-night.

The scheme of the membrane coating preparation is shown in Fig.1.

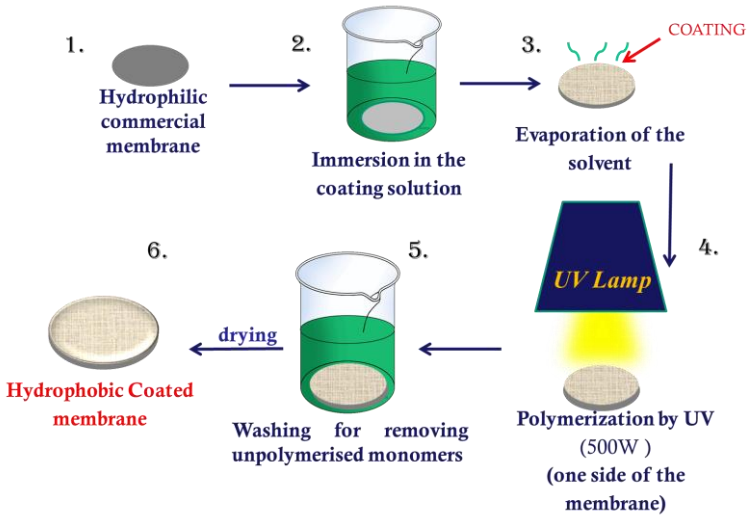

Figure 1. Dip-coating procedure using Fluorolink® AD1700

3.3 Membrane characterization

3.3.1 Scanning Electron Microscopy (SEM)

The morphology of the coated membranes (cross section, top and bottom side) was observed by using the Scanning Electron Microscope (Zeiss EVO, MA100, Assing, Italy). To obtain a clear cross-section, membranes samples were freeze fractured in liquid nitrogen. Sample specimens were sputter-coated with a thin gold film prior to SEM observation.

3.3.2 Atomic Force Microscopy (AFM)

Atomic force microscopy was used to study the surface morphology and roughness of the prepared membranes. The AFM device was a Bruker Multimode 8 with Nanoscope V controller. Data were acquired in tapping mode, using silicon cantilevers (model TAP150, Bruker). The coated membrane surfaces were imaged in a scan size of 10 μm x 10 μm.

3.3.3 Contact Angle

The hydrophilic/hydrophobic nature of the membrane was evaluated using CAM200 as instrument. The measurements were performed using ultrapure water (5μL). For all membranes, at least five measurements were taken the average value and the corresponding standard deviations were calculated.

3.3.4 Liquid entry pressure of water measurements (LEPw)

LEPw was measured using a Millipore cell. The maximum pressure operated limit was 4 bar and the maximum processing volume was 10mL. The cell diameter was 2.2 cm. To determine the LEPw, the cell was filled with water (trans-membrane pressure (TMP)), and the experiments were carried out by applying different pressures of nitrogen, which was in contact with the coated side of the membrane. LEPw was the TMP value at which the liquid water started to permeate in the other side of the cell (kept at atmospheric pressure). For all membranes, at least 5 measurements were taken; the average value and the corresponding standard deviation were, then, calculated.

3.3.5 Porosity

Membrane porosity was defined as the volume of the voids in the membrane itself, divided by the total volume of the membrane. Porosity measurement (ε_m) was determined in according to the gravimetric method. Dry membrane samples were weighed and impregnated in 2-propanol for 24h;

before the test, in order to remove the residual liquid, membrane was blotted using tissue paper, and after, membranes weight was measured again. Finally, the porosity was calculated applying to this formula:

$$\varepsilon(\%) = \{\frac{(Ww-Wd)\,/\rho i}{(Ww-Wd)/\rho i+(\frac{Wd}{\rho P})}\}\, x\, 100 \qquad (1)$$

Where W_w is the weight of the wet membrane, W_d is the weight of the dry membrane, ρ_i is the 2-propanol density (0.78 g/cm^3) and ρ_P is the polymer density. For all membranes, three measurements were performed; then, the average values and corresponding standard deviation were calculated.

3.3.6 Bubble point and pore size measurement

Pore size distribution, largest pore size and bubble point were determined using a PMI Capillary Flow Porometer (CFP1500 AEXL, Porous Materials Inc., USA). For each test, membrane samples were initially fully wetted using 2-propanol (21.7 dyne/cm) for 24h and placed in the sample holder. Inert gas (nitrogen) was fed to the sample with increasing pressure. The operating mode used was wet-up/dry-up, and the data was analysed using the software Capwin. The measurement of bubble point, largest pore size and pore size distribution is based on the Laplace's equation:

$$dp = 4\,\tau\cos\theta / P \qquad (2)$$

where dP is the pore diameter, τ is the surface tension of the liquid, θ is the contact angle of the liquid (assumed to be 0 in case of full wetting, which means $\cos\theta = 1$) and P is the external pressure. The results of each test were imported as an excel file using the software Caprep for further processing.

3.3.7 DCMD experiments

The membrane module consisted of a cell in which the membrane was placed between two chambers (feed and permeate sides). Deionized water was used at the permeate side (cold side), whereas both deionized water and salty solution 0.6 M were considered as feed (hot side). The feed was kept in contact with the hydrophobic coating layer (active side) and the cold permeate was in contact with the hydrophilic side of the membrane. The effective membrane area was 4 cm^2. Temperature, pressure, and flow-rate were continuously monitored; the feed side was constantly heated (±0.5 °C) at the desired feed temperature (40-50-60°C). The cold permeate side was kept at 14±0.5 °C in all cases. The bulk feed and permeate temperatures were measured, after steady state was reached, using thermocouples. The pressure of the hot and cold side was measured using two manometers (0-1 bar). The flow-rate (Q) of the feed and permeate side (80 and 60 L/h, respectively) was measured using

ASA flow meters. All experiments were repeated three times and the average values and corresponding standard deviation were calculated.

Water vapor flux (J), through the coated membranes, was defined as the quantity permeated per unit of area and per unit of time. The flux was calculated by Eq.3:

$$J = \frac{m\ (kg)}{m^2 * h} \quad (3)$$

Where m (kg) was the mass of permeate recovered at the cold side and measured by a balance (resolution: 0.1 g), m^2 was the membrane area, and h was the operating time.

After tests on salty solution a total washing with deionized water of the plant was performed until the complete elimination of all traces of salt. Finally, a DCMD test with deionized water at Tfeed=50°C was carried out to verify the performance of the membrane after the washing step.

3.4 Results and Discussion

3.4.1 Coated membrane preparation

Fluorolink® AD1700 dope solution was prepared as reported in section 2.2. The commercial polyamide (PA) membranes, having different pore size (0.1; 0.22; 0.45 µm), were used as support. The dip-coating procedure was described in section 2.3

All the coated membranes prepared are reported in Table 1.

Table 1: Coated Fluorolink® AD1700 membranes prepared using PA commercial membranes as support

Membrane type	Pore size (µm)	Oligomer concentration (wt%)	Solvents
10-P5	0.1	5	BUTYLACETATE + HFE7100 (70-30wt %)
10-P10		10	
10-P20		20	
22-P5	0.22	5	
22-P10		10	
22-P20		20	
45-P5	0.45	5	
45-P10		10	

45-P20		20	

3.4.2 Membranes Characterization

- SEM, AFM and contact angle analyses

In order to study the presence of Fluorolink® on membranes surface and the effect on their cross-section, commercial PA membranes, with and without coating, were analysed using SEM. In Fig.2, the cross section, top and bottom side of commercial PA membrane (0.22µm pore size) is reported. As it can be seen, the membrane presents a symmetric sponge porous structure.

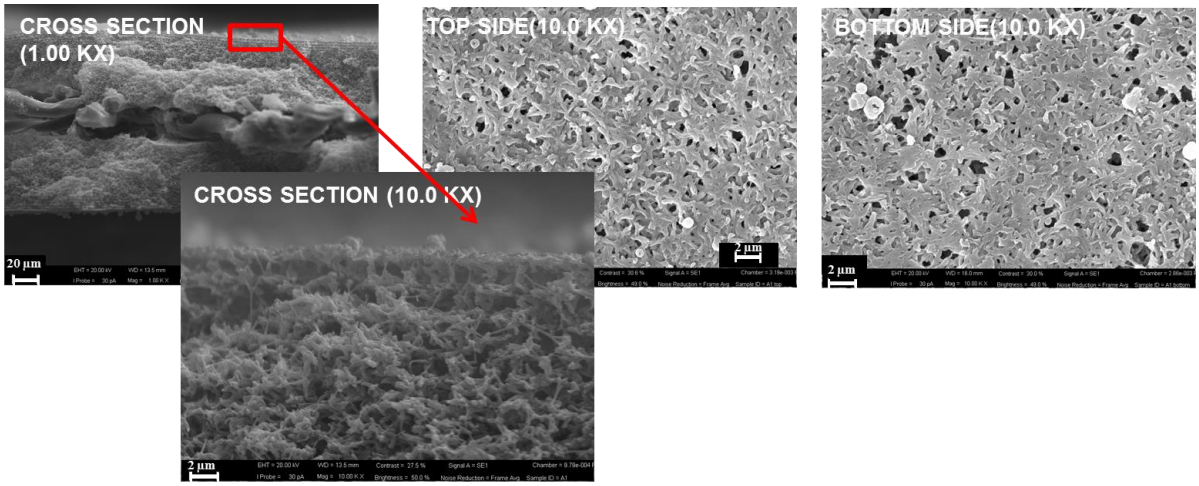

Fig.2: Morphology of commercial PA membrane (pore size 0.22µm)

The pictures of coated membranes are shown in Fig.3. Looking at the cross sections, it is possible to observe as increasing the oligomer concentration (from 5 to 20wt.%) the coated layer becomes more visible. Moreover, the coating did not completely close the pore structure of the pristine membranes. These results indicate that Fluorolink® coating did not significantly modify the original commercial membrane morphology.

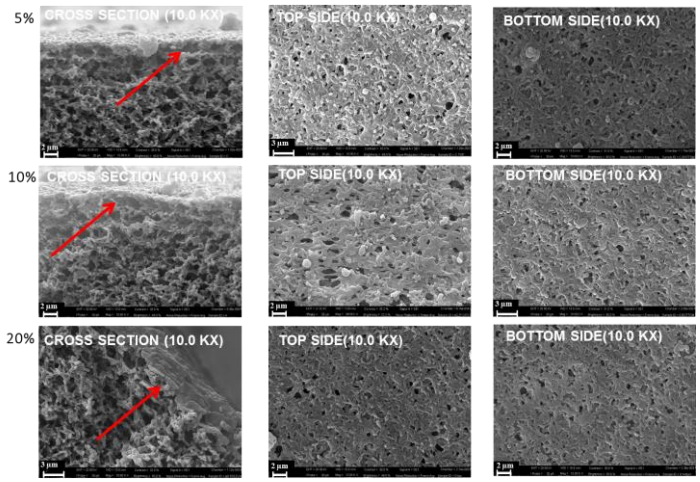

Figure 3. Morphology of coated polyamide membrane (pore size, 0.22µm) with different Fluorolink® AD1700 concentration (5-10-20wt.%)

The membrane surface properties were investigated using AFM. Fig.4 shows the images of PA membrane with and without the Fluorolink® treatment. In the Fig.4a are shown the surfaces topography of the unmodified commercial PA membrane and of the coating commercial PA membranes (5-10-20wt.%), while Fig.4b shows the correspondent 3D views.

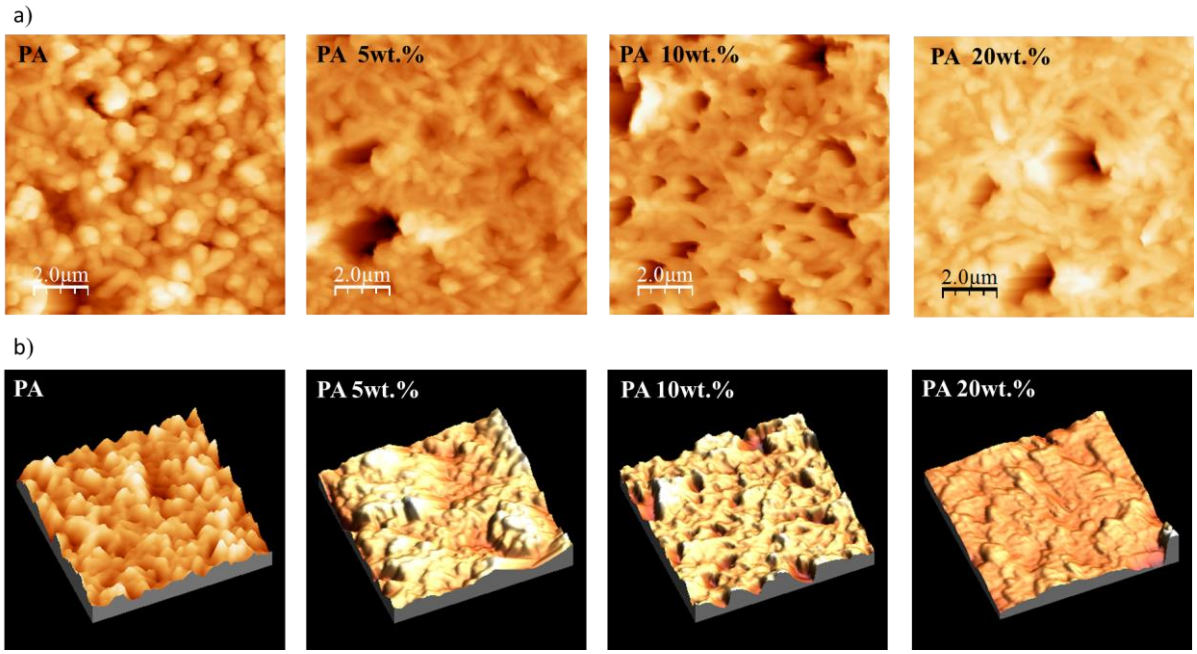

Figure 4. AFM images of PA commercial membranes (pore size, 0.22µm) and coated PA membranes with of Fluorolink® AD1700 in different concentrations (5-10-20wt.%)

The topography was measured on five different areas of the sample surface and the RMS roughness (Sq), roughness average (Sa), and peak to peak value (Sz) were calculated. The obtained data and the respectively standard deviation are reported in Table 2. On the basis of the images and the respectively

extrapolated data, it was possible to observe that the roughness is constant (average of about 0.22 μm) up to 10wt.% of Fluorolink® AD1700. Only at 20wt.% of oligomer the roughness value drastically dropped to about 0.15 μm. This result is in agreement with the SEM pictures (Fig.5 20wt.%), the higher concentration of oligomer increases the thickness of the coated layer covering the porous structure and reducing the surface roughness.

Table 2. Surface roughness of PA 0.22 μm with and without coating

Membrane type	Roughness average, Sa (μm)	RMS Sq (μm)	Peak to peak Sz (μm)
PA	0.21 ±0.08	0.26 ±0.1	2.01 ±0.8
PA 5	0.21 ±0.08	0.28 ±0.1	2.36 ±0.5
PA 10	0.23 ±0.04	0.34 ±0.09	2.71 ±0.6
PA 20	0.14 ±0.07	0.19 ±0.09	1.91 ±0.07

The same trend in terms of morphology and roughness was also observed for the 0.1 and 0.45 μm coated membranes.

Contact angle (CA) measurements also confirmed the presence of Fluorolink® AD1700 on membranes surface. Wenzel [25] proposed a phenomenological model for understanding how roughness affects wetting:

$\cos\theta_m = r \cos\theta_y$

where r is the ratio of the actual to projected surface area (r = 1 for a smooth surface and r > 1 for a rough surface), and θ_y is the Young contact angle, which is equal to θ_m if r = 1. According to this equation, hydrophobicity is reinforced by roughness [26]. The CA results for the different membranes produced are shown in Fig.5.

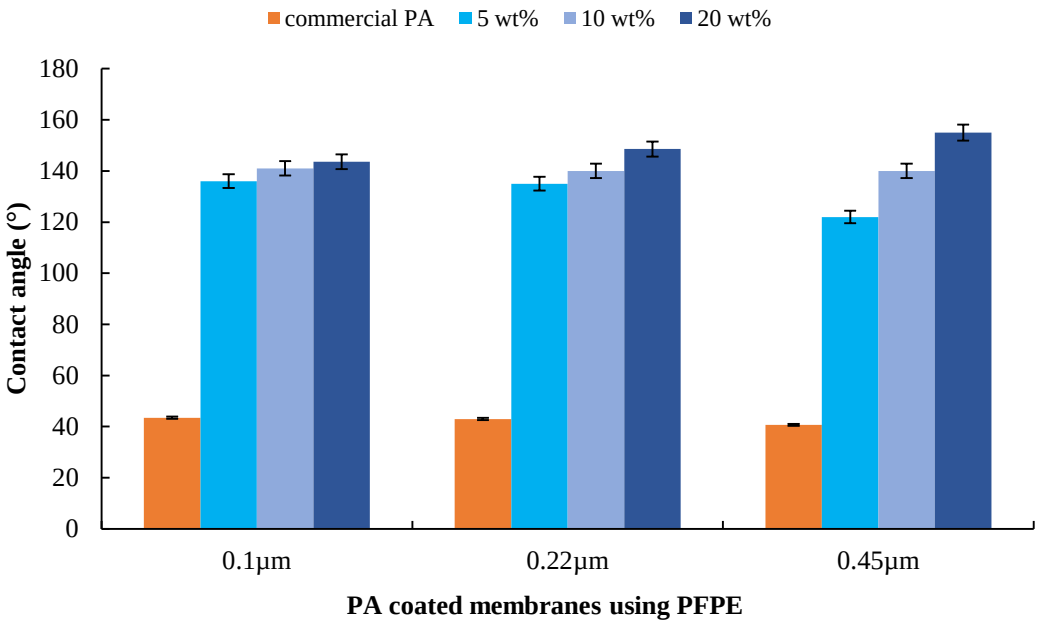

Figure 5. Contact angle results for Fluorolink® AD1700 coated PA membranes (0.1-0.22-0.45µm pore size)

The results of surface roughness parameters confirm that the coating is present and affects the PA membrane surface. Considering the obtained results, it is possible to observe that:

- CA and roughness increased in case of 5wt.% and 10wt.% of oligomer, and only for 20wt.% of oligomer, the roughness decreased. Although the coating PA membranes at 20wt.% of Fluorolink® AD1700 have smoother surface compared to unmodified PA membrane, the PFPE functional groups introduced on the PA membranes are responsible of their higher hydrophobicity.
- CA increases from 120° to 155° at higher oligomer concentration (from 5 to 20 wt.%). Moreover, the increase of the membrane pore size (from 0.1 to 0.45 µm) brings to an decrease of the CA for membranes prepared with 5 wt.%, while the opposite is observed for membranes prepared with 20 wt.%. This is probably due to the fact that low oligomer concentration (5 wt.%) penetrates more in the bigger pore size. The effect of the concentration on the CA is larger for the 0.45 µm membrane, compared to the 0.1 and 0.22 µm membrane.

The CA measurements were also conducted during time in order to evaluate the effective stability of the coating on membrane surface, as shown in Fig.6. In Fig.6a the commercial PA membrane presents a high hydrophylicity being the water drop already absorbed after 5 sec (From 46.27° to 26.3°). On the contrary, the data shown in Fig.6b indicate that the coating was stable in time and the water drop was not absorbed on membrane surface of the coated membranes. Therefore starting from hydrophilic PA membranes with a CA of around ~40°, hydrophobic coating membranes were obtained.

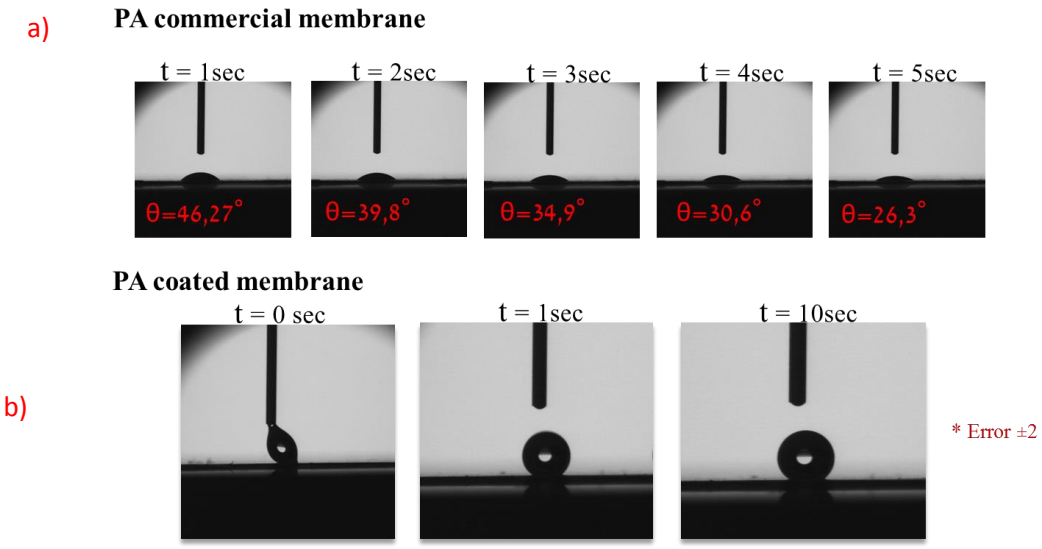

Figure 6. Contact angle measurements during time for (a) commercial PA (0.22 μm pore size) and b) coated PA membranes

- Water Liquid Entry Pressure Measurements (LEPw)

LEP_w measurements indicate the pressure that if applied across the membrane, allows the liquid (water) passage through the hydrophobic membrane. LEPw depends on the maximum pore size and the membrane hydrophobicity. In fact, membranes with higher CA and smaller pore size show higher LEPw. As expected, the highest LEP results were achieved using membranes at 0.1μm, and increasing in oligomer concentration. The LEP_w values are in the range of 2-3.5 bar. The results of LEPw measurements of the commercial PA and coated PA membranes are shown in Fig.7.

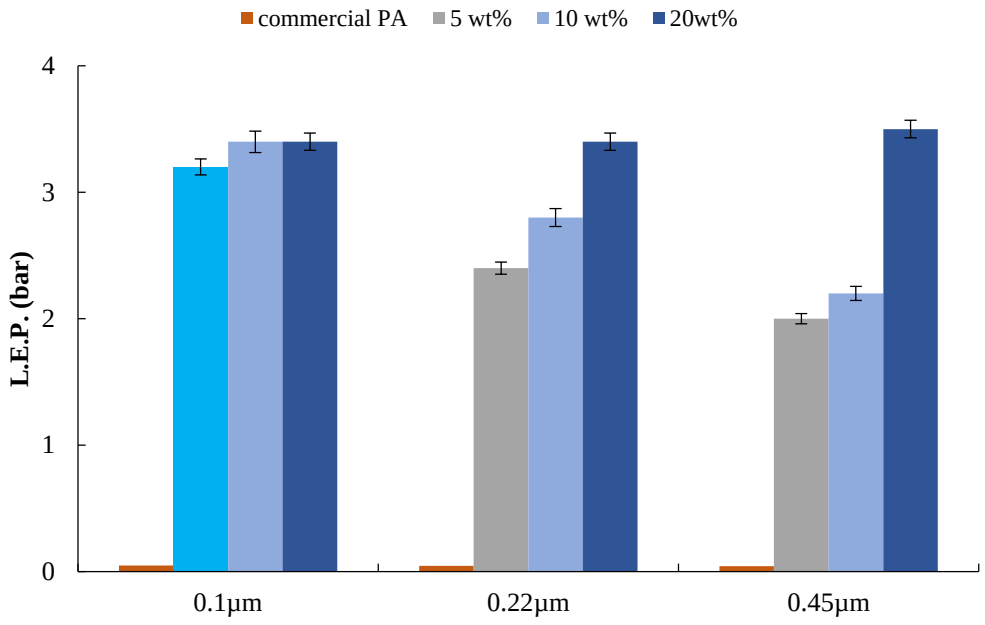

Figure 7. LEP_w measurements of PA membranes and PA membranes (0.1-0.22-0.45µm, pore size) coated with Fluorolink®AD1700

The obtained LEPw results are comparable with most of the commercial hydrophobic membranes commonly used in MD, as shown in Table 3.

Table 3. LEPw values of commercially available hydrophobic membranes [27-28]

Membrane	Material	Manufacturer	Pore size (µm)	LEPw (bar)
TF450	PTFE/PP	Gelman	0.45	1.38
HVHP/Durapore	PVDF	Millipore		1.05
Gore (PT45)	PTFE			2.88
TF200	PTFE/PP	Gelman	0.20	2.82
GVHP/ Durapore	PVDF	Millipore		2.04
Gore (PT20)	PTFE			3.68

- Porosity and Pore size measurements

In Fig.8, it is reported the porosity of the coated PA membranes. Generally, the data indicate that porosity decreases at higher oligomer concentration, and with lower pore size of the support commercial PA membranes. In fact, comparing the porosity results with the commercial PA membranes, without coating, only in case of 20 wt.% of oligomer the porosity decreases more significants. This trend was observed for PA membranes at 0.22-0.1µm. Using commercial PA membranes at 0.45µm no differences in porosity between membranes, with or without coating, was observed.

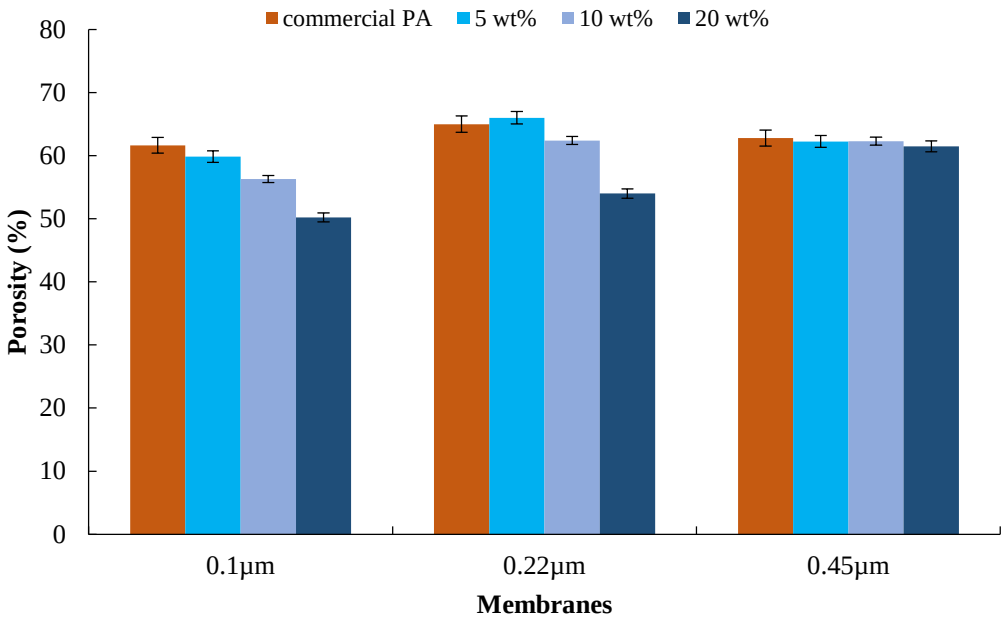

Figure 8. Porosity measurements for Fluorolink® AD1700 coated membranes using PA membranes with 0.1-0.22-0.45µm pore size

In Table 4**,** the pore size data are reported. The coated membranes show similar mean flow pore diameter and diameter at maximum pore size distribution than the unmodified membranes (commercial PA membranes 0.45-0.22-0.1 µm). This result indicates that the presence of Fluorolink® does not strongly affect the pore size of the pristine membranes. In fact, increasing the oligomer concentration a slight decrease of the pore size is evident in all cases. Moreover, the presence of the coating is also noticeable by the bubble point values (largest detected pore diameter), that increase at higher oligomer concentration (5-10-20wt.%).

Table 4. Bubble point and pore size distribution for Fluorolink® AD1700 coated membranes (0.45-0.22-0.1 µm)

MEMBRANE TYPE	BUBBLE POINT (bar)	LARGEST DETECTED PORE DIAMETER (µm)	MEAN FLOW PORE DIAMETER (µm)	DIAMETER AT MAXIMUM PORE SIZE DISTRIBUTION (µm)
Commercial PA 0.45 µm	0.45	1.40	0.55	0.35
45-P5	0.92	0.7	0.41	0.35
45-P10	0.87	0.7	0.4	0.30
45-P20	0.90	0.7	0.35	0.30
Commercial PA 0.2 µm	0.78	0.79	0.33	0.30
22-P5	1.20	0.52	0.32	0.30
22-P10	1.16	0.53	0.30	0.32
22-P20	1.20	0.50	0.35	0.25
Commercial PA 0.1 µm	1.72	0.35	0.20	0.20
10-P5	1.65	0.35	0.28	0.20

10-P10	1.91	0.30	0.30	0.30
10-P20	2.05	0.30	0.20	0.20

Note: The relative standard error is less than 5% in all cases

- DCMD tests

In order to determine the vapour permeate flux of the prepared Fluorolink® AD1700 coated membranes. DCMD experiments were carried out using deionized water and salty solution as feed. The hydrophobic coated side of the membrane was in contact with the hot feed, whose temperature was varied from 40°C to 60°C. while the hydrophilic PA side of the membrane was in contact with cold water at fixed temperature of 14°C. In Fig.9, the results of the DCMD tests with deionized water as feed are reported varying the concentrations of oligomer used on the commercial PA membranes and the temperatures of the feed side.

a)

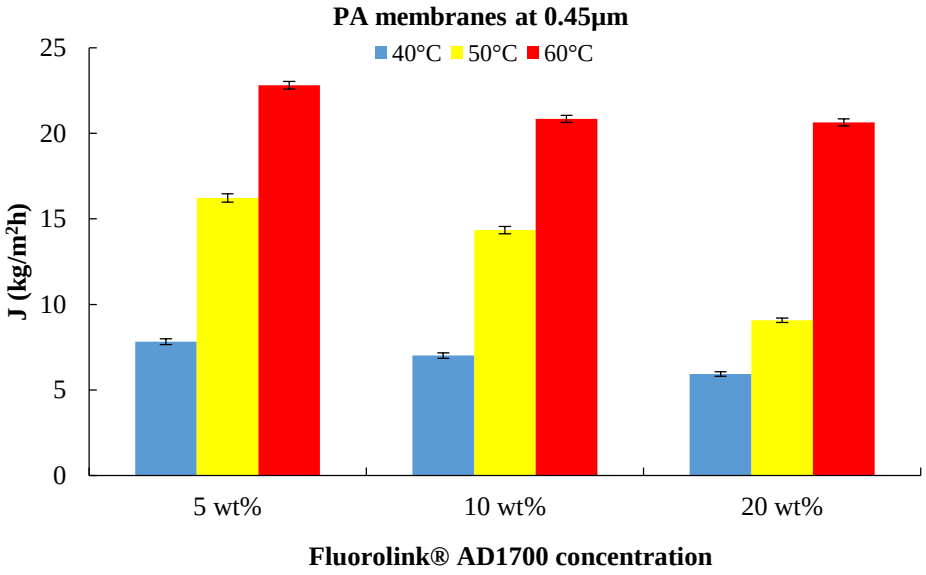

b)

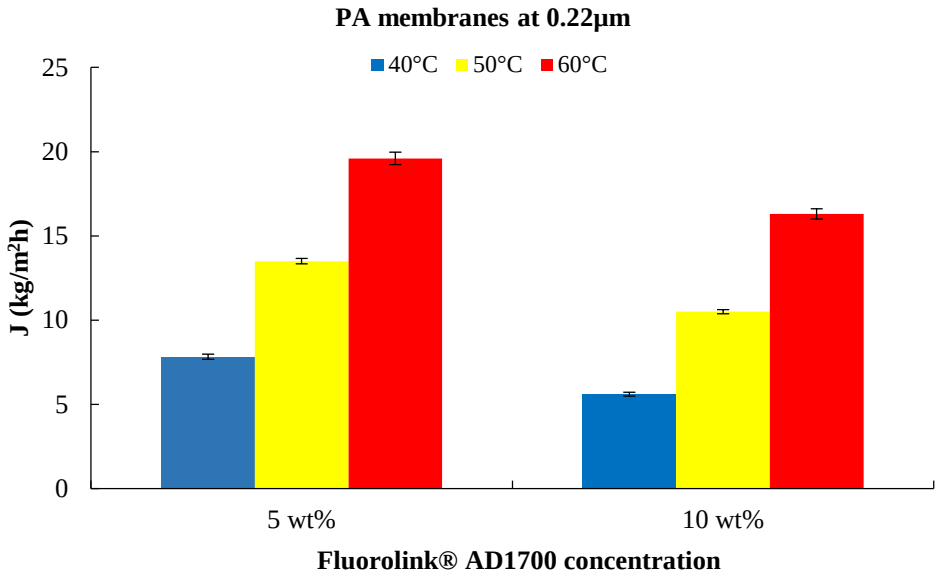

c)

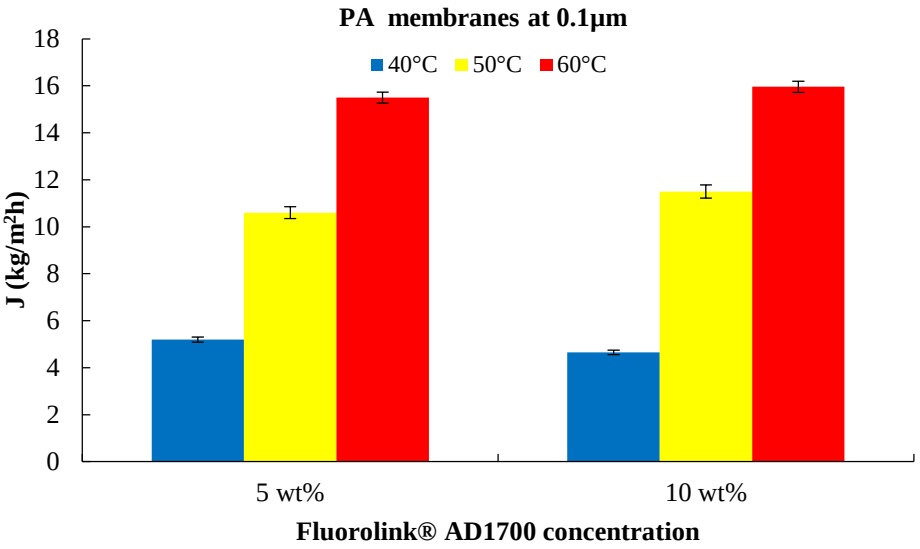

Figure 9. DCMD results for Fluorolink ® AD1700 coated membranes using polyamide of different pore size: a) 0.1µm; b) 0.22 µm and c) 0.45 µm;

In all cases. the flux increased with the feed temperature as expected [16]. It also decreased with the Fluorolink ® AD1700 concentration for the 0.22 µm and 0.45 µm pore size membranes, while it was almost constant for the 0.1 µm membrane. This result could be justified by considering the smaller pore size of the membranes. Fluorolink® concentrations of 5 and 10wt% might occlude in a similar way the inner of pore keeping constant the flux.

Furthermore, coating made on the 0.22 and 0.1 µm membranes with 20wt% of Fluorolink® did not allow to obtain appreciable trans-membrane fluxes, probably due to a significant occlusion inside the pores.

The maximum value of the permeate flux was around 22 kg/m^{2}h at 60 °C and 5wt% oligomer coating on the 0.45 μm PA membrane. Moreover, it is possible to observe that the flux decrease, decreasing the pore size of the commercial PA membranes, from 0.45 to 0.1 micron, as shown in Fig.10.

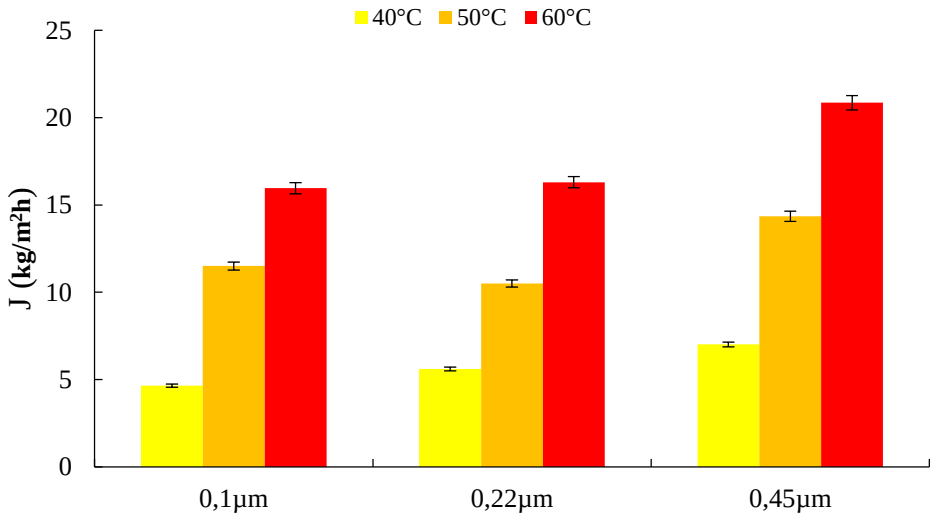

Figure 10. DCMD summary results for Fluorolink® AD1700 coated membranes using 10wt.% of oligomer concentration

Fig.11 shows the trend of the permeate flux in time for the 5wt% oligomer coating on the 0.45 μm PA membrane at T_{feed}=50°C. The time dependence of flux is a sort of "stabilization time" of the system. Being the membrane area quite small (4 cm^2), the amount of water vapor that evaporates and condenses is low, and the time to reach the steady-state condition is long. From the graph it is possible to observe that after 110 minutes the permeate flux reaches an asymptotic value of around 16 kg/m^{2}h for all three tests carried out, that means a good reproducibility. Moreover, the membrane results to be stable after 90 minutes (3 tests of 3 h each) of operation.

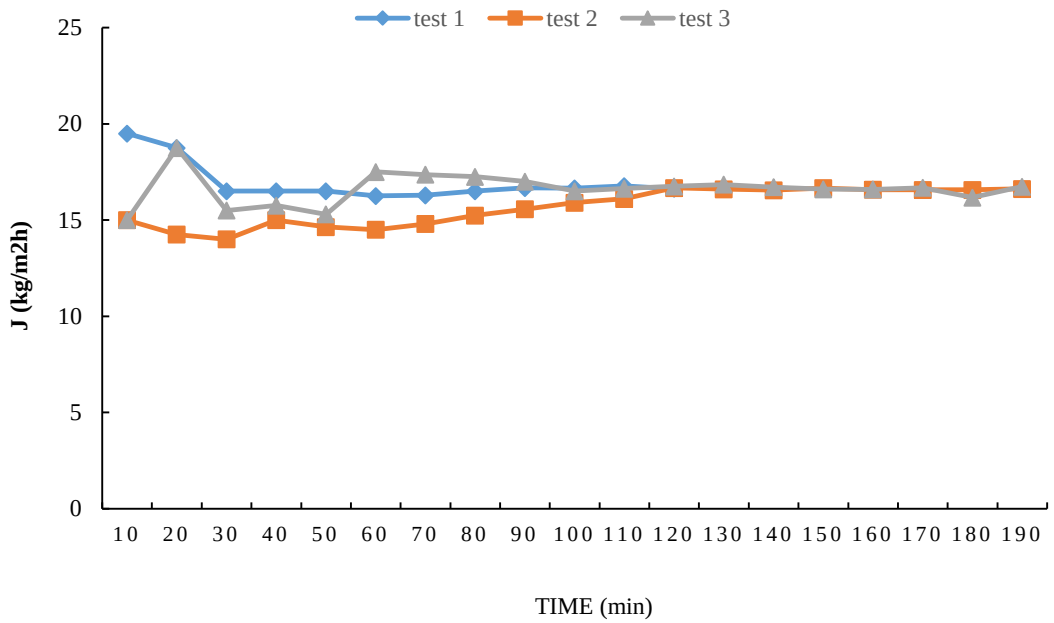

Figure 11. Trend of the permeate flux in the time; 5wt% oligomer coating on the 0.45 μm PA membrane; Tfeed=50°C; Qfeed= 80L/h; Tp=14°C; Qp=60 L/h.

In Fig.12 a comparison, at the same operating conditions, among the permeate fluxes obtained when deionized water and salty solution are feed is reported.

Concerning the test with deionized water, Fig.11 shows that after 110 minutes of unsteady state there is a stabilization of the flux at around 16.6 kg/m2h whereas for test with salty solution a lower constant value of 11 kg/m2h was obtained as flux, due to the lower water activity. It has to be also noticed that variations in flux feeding the salty solution are more significant. This could be attributed to the low resolution of the balance used (0.1 g) whose performance can be affected by a lower quantity of permeate produced. The values obtained in case of salty solution as feed were lower than those of deionized water due to the lower water activity.

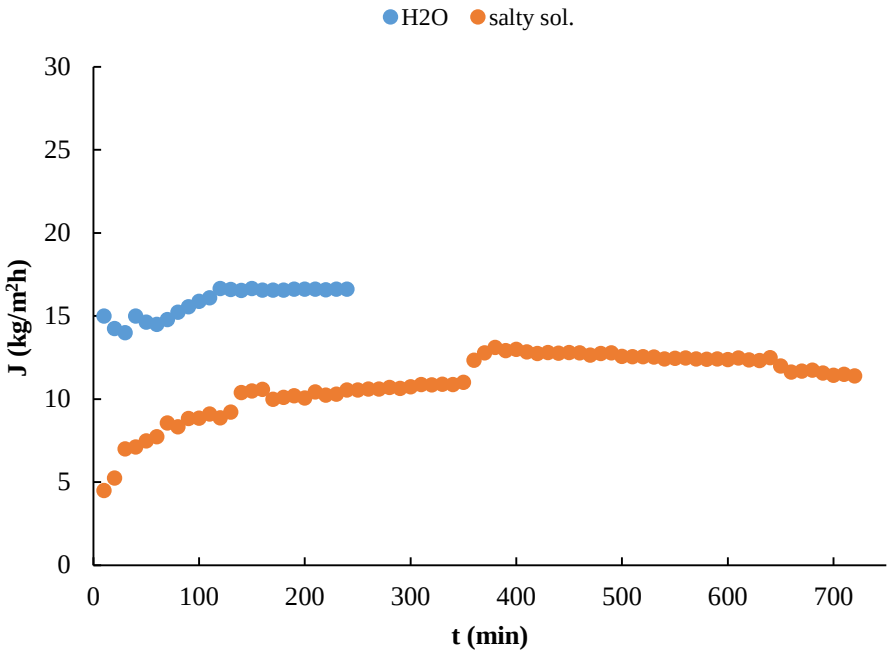

Figure 12. Comparison among permeate fluxes as function of different feed (deionized water and salty solution 0.6 M); 5wt% oligomer coating on the 0.45 μm PA membrane; Tfeed=50°C; Qfeed= 80L/h; Tp=14°C; Qp=60 L/h

After tests a washing step was necessary to restore the initial performance of the membrane as shown in Fig.13 where a comparison among the permeate fluxes before and after the test with salty solution is reported. It can be noticed that the membrane was able to recover its original performance after the washing step.

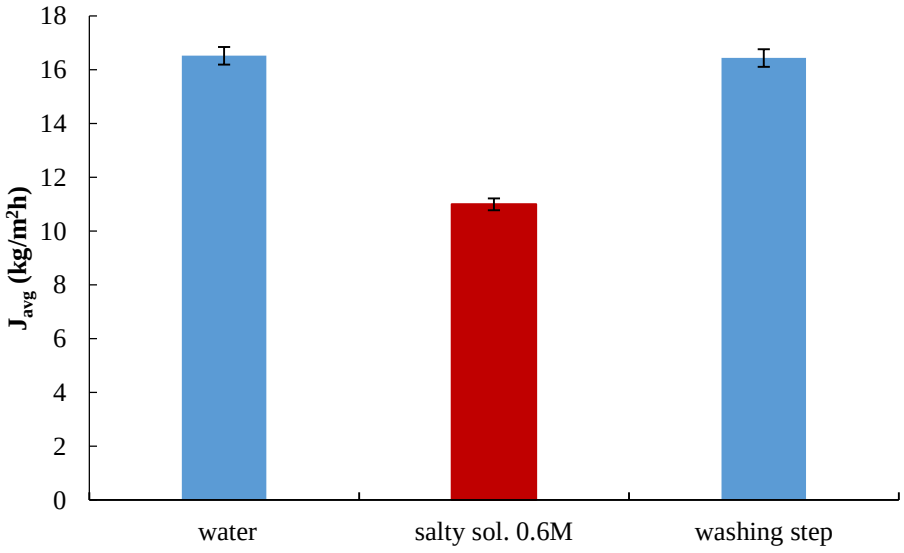

Figure 13. Trend of permeate fluxes before and after the washing step; Tfeed=50°C; Qfeed= 80L/h; Tp=15°C; Qp=60 L/h.

Fig.14 shows the trend of the salt rejection in time for tests with salty solution: after 15 hours the value is almost constant and around at the average value of 99.6%.

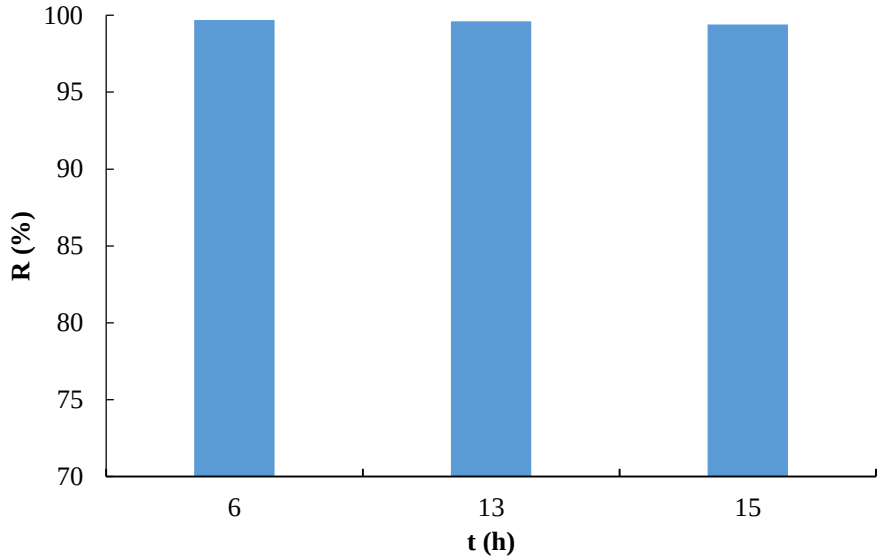

Figure 14. Trend of salt rejection in time; Tfeed=50°C; Qfeed= 80L/h; Tp=15°C; Qp=60 L/h.

The obtained DCMD results are comparable with those reported in literature for fluorinated flat hydrophobic membranes, as shown in Table 5.

Table 5. DCMD values of hydrophobic membranes reported in literature

Membrane type	**Pore size (µm)**	**Solution**	**Tf (°C)**	**Feed velocity (m/s)**	**J (kg/m^{2}h)**	**Ref.**
PVDF	0.22	Pure water	50	1.8-2.3	~ 18–20 l/m2h	[29]
PVDF	0.22	Pure water	40–70	0.23	~7–33 l/m2h	[29]
PVDF	0.22	Pure water	40–70	0.1	~3.6–16.2	[30]
PTFE	0.2	Pure water	40-70	-	~5.8–18.7	[31]
PVDF	0.4	Pure water	36-66	0.145	~5.4–36	[32]

3.5 Conclusions

Novel membranes by coating the hydrophobic Flurolink® AD 1700 on commercial hydrophilic PA membranes were prepared by dip-coating technique followed by photo-polymerization process. The use of different oligomer concentrations (5. 10 and 20 wt.%) and different commercial PA membrane pore sizes (0.1. 0.22 and 0.45 μm) has been investigated. The characterization results proved that the novel coating has been successfully added on the membranes. In particular. the hydrophobic coating did not change the original membrane morphology preserving the porous structure of the supporting PA membrane. On the other hand. the coating drastically increased the hydrophobicity of the membrane leading to the production of super-hydrophobic membranes made up of a thin highly hydrophobic layer (contact angle up to 150° in the best case) and a porous hydrophilic sub-layer (contact angle of about 45°) which acts as a mechanical support. The increasing concentration of oligomer (from 5 to 20 wt.%) determined an increase in LEPw values (due to the higher hydrophobicity of the membrane) and a decrease in membrane porosity (due to a partial penetration of the coating within the membrane sub-layer). Pore size measurements of the coated membranes reported an increase in bubble point pressure (up to 2.05 bar) in comparison to pristine commercial PA membranes due to the reduction of the biggest pores of the membrane. However. the mean pore diameter of the PA membrane was preserved and not influenced by the coating even when higher concentration of oligomer (20 wt.%) was adopted. DCMD tests demonstrated the stability of the coating in time (about 11h) and the good performance of the membranes. During tests with deionized water. membranes prepared with the lower concentration of oligomer (5 wt.%) presented the highest values of permeate flux (about 22 Kg/m^2h at 60°C and 16.6 Kg/m^2h at 50°C). The flux was also positively influenced by increasing the temperature (from 40 to 60°C) and the pore size (from 0.1 to 0.45 μm) of the commercial PA membranes.

Regarding the test carried out with salty solution as feed (0.6 M) at Tfeed=50°C. a high rejection (99.3% after 15 hours of process) and permeate flux of 11 kg/m^2h were obtained. Moreover the membrane was able to recover to its original performance after washing.

References

[1] Z. Cui, E. Drioli, Y. M. Lee, Recent progress in fluoropolymers for membranes, Progress in Polymer Science. 39 (2014) 164– 198. doi.10.1016/j.progpolymsci.2013.07.008.

[2] E. Giannetti, Semi-crystalline fluorinated polymers, Polymer International. 50:1, (2001) 10–26. Doi.10.1002/1097-0126(200101)

[3] S. Ebnesajjad, Introduction to Fluoropolymers- Materials, Technology and Applications, Applied Plastics Engineering Handbook: Processing and Materials, Myer Kutz (Elsevier, 2011).

[4] H. Teng, Overview of the Development of the Fluoropolymer Industry, Applied Sciences. 2, (2012) 496-512. doi:10.3390/app2020496

[5] S. Simone, A. Figoli, A. Criscuoli, M.C. Carnevale, S.M. Alfadul, H.S. Al-Romaih, F.S. Al Shabouna, O.A. Al-Harbi, E. Drioli, Effect of selected spinning parameters on PVDF hollow fiber morphology for potential application in desalination by VMD, Desalination. 344 (2014) 28–35. doi.10.1016/j.desal.2014.03.004.

[6] S. Simone, A. Figoli, S. Santoro, F. Galiano, S.M. Alfadul, O.A. Al-Harbi, E. Drioli, Preparation and characterization of ECTFE solvent resistant membranes and their application in pervaporation of toluene/water mixtures, Separation and Purification Technology. 90 (2012) 147–161. doi.10.1016/j.seppur.2012.02.022.

[7] F. Falbo, S. Santoro, F. Galiano, S. Simone, M. Davoli, E. Drioli,A. Figoli, Organic/organic mixture separation by using novel ECTFE polymeric pervaporation membranes, Polymer. doi.10.1016/j.polymer.2016.06.023

[8] D. Sianesi, G. Marchionni, R.J. De Pasquale, Perfluoropolyethers (PFPEs) from Perfluoro Olefin Photooxidation: Fomblin® and Galden® Fluids, in Organofluorine Chemistry Principles and Commercial Applications, Ed. by Banks R.E., Smart B. E. and Tatlow J.C., Chapt. 20, Springer Science Business Media, LLC (1994).

[9] T. Temtchenko, R. Marchetti, A. Locaspi, Self-cleaning perfluoropolyether based coatings, Surface Coatings International. 81 (1998) 448-450. doi.10.1007/BF02692975

[10] R. Bongiovanni, G. Malucelli, A. Pollicino, C. Tonelli, G. Simeone, A. Priola, Perfluoropolyether structures as surface modifying agents of UV-curable systems, Macromolecular Chemistry and Physics. 199 (1998) 1099–1105. doi. 10.1002/(SICI)1521-3935(19980601)199:6

[11] V. Oldani, R. Del Negro, C.L. Bianchi, R. Suriano, S. Turri, C. Pirola, B. Sacchi, Surface properties and anti-fouling assessment of coatings obtained from perfluoropolyethers and ceramic oxides nanopowders deposited on stainless steel, Journal of Fluorine Chemistry, 180 (2015) 7‑14. doi./10.1016/j.jfluchem.2015.08.019

[12] M. Avataneo, U. De Patto, P. A. Guarda, G. Marchionni, Perfluoropolyether-tetrafluoroethylene (PFPE‑TFE) block copolymers: An innovative family of fluorinated materials, Journal of Fluorine Chemistry. 132 (2011) 885‑891. doi.10.1016/j.jfluchem.2011.06.034

[13] B. Bertolotti, H. Messaoudi, L. Chikh, C. Vancaeyzeele, S. Alfonsi, O. Fichet, Stability in alkaline aqueous electrolyte of air electrode protected with fluorinated interpenetrating polymer network membrane, Journal of Power Sources. 274 (2015) 488-495. doi./10.1016/j.jpowsour.2014.10.059

[14] A. Sanguineti, E. Di Nicolò, P. Campanelli , Coated membrane comprising layer of perfluoropolyether on hydrophilic substrate, WO 2013164287 A1 (2013)

[15] L. Garcìa-Fernàndez, M. Khayet, M.C. Garcìa-Payo, Membrane used in membrane distillation: preparation and characterization in: A.Basile, A.Figoli, M. Khayet (Eds), Pervaporation, Vapour Permeation and Membrane Distillation, chap. 11 (2015) Woodhead publishing.

[16] A. Criscuoli, M.C. Carnevale, E. Drioli, Evaluation of energy requirements in membrane distillation, Chemical Engineering and Processing: Process Intensification. 47: 7 (2008) 1098-1105. doi./10.1016/j.cep.2007.03.006

[17] M. Khayet, T. Matsuura, J.I. Mengual, Porous hydrophobic/hydrophilic coated membranes: estimation of the hydrophobic layer thickness, Journal of Membrane Science. 266 (2005) 68–79 (a). doi.10.1016/j.memsci.2005.05.012

[18] M. Khayet, T. Matsuura, Application of surface modifying macromolecules for the preparation of membranes for membrane distillation, Desalination, 158 (2003) 51–6. doi.10.1016/S0011-9164(03)00432-6

[19] M. Khayet, D.E. Suk, R.M. Narbaitz, J.P. Santerre, T. Matsuura, Study on surface modification by surface-modifying macromolecules and its applications in membrane-separation processes, Journal Applied Polymer Science.89:11 (2003) 2902–2916. doi.10.1002/app.12231

[20] R. Huo, Z. Gu, K. Zuo, G. Zhao, Preparation and humic acid fouling resistance of poly(vinylidene fluoride)–fabric composite membranes for membrane distillation, Journal Applied Polymer Science.117 (2010), 3651–3658. doi. 10.1002/app.32271

[21] K. Hintzer, T. Zipplies, D.P. Carlson, W. Schmiegel, Fluoropolymers, Organic, Ullmann's Encyclopedia of Industrial Chemistry, Wiley-VCH Verlag GmbH & Co (2014).

[22] R.W. Gore, Process for producing filled porous PTFE, US patent 4096227 (1978).

[23] Y. Mutoh, M. Miura, Porous fluorine resin membrane and process for preparing the same. US Patent 4,702,836 (1987).

[24] S. Lee, J.S. Park, T.R. Lee, The wettability of Fluoropolymer Surfaces: Influence of Surface Dipoles, Langmuir 24:9 (2008) 4817–4826.

[25] R.N. Wenzel, Resistance of solid surfaces to wetting by water, Industrial and Engineering Chemistry Research. 28 (1936) 988–994. doi. 10.1021/la700902h

[26] D. Quèrè, Rough ideas on wetting, Physic A, 313 (2002) 32 – 46. doi.10.1016/S0378-4371(02)01033-6

[27] A. Alkhudhiri, N. Darwish, N. Hilal, Membrane distillation: A comprehensive review, Desalination 287 (2012) 2–18. doi.10.1016/j.desal.2011.08.027

[28] G. Rácz, S. Kerker, Z. Kovács, G. Vatai, M. Ebrahimi, P. Czermak, Theoretical and Experimental Approaches of Liquid Entry Pressure Determination in Membrane Distillation Processes, Periodica Polytechnica Chemical Engineering. 58:2 (2014) 81-91. doi.10.3311/PPch.2179

[29] S. Srisurichan, R. Jiraratananon, A. G. Fane, Mass transfer mechanisms and transport resistances in direct contact membrane distillation process, Journal of Membrane Science 277 (1–2) (2006) 186–194. doi.10.1016/j.memsci.2005.10.028

[30] J. Phattaranawik, R. Jiraratananon, A. G. Fane, Heat transport and membrane distillation coefficients in direct contact membrane distillation, Journal of Membrane Science 212 (1–2) (2003) 177–193. doi.10.1016/S0376-7388(02)00498-2

[31] J. Phattaranawik, R. Jiraratananon, A. G. Fane, Effect of pore size distribution and air flux on mass transport in direct contact membrane distillation, Journal of Membrane Science. 215 (1–2) (2003) 75–85. doi.org/10.1016/S0376-7388(02)00603-8

[32] Y. Yun, R. Ma, W. Zhang, A. G. Fane, J. Li, Direct contact membrane distillation mechanism for high concentration NaCl solutions, Desalination. 188 (1–3) (2006) 251–262. doi.10.1016/j.desal.2005.04.123

Chapter 4.

Development of a novel perfluoropolyether (PFPE) hydrophobic/hydrophilic coated membranes for water treatment application

4.1 Introduction

Thanks to the great technological advancement, membrane separation processes have become an emerging technology for the treatment of water in different fields, such as wastewater treatment, oily wastewater treatment, desalination etc. In fact, the re-use of wastewater and water desalination from sea and inland saline aquifers represents a problem in growth. Moreover, demand of fresh water is required by different sectors such as agriculture, livestock, food production and industrial output. The growing attention to the environment, leads to develop an appropriate water treatment techniques in order to ensure a sustainable freshwater [1]. Near the commonly membranes preparation techniques, several studies focus the attention in order to achieve high-performance membranes, and a new way is the preparation of tailored membranes via coating technique. These novel membranes are a perfect fusion between the useful properties of the base membrane and the novel functional polymer (layer) [2]. In fact, an important advantage of the composite membranes is that, the top-separating layer is formed in situ and hence the chemistry and performance of the top and bottom substrate can be independently studied and modified to maximize the overall membrane performance [2,3]. Much of the research, that has been done up to improve membrane performance for aqueous applications, has centered on both changing the chemistry or morphology of the selective layer and measuring its flux and selectivity. Several methods can be used in order to prepare coated membranes, as solution coating or polymerization reactions [4]. Hydrophilic and hydrophobic membrane surface modifications were used in different fields; in particular surface hydrophilization is beneficial, for all those polymeric materials that are applied in aqueous systems, e.g. in order to control the fouling [5,6] while hydrophobilization can be necessary in case of pervaporation (PV), VOCs' recovery, or in membrane distillation (MD) [7,8]. Hydrophobilization processes often involves several step, such as plasma polymerization, grafting or interfacial polymerization [9,10]. Several authors reported different methods in order to modified membranes from hydrophilic to hydrophobic, for MD applications. In particular, the concept of composite hydrophilic/hydrophobic membranes, using fluorinated modified macromolecules (SMM) was firstly introduced by Khayet et al. [11], and applied in DCMD process. Recently, Shaulsky et al. [12] reported a versatile approach using Poly(vinylidene fluoride-hexafluoropropylene) (PVDF-HFP) to produce a highly porous electrospun fiber mat, coated with Poly(vinylidene fluoride) (PVDF) that are enabled to control the membrane

pore size, and tested in direct contact MD experiments with 40 °C temperature. Zhao et al., produced high DCMD hydrophobic PVDF membranes by depositing fluorographite particles on the membrane surface [13]. Poly(vinylidene fluoride) (PVDF) flat sheet nano-composite membranes using SiO2 nano-particles, were surface modified by coating with electro-spun PVDF nanofibres to increase the surface hydrophobicity by Efome et al. [14]. Composite hollow fiber membranes for vacuum membrane distillation were produced by Tong et al. [15], by coating a copolymer (Hyflon AD60) of tetrafluoroethylene (TFE) and 2,2,4-trifluoro-5-trifluoro methoxy-1,3-dioxole (TTD) on PVDF membranes. In fact, the hydrophobicity of the membrane material play a crucial role in MD, inasmuch prevents that the liquid solution penetrate into the pore structure of the membrane [16] and an increase in surface hydrophobicity increase the wetting resistance [17,18]. In fact, despite typically materials using in MD are hydrophobic polymer, such as Polypropylene (PP), PVDF, and Poly(tetrafluroethylene) (PTFE), are not specifically designed for MD applications [7,19,20]. Moreover, some coating methods are not easy to produce on an industrial scale.

In this work a novel easy method was presented, in order to produce hydrophobic or super hydrophobic and oleophobic coated membranes, starting from hydrophilic commercial membranes. Flurolink® Perfluoropolyethers (PFPEs) compounds UV or thermally cross-linkable, produced by Solvay Specialty Polymers, were used as coating materials [21]. These materials are based on bi-functional perfluoropolyether structure, perfluorinated carbon units, as –CF2– and –CF2–CF2–, separated by oxygen atoms [22], with a high molecular weight. Their properties including water/oil repellence, better chemical resistance, low coefficient of friction and high degree of hydrophobicity. Bongiovanni et al., studied the possibility of using two PFPEs bis-urethane methacrylates as novel additives for the preparation of UV-cured acrylic films [23], and in other work reported modification surface of cellulose using a highly fluorinated acrylic monomer, characterized by a long perfluoropolyether chain [24]. In a recent work, Figoli et al.[7], studied the effect of different Fluorolink® AD1700 concentrations (5, 10 and 20wt%) as coating materials, using polyamide PA (0.45, 0.22 and 0.1 μm) as starting material, for DCMD. In this work, Fluorolink® MD700 was used as coating materials on two different commercial hydrophilic membranes: PA, and polyethersulfone (PES), at three different pore size (0.45, 0.22 and 0.1 μm). This materials have been recently applied by Bertolotti et al. [25], in an interpenetrating polymer network for the production of anion exchange membranes to protect air electrodes functioning in aqueous lithium-air battery configuration. Respect to Fluorolink® AD1700, the functional group of Fluorolink® MD700 consisting in (Meth) Acrylates, which make them more cross-linkable and consequently more stable in time. Fluorolink® MD700 coated membranes were simply produced by dip-coating and in situ polymerization. The influences

of starting material (PA-PES), was initially studied in terms of water/oil repellence by a contact angle measurements. Prepared membranes were characterized in terms of surface morphology (EPMA and AFM), porosity, pore size, liquid entry pressure and mechanical tests. Coating stability was evaluated during time using salty solution NaCl 0.6M and with chemicals cleaning agents (KMnO4 0.1wt%, Hypochlorite NaClO pH 4.25, HCl pH 2.5, NaOH pH 11.5). Experiments in DCMD were carried out in order to evaluated membranes performance.

4.2. Experimental

4.2.1 Materials

Fluorolink® MD700 (PFPE backbone Mw = 1500 g mol^{-1}) was supplied form Solvay Specialty Polymers S.p.A., Bollate (Italy). Its chemical structure is reported in Fig. 1. Butyl acetate, 2-Propanol (IPA), 2-Hydroxy-2-methylpropiophenone (Darocure 1173), $KMnO_4$, NaClO, NaOH, HCl, hexadecane C_{16} and Sodium chloride were purchased from Sigma-Aldrich and used without any further purification. Liquid nitrogen was purchased from Pirossigeno (Italy). Polyamide PA, and Polyethersulfone PES (0.1-0.22-0.45µm) were supplied from Sterlitech (USA).

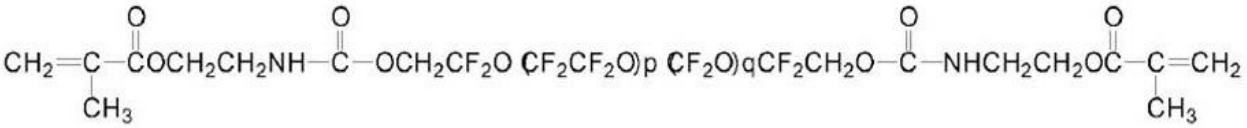

Figure 1: Chemical structure of Fluorolink® MD700

4.2.2 Polymeric dope solution preparation

Fluorolink® MD700 solution was prepared using 5wt.% of oligomer concentration. Butyl acetate was used as solvents and Darocure 1173 was used as photo-initiator (1wt.%)**.** The solution was stirred for 2h at a room temperature until complete dissolution of the oligomers was achieved. This solution was allowed to degas for 30' before using it.

4.2.3 Coated membrane preparation by Dip-Coating and In-situ polymerization

Commercial membranes, used as supporting material, were dipped into the oligomer solution for 10 min, and dried over-night. The coated membranes were exposed for 5 min at UV lamp (500Watt - Purchased from Helios Italquartz LTD), in order to activate the photo-initiator in polymerization reaction. The un-polymerized oligomer was removed washing the coated membranes using a solution of butyl acetate for 10 min. The membranes were then dried in air, and put in an oven, at 40°C, over-night.

The scheme of the membrane coating preparation is shown in Fig.2.

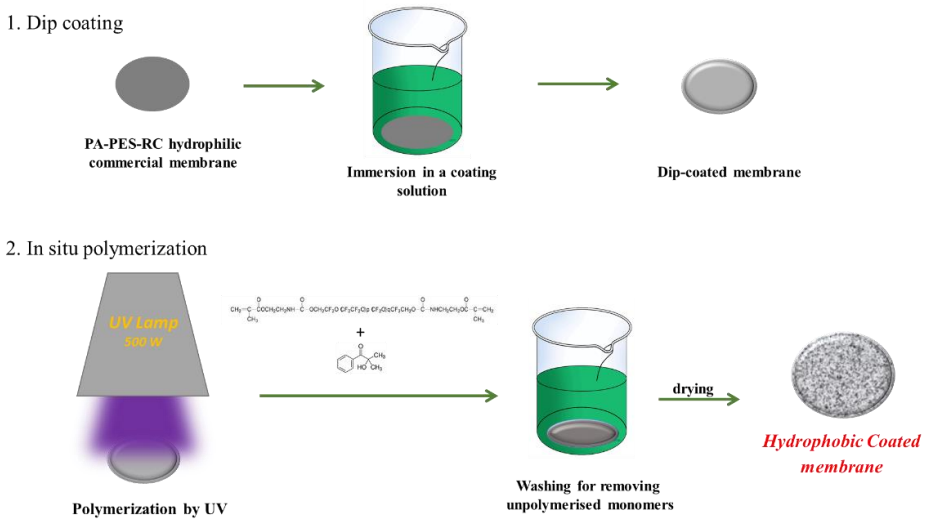

Figure 2. Dip-coating/ In situ polymerization procedure using Fluorolink® MD700

4.3 Membrane characterization

4.3.1 Electron Probe Microanalyzer (EPMA)

The morphology of the coated membranes (cross section, top and bottom side) was observed by using the Electron Probe Microanalyzer (EPMA) (JXA-8230, Jeol, USA). To obtain a clear cross-section, membranes samples were freeze fractured in liquid nitrogen. Sample specimens were sputter-coated with a thin graphite film prior to observation.

4.3.2 Atomic Force Microscopy (AFM)

Atomic force microscopy was used to study the surface morphology and roughness of the prepared membranes. The AFM device was a Bruker Multimode 8 with Nanoscope V controller. Data were acquired in tapping mode, using silicon cantilevers (model TAP150, Bruker). The coated membrane surfaces were imaged in a scan size of 10 µm x 10 µm.

4.3.3 Contact Angle

The hydrophilic/hydrophobic and oleophobic nature of the membrane was evaluated using CAM200 as instrument. The measurements were performed using ultrapure water (72,1 mN m^{-1}), and hexadecanoic acid C_{16} (28,1 mN m^{-1}) (5µL). For all membranes, at least five measurements were taken the average value and the corresponding standard deviations were calculated.

4.3.4 Liquid entry pressure of water measurements (LEP_w)

LEP_w set-up was described in Figoli et al. [7] (section 2.4.4.). To determine the LEP_w, the cell was filled with water (trans-membrane pressure (TMP)), and the experiments were carried out by applying different pressures of nitrogen, which was in contact with the coated side of the membrane. LEP_w was the TMP value at which the liquid water started to permeate in the other side of the cell (kept at atmospheric pressure). For all membranes, at least 5 measurements were taken; the average value and the corresponding standard deviation were, then, calculated.

4.3.5 Porosity

Membranes porosity was calculated by measuring the void fraction, i.e., is the volume of the pores divided by the total volume of the membrane, by the gravimetric method reported in literature [7,27,28]. Dry membrane samples were weighed and impregnated in 2-propanol for 24h; before the test, in order to remove the residual liquid, membrane was blotted using tissue paper, and after, membranes weight was measured again. Finally, the porosity was calculated applying to this formula:

$$\varepsilon(\%) = \left\{\frac{(Ww-Wd)/\rho i}{(Ww-Wd)/\rho i+(\frac{Wd}{\rho P})}\right\} x\ 100 \quad (1)$$

Where W_w is the weight of the wet membrane, W_d is the weight of the dry membrane, ρ_i is the 2-propanol density (0.78 g/cm^3) and ρ_P is the polymer density (PA 1.13 g/cm^3- PES 1.37 g/cm^3). For all membranes, three measurements were performed; then, the average values and corresponding standard deviation were calculated.

4.3.6 Bubble point and pore size measurement

The mean pore size, bubble point and distribution in coated membranes were determined using a PMI capillary flow porometer (Porous Materials Inc., CFP 1500, A6XL, USA). 2-propanol was used as wetting liquid (21.7 dyne/cm). The operating mode used was wet-up/dry-up method. The measurement of bubble point, largest pore size and pore size distribution is based on the Laplace's equation:

$$dp = 4\ \tau \cos\theta / P \quad (2)$$

where dP is the pore diameter, τ is the surface tension of the liquid, θ is the contact angle of the liquid (assumed to be 0 in case of full wetting, which means $\cos\theta = 1$) and P is the external pressure.

4.3.7 Mechanical tests

The Young's or elastic modulus (Emod), the tensile stress at break (Rm) and breaking elongation or stress at break (eBreak) were measured by means of a ZWICK/ROELL Z 2.5 test unit. Each sample

was stretched unidirectionally at a constant rate of 5 mm/min; the initial distance between the clamps was of 50 mm. Five specimens were tested for each sample.

4.3.8 Coating stability

Coating stability was evaluated by exposing membranes at different hard conditions, some of these, usually used as cleaning procedures [29]. Samples were kept totally immersed in one of the following solution: NaCl 0.6M, KMnO4 0.1wt%, Hypochlorite NaClO pH 4.25, HCl pH 2.5, NaOH pH 11.5. Coating stability in NaCl, was evaluated during time. CA measurements was carried out every 7 days for 4 weeks. Salty solution was used in order to investigate the membranes strength for desalination treatment. Coating stability in chemicals cleaning agents was evaluated with different protocols: concerning KMnO4 0,1wt%, membranes were immersed for 1h. After this time, membranes were washed and dried. Membranes treatment in NaClO, HCl and NaOH were conducted overnight, and after this time were washed using hot water (60°C) for three times and dried.
After each treatments, the presence and stability of the coating was analysed by water contact angle measurements. Before each test, membrane was washed using deionized water and dried.

4.3.9 DCMD experiments

The membrane module consisted of a cell in which the membrane was placed between two chambers (feed and permeate sides). Deionized water was used at the permeate side (cold side), and as feed (hot side). The feed was kept in contact with the hydrophobic coating layer (active side) and the cold permeate was in contact with the hydrophilic side of the membrane. The effective membrane area was 4 cm^2. The cold permeate side was kept at 14±0.5 °C, while the feed side was constantly heated (±0.5 °C) at the desired feed temperature (40-50-60°C). The bulk feed and permeate temperatures were measured, after steady state was reached, using thermocouples. The pressure of the hot and cold side was measured using two manometers (0-1 bar). The flow-rate (Q) of the feed and permeate side (80 and 60 L/h, respectively) was measured using ASA flow meters. The DCMD set-up was reported in Fig. 3. All experiments were repeated three times and the average values and corresponding standard deviation were calculated.

Water vapor flux (J), through the coated membranes, was defined as the quantity permeated per unit of area and per unit of time. The flux was calculated by Eq.3:

$$J = \frac{m\ (kg)}{m^2 * h} \quad (3)$$

Where m (kg) was the mass of permeate recovered at the cold side and measured by a balance (resolution: 0.1 g), m^2 was the membrane area, and h was the operating time.

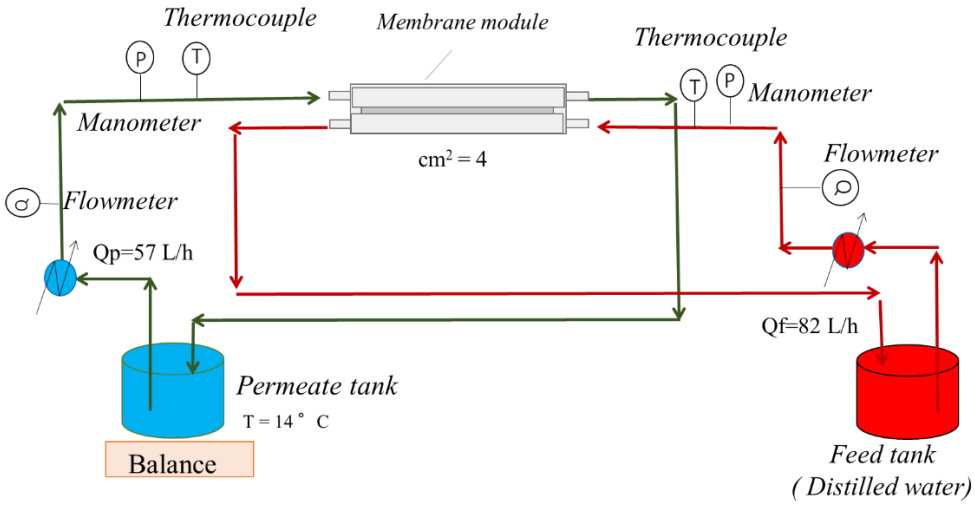

Figure 3. DCMD set-up

4.4. Results and discussion

4.4.1 Coated membrane preparation

Fluorolink® MD700 dope solution was prepared as reported in section 4.2.2. The commercial polyamide (PA), and polyethersulfone (PES) membranes, having different pore size (0.1; 0.22; 0.45 µm), were used as support. The dip-coating/ in-situ polymerization procedure was described in section 4.2.3. The photopolymerization kinetic, reported by Vitale et al. [26] shows that in correspondence of the highest conversion, PFPE methacrylate gives a fully crosslinked material where the residual presence of uncured monomers is negligible (gel content = 97%).

All the coated membranes prepared are reported in Table 1.

Table 1: Coated Fluorolink® MD700 membranes prepared using PA and PES commercial membranes as support

Membrane type	Material	Pore size (µm)	Oligomer concentration (wt%)	Solvent
COATED PA-01	PA	0.1	5	BUTYLACETATE
COATED PES-01	PES			
COATED PA-22	PA	0.22	5	
COATED PES-22	PES			
COATED PA-45	PA	0.45	5	
COATED PES-45	PES			

4.4.2 Membranes Characterization

- EPMA, AFM and contact angle analyses

Morphology of the commercial PA and PES membranes, with and without coating, were analysed using Electron Probe Microanalyzer. In order to study the presence of Fluorolink® MD700, in Fig. 4, the cross section and top side of commercial membranes (a), and cross section and top side of the coated membrane (b), is reported. As it can be seen, commercial PA and PES membranes present a sponge porous structure.

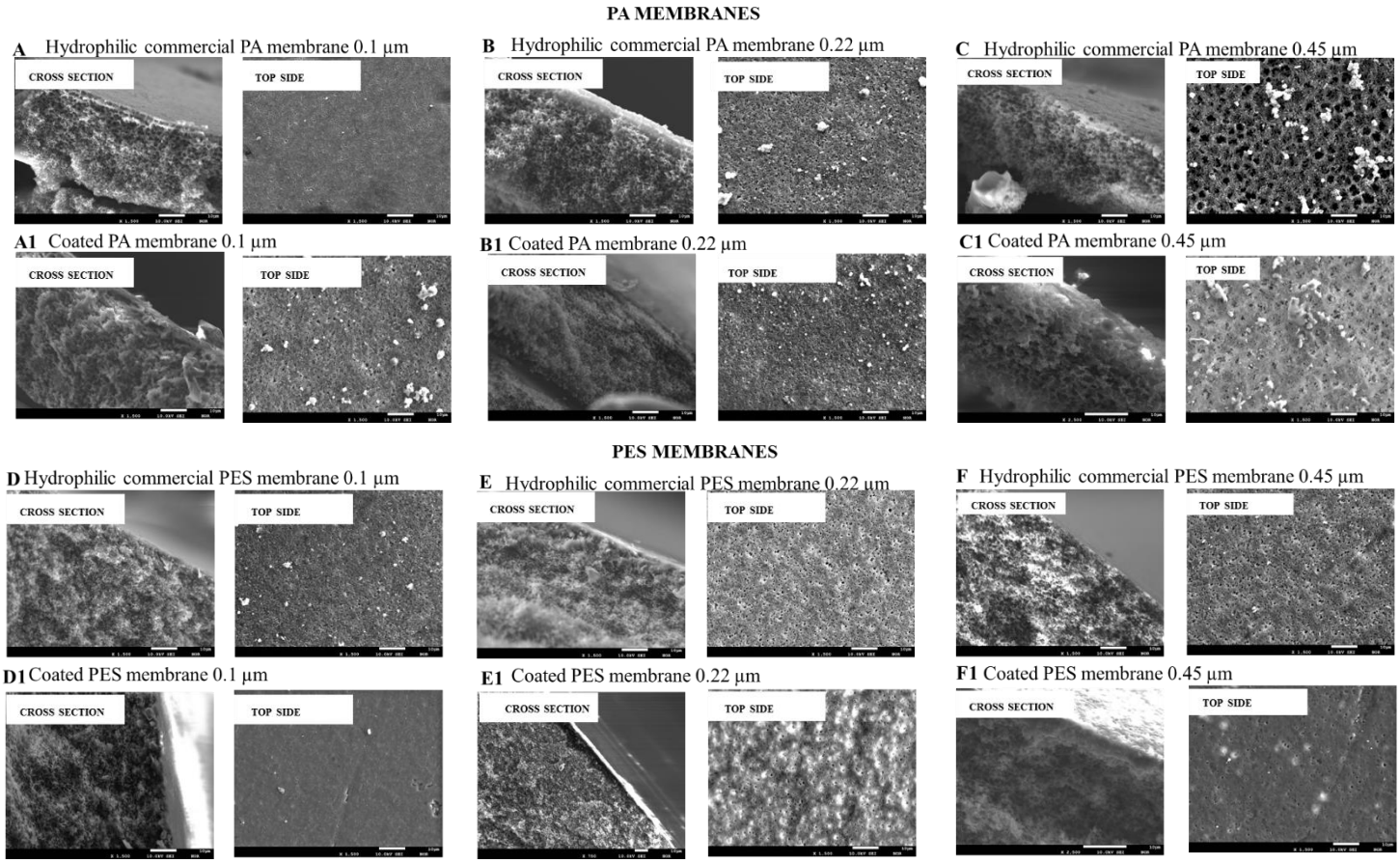

Figure 4. Morphology of PA and PES membranes with (A1-F1) and without (A-F) coating at different pores size (pore size 0.10-0.22-0.45µm)

The pictures of coated membranes show that the coating did not completely cover the pore structure of the starting membranes. However, looking at the cross sections, it is possible to observe the presence of the coating layer, in all cases. This result is more visible when membrane with pore size of 0.1µm were used (Fig. 4, A and D), in fact the thickness increases from 110 to 125 µm for PA membranes, and from 152 to 161 µm for PES membranes.

The membrane surface properties were investigated using AFM. The topography was measured on five different areas of the sample surface and the RMS roughness (Sq), roughness average (Sa), and

peak to peak value (Sz) were calculated. The obtained data and the respectively standard deviation are reported in Table 2.

Table 2: Surface roughness of PA and PES (0.1-0.22-0.45µm) with and without coating

Membranes	Material	Roughness average Sa (µm)	RMS Sq (µm)	Peak to peak Sz (µm)
Commercial PA 0.1 µm	PA	0,07 ± 0,01	0,09 ± 0,01	1,07 ± 0,26
COATED PA-01		0,10 ± 0,1	0,17 ± 0,1	1,71 ± 0,13
Commercial PA 0.2 µm		0,11 ± 0,01	0,14 ± 0,01	1,11 ± 0,13
COATED PA-22		0,13 ± 0,2	0,17 ± 0,2	1,55 ± 0,1
Commercial PA 0.45 µm		0,21 ±0,08	0,26 ±0,1	2,01 ±0,8
COATED PA-45		0,15 ± 0,02	0,21 ± 0,04	2,06 ± 0,6
Commercial PES 0.1 µm	PES	0,03 ± 0	0,04 ± 0	0,44 ± 0,12
COATED PES-01		0,03 ± 0	0,03 ± 0	0,38 ± 0,02
Commercial PES 0.2 µm		0,06 ± 0	0,10 ± 0	0,98 ± 0
COATED PES-22		0,06 ± 0	0,08 ± 0	0,78 ± 0,07
Commercial PES 0.45 µm		0,06 ± 0	0,08 ± 0	0,79 ± 0,06
COATED PES-45		0,06 ± 0	0,08 ± 0	0,78 ± 0,07

Based on the images, shown in fig.6, and the data reported in Table 2, it was possible to observe that:

- The roughness increases when PA membranes with pore size of 0.1 and 0.22 were used as starting materials.
- In all cases, when membranes at 0.45 µm (PA and PES) were used as starting materials, the coating layer did not modified the roughness.
- The roughness of the PES membranes (0.1-0.22-0.45 µm), has not been affected by the coating layer. In all cases the surface was smooth (RMS S_q from 0.10 to 0.03 µm).

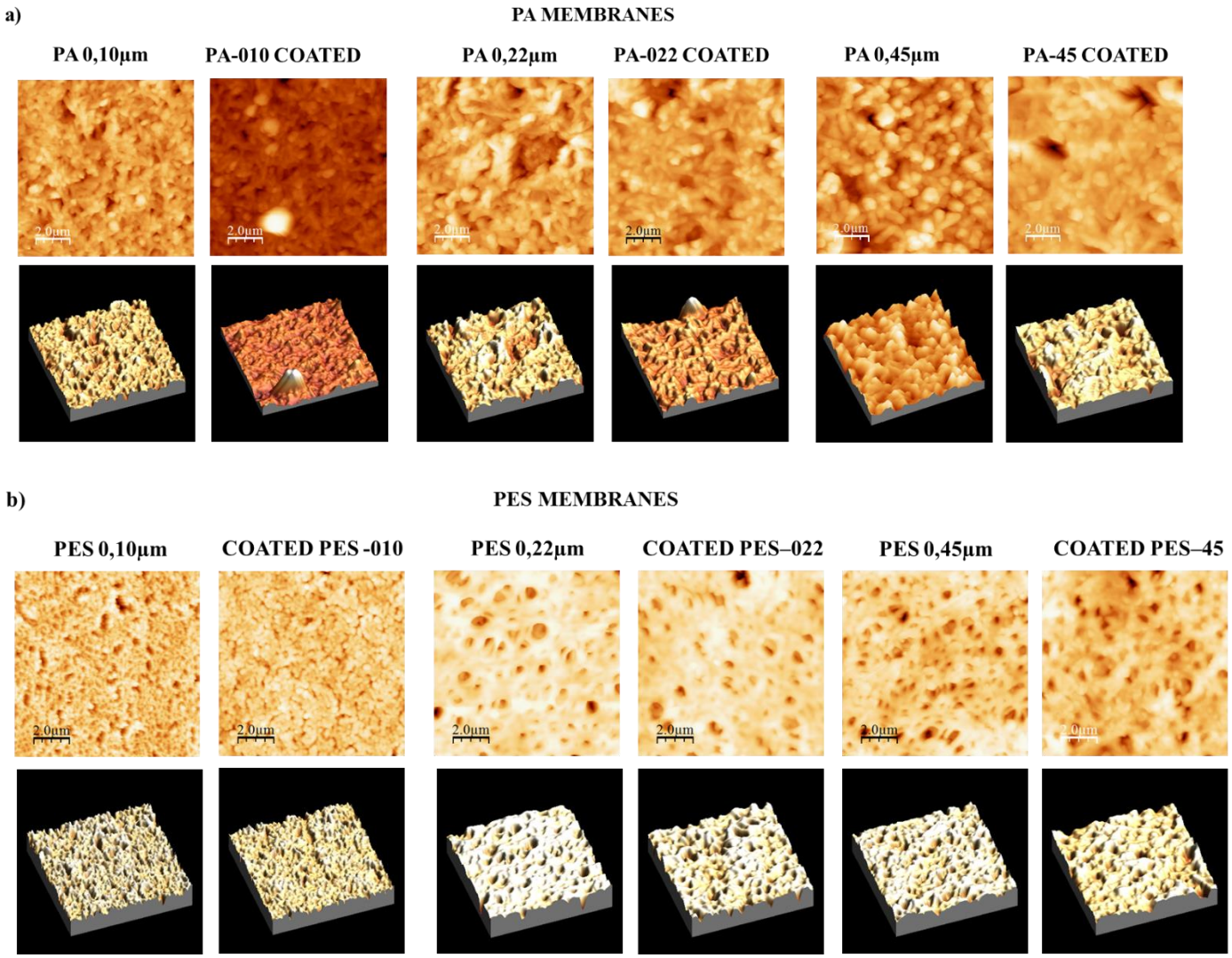

Figure 6. a) AFM images of PA commercial membranes (0.1-0.22-0.45µm) and coated PA membranes with of Fluorolink® MD700; b) AFM images of PES commercial membranes (0.1-0.22-0.45µm) and coated PES membranes with of Fluorolink® MD700

Contact angle (CA) measurements confirmed the presence of Fluorolink® MD700 on membranes surface. Water/oil repellence was studied by measuring the contact angle of the substrate with water and hexadecanoic acid C_{16} as liquids. Correlation of CA and roughness was analysed according to Wenzel equation [30]:

$$\cos \theta^* = \cos \theta \times r \quad (4)$$

Where θ is the Young's angle and r the surface area of the solid.

According to this equation, hydrophobicity is reinforced by roughness [31]. The water CA results for the different membranes produced are shown in Fig.5. The wettability of the membranes does not change over time, as already reported by Figoli et al [7]. Looking at the graphs it is possible to

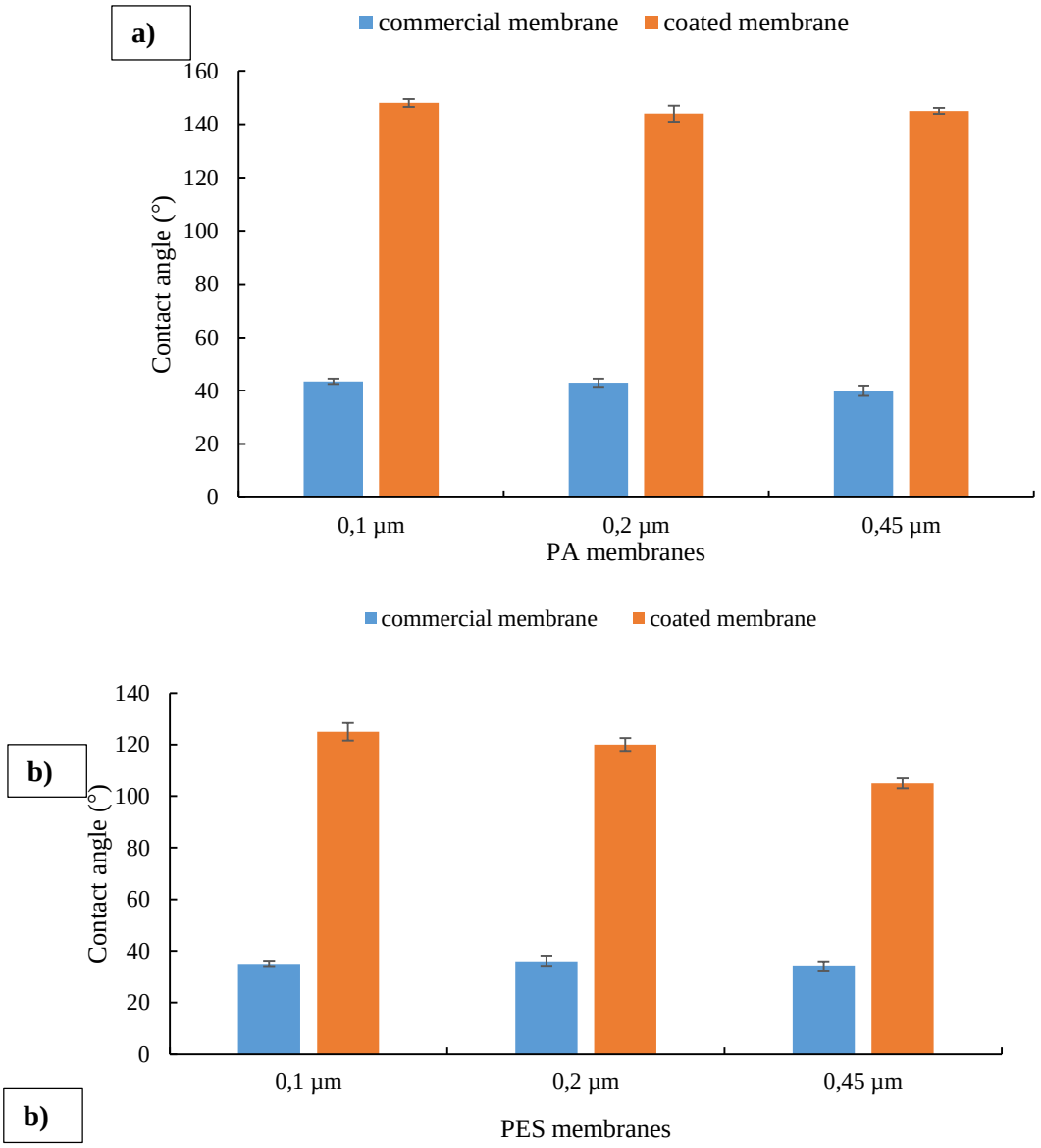

Figure 5. a) Contact angle for PA membranes (0.1-0.22-0.45µm) with and without coating; b) Contact angle for PES membranes (0.1-0.22-0.45µm) with and without coating

observe that in all cases, starting from hydrophilic commercial membranes, hydrophobic coated membranes were obtained. Water CA, was up to 140° for PA coated membranes, and up to 100° for PES coated membranes. The low CA obtained for PES coated membranes, could depend by the photo-degradation of the PES membranes during the UV treatment [32]. According to EPMA images (fig.4 A and D), higher contact angle was obtained using membranes at 0.1µm, this result could be explained by the thicker coated layer, that increases the presence of PFPE on membrane surface.

Contact angle results using hexadecane C_{16} is reported in Table 3.

Table 3. Contact angle results *vs* hexadecane C_{16} of PA and PES membranes with and without coating

Membranes	**Contact angle (C_{16})**
Commercial PA 0.1 µm	33 ± 0,5
COATED PA 0.1 µm	96,1 ± 0,9
Commercial PA 0.22 µm	34 ± 0,7
COATED PA 0.22 µm	91 ± 1,4
Commercial PA 0.45 µm	32 ± 1,5
COATED PA 0.45 µm	93 ± 1,8
Commercial PES 0.1 µm	28 ± 1
COATED PES 0.1	70 ± 0,9
Commercial PES 0.22 µm	27 ± 1,4
COATED PES 0.22	72,5 ± 1,4
Commercial PES 0.45 µm	27 ± 0,8
COATED PES 0.45	68 ± 1,2

The results confirmed that the coating treatment increases the oleophobicity of the membranes, in particular a CA_{C16} around 96° was obtained for Fluorolink®MD700 PA 0.1 µm membrane. Coated membranes are both hydrophobic and oleophobic: in all cases water contact angle was higher than 90° and the angle with hexadecane C_{16}, indicate good oleophobicity [26].

- Liquid entry pressure of water measurements (LEP_w)

LEP is defined as the pressure difference at which the liquid wets the hydrophobic membrane, its value depends on the maximum pore size and the membrane hydrophobicity. As expected, the highest LEP results were achieved using membranes at 0.1µm. The LEPw values are in the range of 4-3 bar for PA coated membranes and in the range of 4-1,9 for PES coated membranes. The results of LEPw measurements of the commercial PA and PES and related coated membranes are shown in Fig.6.

a)

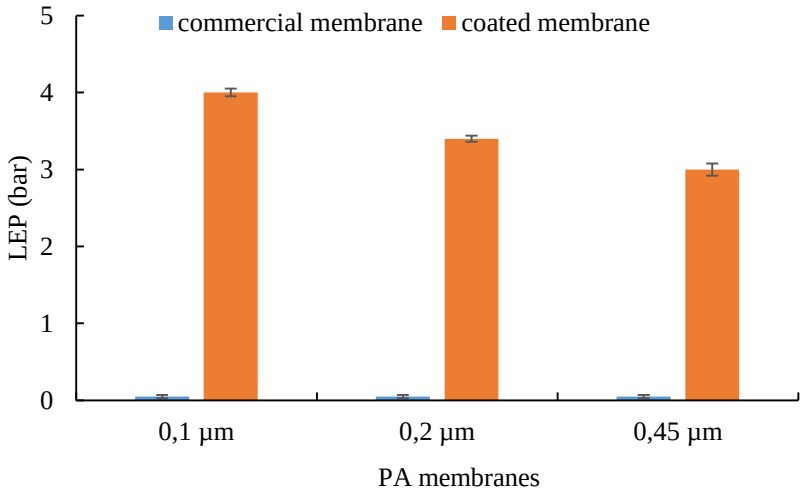

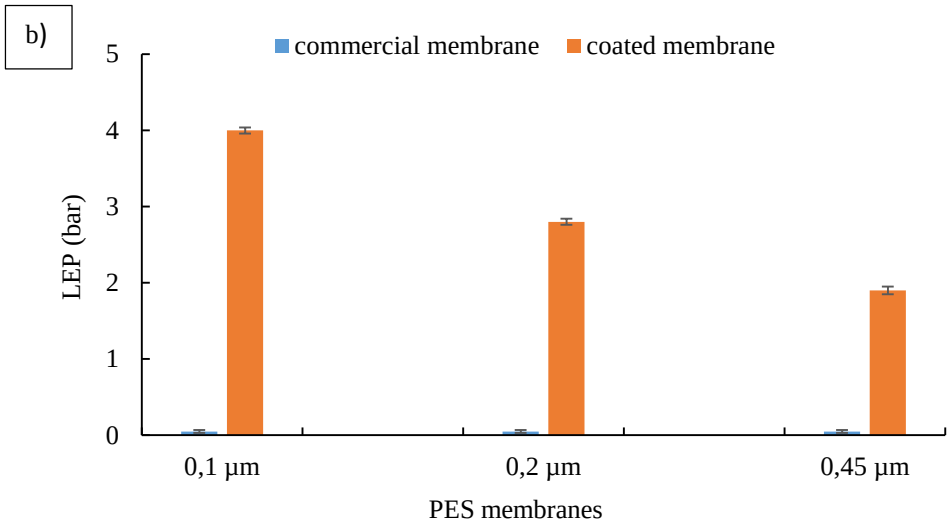

Figure 6. a) LEP_w measurements of PA membranes and PA membranes (0.1-0.22-0.45µm, pore size) coated with Fluorolink®MD700; b) LEP_w measurements of PES membranes and PES membranes (0.1-0.22-0.45µm, pore size) coated with Fluorolink®MD700

- Porosity and Pore size measurements

In Fig.7, the porosity of the coated PA and PES membranes are reported. The data show a lower decrease of porosity for the coated membranes. This trend was more evident when PES commercial membranes were used as support. Using commercial membranes at 0.45µm no differences in porosity between membranes, with or without coating, was observed, probably because parts of the coating penetrates inside of the bigger pore size.

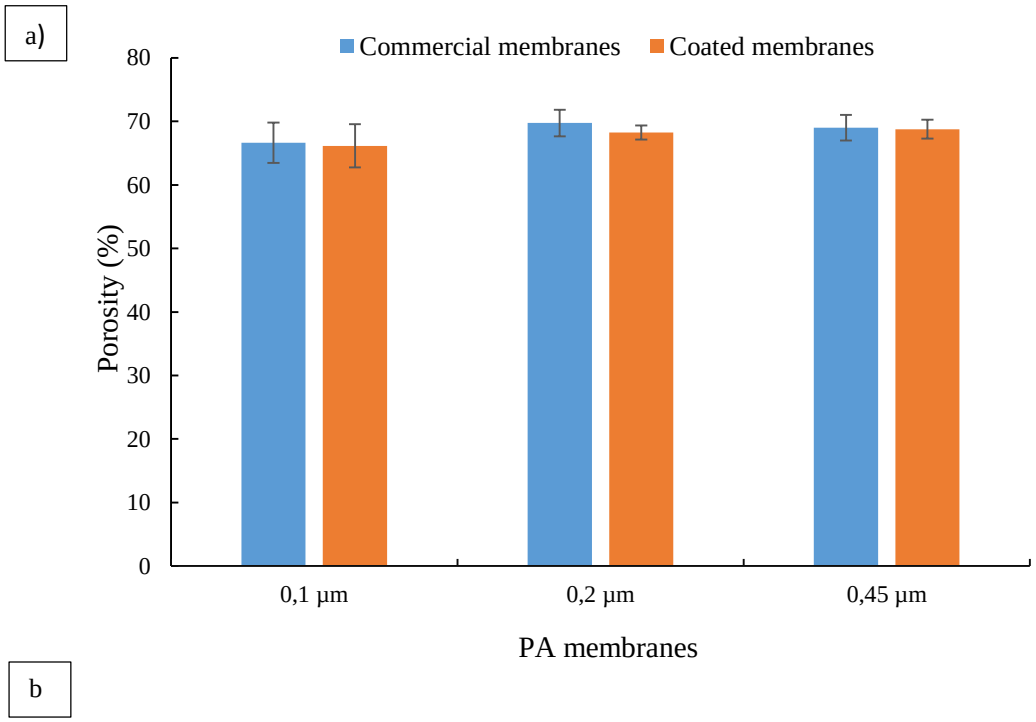

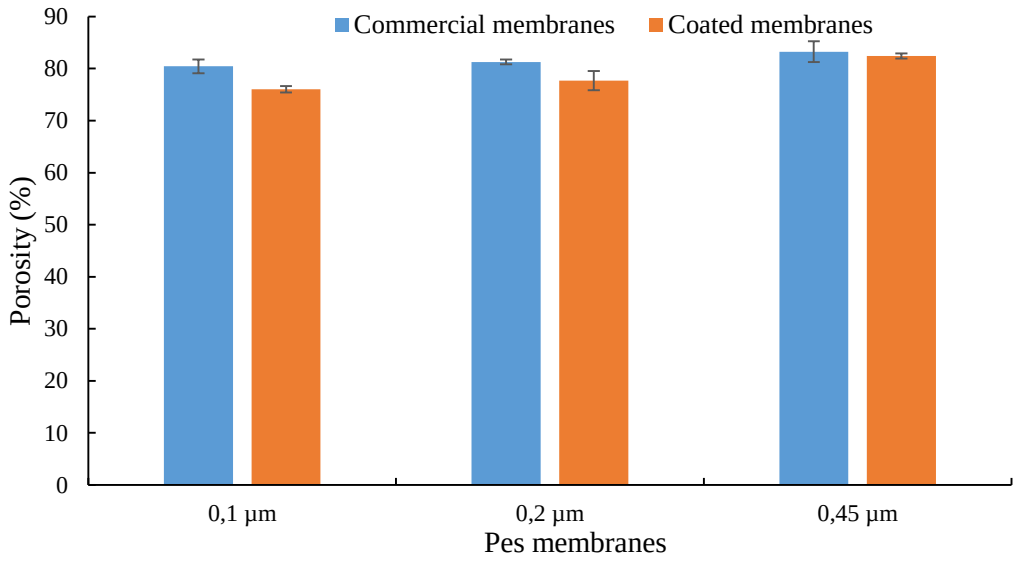

Figure 7. a) Porosity measurements for PA membranes (0.1-0.22-0.45µm); b) Porosity measurements for PES membranes (0.1-0.22-0.45µm), with and without Fluorolink® MD700

Table 4 shows the pore size analysis. The coated membranes show similar mean flow pore diameter and diameter at maximum pore size distribution than the unmodified membranes (commercial PA and PES membranes 0.45-0.22-0.1 µm). The mean pore size remains unchanged also when the thickness increases (PA 0.1 µm, from 110 to 125, and PES 0.1 µm, from 152 to 161 µm); this result suggests that the coating layer, even when the top layer increases, does not affect the pores size. The presence of the coating is only noticeable by the bubble point values, that increase after the treatments, in fact looking at the data, it is possible to observe that the largest detected pore diameters are partially covered.

Table 4: Bubble point and pore size distribution for Fluorolink® MD700 PA and PES coated membranes (0.1-0.22-0.45µm)

Membranes	Thickness (µm)	Bubble point (bar)	Largest detected pore diameter (µm)	Mean flow pore diameter (µm)	Diameter at maximum pore size distribution (µm)
Commercial PA 0.1 µm	110 ± 3	1,72	0,35	0,20	0,20
COATED PA-01	125 ± 3	1,60	0,38	0,18	0,17
Commercial PA 0.2 µm	124 ± 2	0,78	0,79	0,33	0,30
COATED PA-22	123 ± 3	1,51	0,40	0,33	0,27
Commercial PA 0.45 µm	114 ± 4	0,45	1,40	0,55	0,35
COATED PA-45	116 ± 1	1,39	0,44	0,35	0,35
Commercial PES 0.1 µm	152 ± 2	2,15	0,27	0,17	0,17
COATED PES-01	161± 4	2,08	0,29	0,16	0,16
Commercial PES 0.2 µm	124 ± 3	1,44	0,43	0,33	0,32
COATED PES-22	122 ± 0,5	1,65	0,37	0,33	0,14
Commercial PES 0.45 µm	141 ± 3	0,87	0,71	0,49	0,42
COATED PES-45	142 ± 5	1,30	0,48	0,40	0,33

*the error was less 5% in all cases

- Mechanical tests

In order to evaluate if the coating treatment affected the mechanicals properties of the membranes, mechanical tests were carried out. The obtained data were reported in Table 5. The data show that in all cases the Young Moduls (elastic modulus, N/mm^2), defined as the relationship between stress and strain, decrease for the coated membranes, although maintaining higher values. This result indicates that the membranes elasticity did not change in comparison with pristine membranes. Elongation at break (ε Break), also known as fracture strain, is the ratio between changed length and initial length after breakage of the sample. It expresses the capability of a material to resist changes of shape without crack formation. Compared the obtained results for PA and PES membranes, mechanical properties are also not modified by the coating treatment.

Table 5: Young moduls, tensile-strenght and ε Break for Fluorolink® MD700 PA and PES coated membranes (0.1-0.22-0.45μm)

Membranes	**Material**	**Young moduls (N/mm^2)**	**Tensile-strength (N/mm^2)**	**ε Break (%)**
Commercial PA 0.1 μm		602 ± 12	25 ± 2	30 ± 6
COATED PA-01		446 ± 50	18 ± 0,6	21 ± 4
Commercial PA 0.2 μm		464 ± 41	18 ± 2	23 ± 4
COATED PA-22		340 ± 17	10 ± 1	19 ± 4
Commercial PA 0.45 μm		411 ± 20	16 ± 2	45 ± 1,5
COATED PA-45		372 ± 15	13 ± 0,3	50 ± 3
Commercial PES 0.1 μm	PES	148 ± 10	4 ± 0,4	19,6 ± 4
COATED PES-01		110 ± 0,9	5,5 ± 0,2	30 ± 2
Commercial PES 0.2 μm		192 ± 8	6 ± 0,3	27 ± 0,3
COATED PES-22		183 ± 13	7 ± 0,2	34 ± 3
Commercial PES 0.45 μm		130 ± 1	4 ± 0,2	26 ± 4
COATED PES-045		115± 5	4 ± 1	28 ± 2,4

- Coating stability

Coating stability was evaluated by exposing coated membranes at NaCl 0.6 M, as typical feed in desalination treatment, and at several common chemical cleaning agents, including caustic (NaOH pH 11.5), acidic (HCl pH 2.5; HClO pH 4,25), oxidative (KMnO4 1wt.%) and disinfectants (NaClO pH 4,25) [33]. The results were showed in fig.8 and fig.9.

Treatment in NaCl 0.6M

Fig.8 show the CA results, after treatment in salty solution. Looking the data, it is possible to observe that for PA coated membranes, the treatment in salty solution did not affected the contact angle during time. On the contrary, for PES coated membranes, contact angle decreases depending of the pore size,

from 125° to 101° for PES-01, from 120° to 96° for PES-022 and from 105° to 95° from PES-045. Nevertheless contact angle decreases, the results show that the membranes keep their hydrophobic nature (CA >90°).

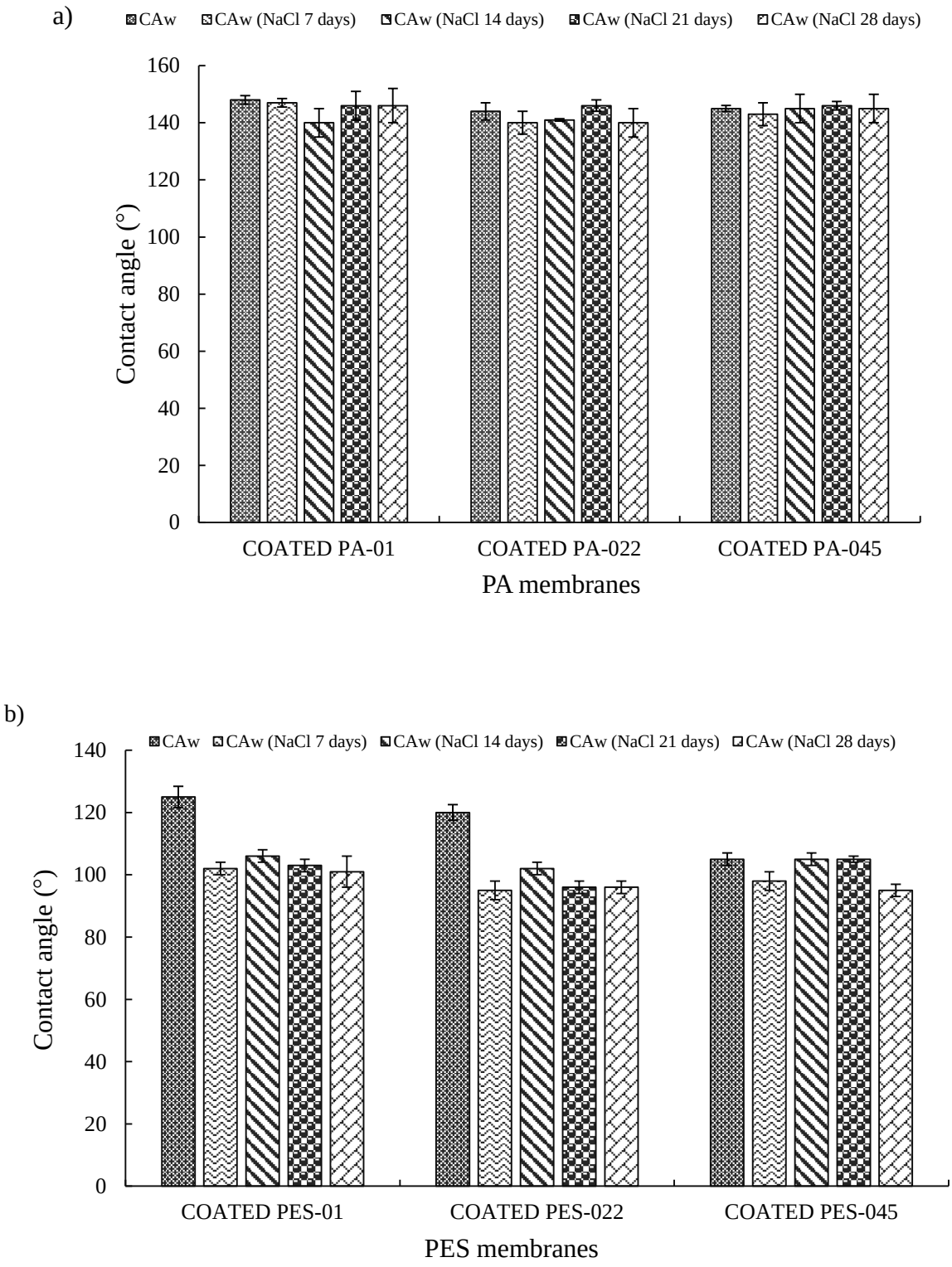

Figure 8. a) Water contact angle results of PA and b) PES coated membranes (0.1-0.22-0.45µm) after and before the treatment in NaCl 0.6M

Chemical cleaning agents

In order to study the influence of the pore size on the coating stability during chemical cleaning, membranes with 0.1 and 0.45 µm were used for these tests. The results of chemical cleaning treatments were reported in fig.9. These treatments were carried out in order to evaluate the performance of coated membranes after the typically chemicals cleanings. In fact, sodium hydroxide, NaOH, encourages dissolution of weakly acidic organic matter, with the generally carboxylic and phenolic functional groups, and promotes cleavage of polysaccharides and proteins into smaller sugars and amides. Acid cleaning aims to remove multivalent cationic species such as in hardness salts and metal hydroxide, moreover acids are mildly oxidative for natural organic matter (fouling), forming soluble aromatic aldehydes [34]. $KMnO_4$ was firstly introduced as a water treatment chemical in 1913 [35]. Generally used as oxidant, where organic compounds are oxidized into water and carbon dioxide (or alcohols, aldehydes, ketones and carboxylic acids) which are easily biodegradable. Using oxidant treatment, phenols, ammonia, dyes, hydrocarbons and other organic pollutants may be removed from the membrane surface. [36]. Sodium hypochlorite generally was used as disinfectant, against bacteria, viruses and fungi.

As reported for the treatment in NaCl 0.6M, the results show that for PA coated membranes, the treatment with chemical cleaning agents, did not affected the contact angle. On the contrary, CA decreases for coated PES membranes, always remaining hydrophobic (>90°).

a)

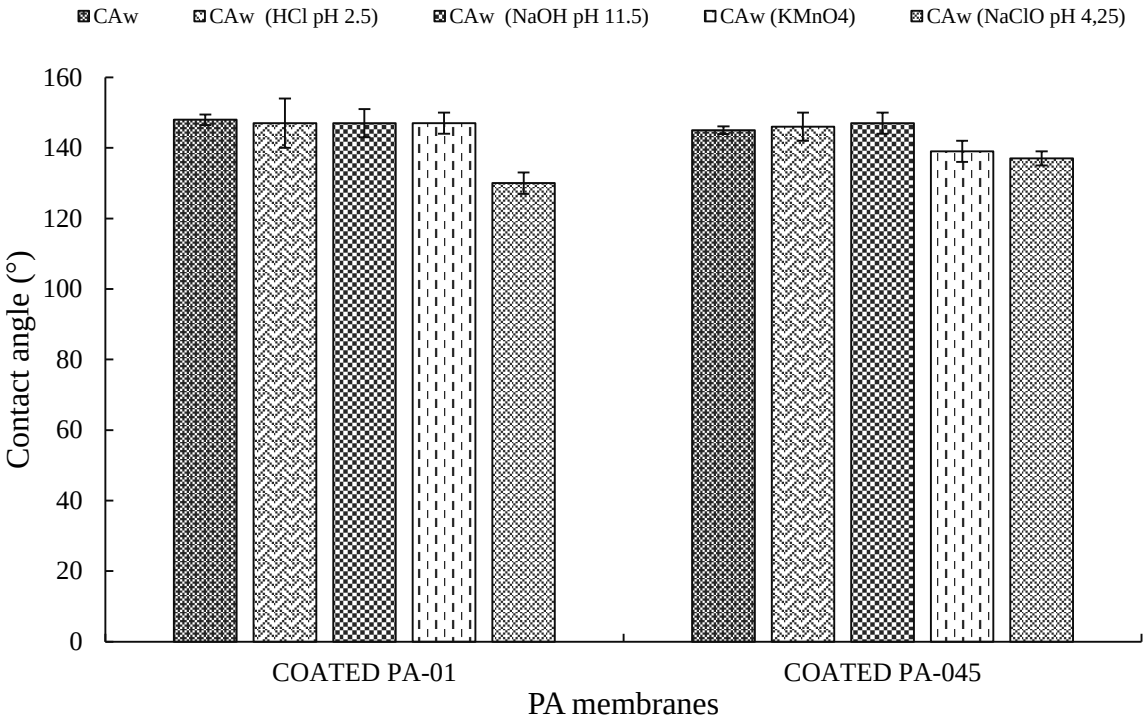

b)

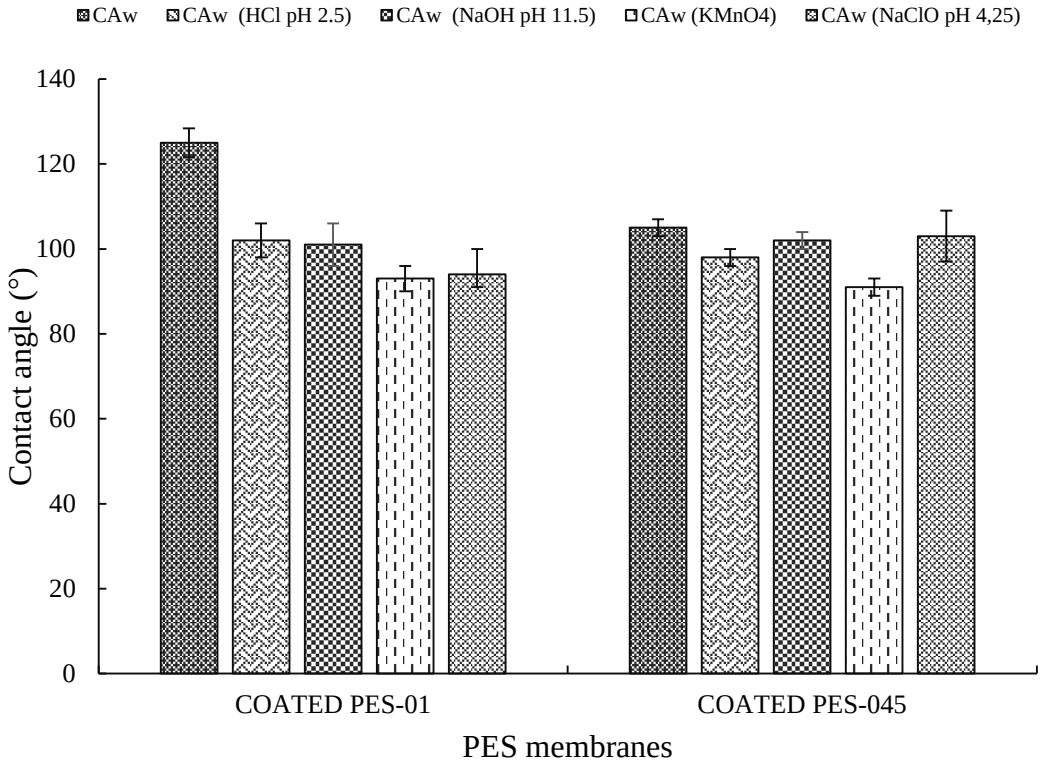

Figure 9. Water contact angle results of PA a) and PES b) coated membranes (0.1-0.45µm) after and before the treatment in chemical cleaning agents

- DCMD tests

Coated membranes performance was determined with DCMD experiments. DCMD tests were carried out using deionized water as feed (from 40°C to 60°C). The hydrophobic coated side of

the membrane was in contact with the hot feed, while the hydrophilic side of the membrane was in contact with cold water at 14°C.

In Fig.10, the results of the DCMD tests with deionized water as feed are reported varying the starting material (PA and PES) and the temperatures of the feed side.

a)

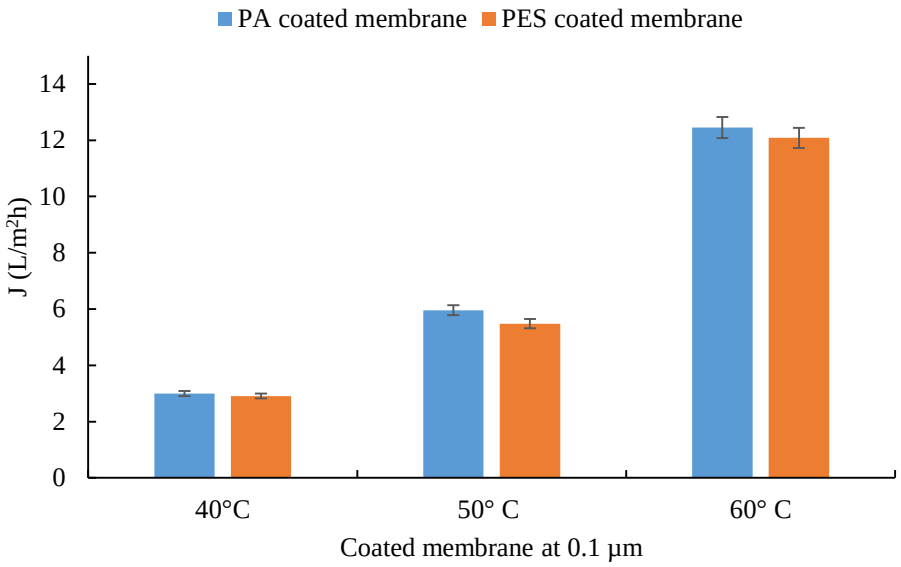

b)

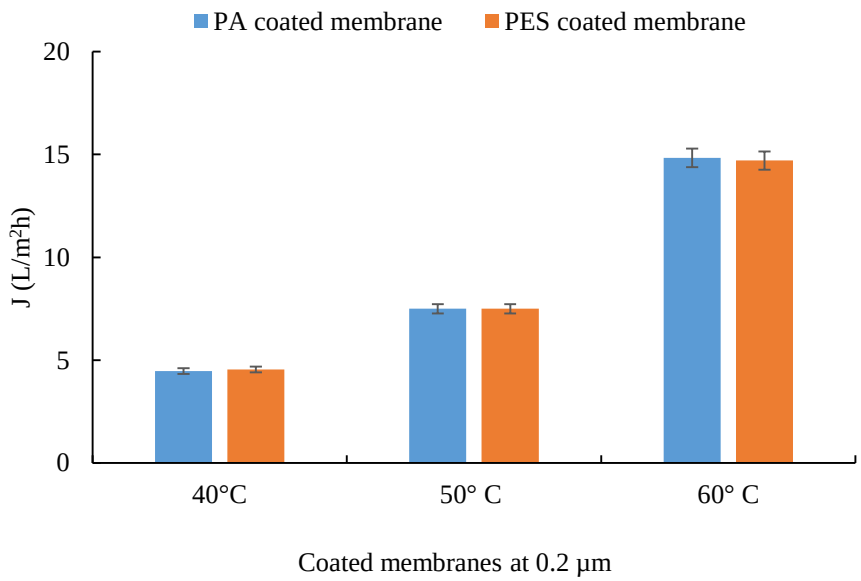

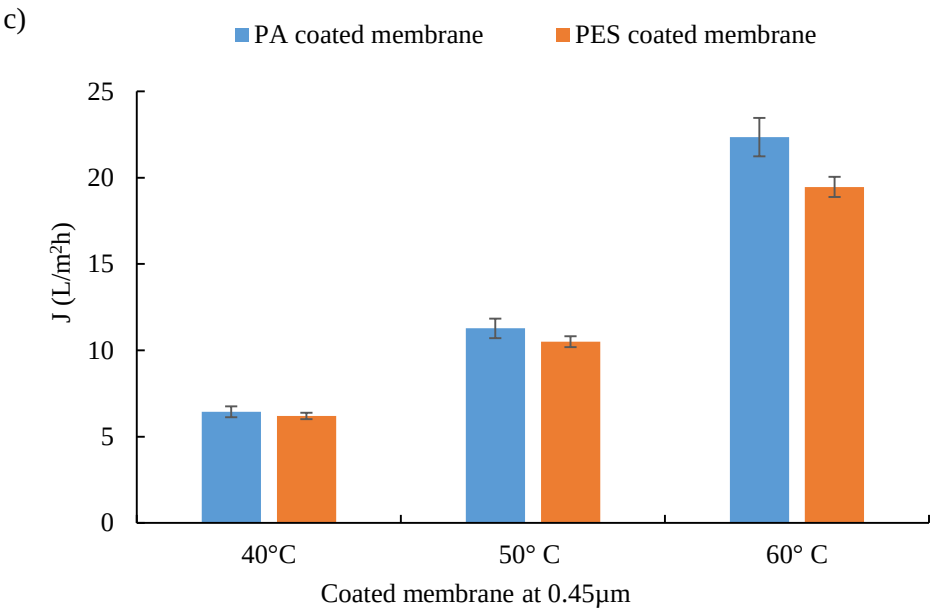

Figure 10. DCMD results for Fluorolink ® MD700 coated membranes using PA and PES as starting materials of different pore size: a) 0.1µm b) 0.22 µm and c) 0.45 µm

As reported in the graphs, in all cases the flux increased with the feed temperature as expected [7,19]. Looking at the data, it is possible to observe that the starting material did not influence the flux when membranes at 0.1 and 0.2 µm are used. The results are comparable, considering the smaller pore size of the membranes. For coated membranes having a pore size of 0.45µm, PA coated membranes show a higher flux (around 22 L/m^{2}h at 60°C), than PES coated membranes (around 19 L/m^{2}h at 60°C). This result is comparable with the flux reported by Figoli et al. [7], using PA 0.45µm pore size membranes coated awith Flurolink®AD1700 (22.81 L/m^{2}h at 60°C).

Conclusions

Innovative hydrophobic/hydrophilic composite membranes were prepared by dip-coating/in situ polymerization using Flurolink® MD700 on commercial membranes. The influence of the starting material (PA and PES) was studied and the use of different pore sizes (0.1, 0.22 and 0.45 μm) has been investigated too. The characterization tests show that the coating has been successfully performed on the membranes. The coating increased the hydrophobicity of the membranes in all cases, and the best results was obtained for PA membranes, with a water CA of about 148°. CA *vs* Hexadecane C_{16} confirmed that the coating increases the oleophobicity of the membranes too. The presence of the hydrophobic coating layer was confirmed by the EPMA images, and as reported by the pore size analysis and AFM pictures, without any change in the membranes morphology. Highest LEP_w results were achieved for both PA and PES coated membranes with pore size of 0.1μm. Coating stability tests show that PA coated membranes are more resistant than PES coated membranes, in fact the treatment with chemical cleaning agents and salty solution 0.6M, did not affected the CA. Coating stability tests, and DCMD tests demonstrated the good performance of the membranes and the potential use in desalination. During tests with deionized water, coated PA membranes at 0.45μm presented the highest values of permeate flux (about 22 Kg/m^2h). The flux was also positively, influenced by increasing the temperature (from 40 to 60°C) and the pore size (from 0.1 to 0.45 μm) of the commercial membranes as reported. The starting membranes with lower pore size (0.1-0.22 μm), did not influence the vapour flux.

References

[1] M.G. Buonomenna, Smart composite membranes for advanced wastewater treatments, in: M.F. Montemor (Ed.), Smart Composite Coatings and Membranes, 1 edition, Elsevier Ltd, 2016: pp. 371–419. doi:http://dx.doi.org/10.1016/B978-1-78242-283-9.00014-2.

[2] M. Ulbricht, Advanced functional polymer membranes, Polymer. 47 (2006) 2217–2262. doi:10.1016/j.polymer.2006.01.084.

[3] A.P. Rao, S. V. Joshi, J.J. Trivedi, C. V. Devmurari, V.J. Shah, Structure-performance correlation of polyamide thin film composite membranes: Effect of coating conditions on film formation, Journal of Membrane Science. 211 (2003) 13–24. doi:10.1016/S0376-7388(02)00305-8.

[4] Drioli E. and Giorno L., Membrane Operations Innovative Separations and Transformations, WILEY-VCH, 2009.

[5] F. Galiano, A. Figoli, S.A. Deowan, D. Johnson, S.A. Altinkaya, L. Veltri, G. De Luca, R. Mancuso, N. Hilal, B. Gabriele, J. Hoinkis, A step forward to a more efficient wastewater treatment by membrane surface modification via polymerizable bicontinuous microemulsion, Journal of Membrane Science. 482 (2015) 103–114. doi:10.1016/j.memsci.2015.02.019.

[6] H. Guo, Y. Deng, Z. Tao, Z. Yao, J. Wang, C. Lin, T. Zhang, B. Zhu, C.Y. Tang, Does Hydrophilic Polydopamine Coating Enhance Membrane Rejection of Hydrophobic Endocrine-Disrupting Compounds?, Environmental Science & Technology Letters. 3 (2016) 332–338. doi:10.1021/acs.estlett.6b00263.

[7] A. Figoli, C. Ursino, F. Galiano, E. Di Nicolò, P. Campanelli, M.C. Carnevale, A. Criscuoli, Innovative hydrophobic coating of perfluoropolyether (PFPE) on commercial hydrophilic membranes for DCMD application, Journal of Membrane Science. 522 (2017) 192–201. doi:10.1016/j.memsci.2016.08.066.

[8] M. Qtaishat, M. Khayet, T. Matsuura, Novel porous composite hydrophobic/hydrophilic polysulfone membranes for desalination by direct contact membrane distillation, Journal of Membrane Science. 341 (2009) 139–148. doi:10.1016/j.memsci.2009.05.053.

[9] Y. Wu, Y. Kong, X. Lin, W. Liu, J. Xu, Surface-modified hydrophilic membranes in membrane distillation, Journal of Membrane Science. 72 (1992) 189–196.

[10] X. Wei, B. Zhao, X. Li, Z. Wang, B. He, T. He, B. Jiang, CF 4 plasma surface modification

of asymmetric hydrophilic polyethersulfone membranes for direct contact membrane distillation, Journal of Membrane Science. 408 (2012) 164–175. doi:10.1016/j.memsci.2012.03.031.

[11] M. Khayet, T. Matsuura, Application of surface modifying macromolecules for the preparation of membranes for membrane distillation, Desalination. 158 (2003) 51–56. doi:10.1016/S0011-9164(03)00432-6.

[12] E. Shaulsky, S. Nejati, C. Boo, F. Perreault, C.O. Osuji, M. Elimelech, Post-fabrication modification of electrospun nanofiber mats with polymer coating for membrane distillation applications, Journal of Membrane Science. 530 (2017) 158–165. doi:10.1016/j.memsci.2017.02.025.

[13] D. Zhao, J. Zuo, K.-J. Lu, T.-S. Chung, Fluorographite modified PVDF membranes for seawater desalination via direct contact membrane distillation, Desalination. 413 (2017) 119–126. doi:10.1016/j.desal.2017.03.012.

[14] J.E. Efome, D. Rana, T. Matsuura, C.Q. Lan, Enhanced performance of PVDF nanocomposite membrane by nanofiber coating: A membrane for sustainable desalination through MD, Water Research. 89 (2016) 39–49. doi:10.1016/j.watres.2015.11.040.

[15] D. Tong, X. Wang, M. Ali, C.Q. Lan, Y. Wang, E. Drioli, Z. Wang, Z. Cui, Preparation of Hyflon AD60/PVDF composite hollow fiber membranes for vacuum membrane distillation, Separation and Purification Technology. 157 (2016) 1–8. doi:10.1016/j.seppur.2015.11.026.

[16] M.S. El-Bourawi, Z. Ding, R. Ma, M. Khayet, A framework for better understanding membrane distillation separation process, Journal of Membrane Science. 285 (2006) 4–29. doi:10.1016/j.memsci.2006.08.002.

[17] M. Gryta, Long-term performance of membrane distillation process, Journal of Membrane Science. 265 (2005) 153–159. doi:10.1016/j.memsci.2005.04.049.

[18] J.T. Simpson, S.R. Hunter, T. Aytug, Superhydrophobic materials and coatings: a review, Reports on Progress in Physics. 78 (2015) 86501. doi:10.1088/0034-4885/78/8/086501.

[19] A. Criscuoli, M.C. Carnevale, E. Drioli, Evaluation of energy requirements in membrane distillation, Chemical Engineering and Processing: Process Intensification. 47 (2008) 1098–1105. doi:10.1016/j.cep.2007.03.006.

[20] E. Drioli, A. Ali, F. Macedonio, Membrane distillation: Recent developments and

perspectives, Desalination. 356 (2015) 56–84. doi:10.1016/j.desal.2014.10.028.

[21] A. Sanguineti, E. Di Nicolò, P. Campanelli, Coated Membrane Comprising Layer of Perfluoropolyether on Hydrophilic Substrate, WO 2013164287 A1, 2013.

[22] S. Ebnesajjad, Introduction to Fluoropolymers, Elsevier, 2011. doi:10.1016/B978-1-4377-3514-7.10004-2.

[23] R. Bongiovanni, G. Malucelli, A. Pollicino, C. Tonelli, G. Simeone, A. Priola, Perfluoropolyether structures as surface modifying agents of UV-curable systems, Macromolecular Chemistry and Physics. 199 (1998) 1099–1105. doi:10.1002/macp.1998.021990625.

[24] R. Bongiovanni, E. Zeno, A. Pollicino, P.M. Serafini, C. Tonelli, UV light-induced grafting of fluorinated monomer onto cellulose sheets, Cellulose. 18 (2011) 117–126. doi:10.1007/s10570-010-9451-5.

[25] B. Bertolotti, H. Messaoudi, L. Chikh, C. Vancaeyzeele, S. Alfonsi, O. Fichet, Stability in alkaline aqueous electrolyte of air electrode protected with fluorinated interpenetrating polymer network membrane, Journal of Power Sources. 274 (2015) 488–495. doi:10.1016/j.jpowsour.2014.10.059.

[26] A. Vitale, M. Quaglio, M. Cocuzza, C.F. Pirri, R. Bongiovanni, Photopolymerization of a perfluoropolyether oligomer and photolithographic processes for the fabrication of microfluidic devices, European Polymer Journal. 48 (2012) 1118–1126. doi:10.1016/j.eurpolymj.2012.03.016.

[27] P. Sukitpaneenit, T.S. Chung, Molecular elucidation of morphology and mechanical properties of PVDF hollow fiber membranes from aspects of phase inversion, crystallization and rheology, Journal of Membrane Science. 340 (2009) 192–205. doi:10.1016/j.memsci.2009.05.029.

[28] C. Ursino, S. Simone, L. Donato, S. Santoro, M.P. De Santo, E. Drioli, A. Figoli, ECTFE membranes produced by non-toxic diluents for organic solvent filtration separation, RSC Advances. 6 (2016) 81001–81012. doi:10.1039/C6RA13343F.

[29] J.M. Arnal, B. García-fayos, M. Sancho, Membrane Cleaning, Expanding Issues in Desalination. chapter 3 (2011) 63–84.

[30] R.N. Wenzel, Resistance of Solid Surfaces To Wetting By Water, Industrial & Engineering

Chemistry. 28 (1936) 988–994. doi:10.1021/ie50320a024.

[31] D. Quéré, Rough ideas on wetting, Physica A: Statistical Mechanics and Its Applications. 313 (2002) 32–46. doi:10.1016/S0378-4371(02)01033-6.

[32] S. Simone, F. Galiano, M. Faccini, M. Boerrigter, C. Chaumette, E. Drioli, A. Figoli, Preparation and Characterization of Polymeric-Hybrid PES/TiO2 Hollow Fiber Membranes for Potential Applications in Water Treatment, Fibers. 5 (2017) 14. doi:10.3390/fib5020014.

[33] J.C.-T. Lin, D.-J. Lee, C. Huang, Membrane Fouling Mitigation: Membrane Cleaning, Separation Science and Technology. 45 (2010) 858–872. doi:10.1080/01496391003666940.

[34] N. Porcelli, S. Judd, Chemical cleaning of potable water membranes: A review, Separation and Purification Technology. 71 (2010) 137–143. doi:10.1016/j.seppur.2009.12.007.

[35] R.M. Galvín, J.M. Rodríguez Mellado, Potassium permanganate as pre-oxidant in a reverse osmosis water plant, Water SA. 24 (1998) 361–363.

[36] V.K. Gupta, I. Ali, T. a. Saleh, A. Nayak, S. Agarwal, Chemical treatment technologies for waste-water recycling—an overview, RSC Advances. 2 (2012) 6380. doi:10.1039/c2ra20340e.

General conclusions

In the last decades, the development of new, facile and cost effective strategies to prepare membranes has received great attention due to the broad range of application fields of membrane processes. Polymeric materials play a key role in determining and influencing the membranes performances and selectivity. In particular, fluoropolymers are materials that possess properties that no other material is capable of emulate. As reported above, substitution of fluorine for hydrogen in a polymer improves important properties:

- Increase thermal resistance and reduce flammability
- Chemical stability
- Hydrophobicity
- Improve low surface energy
- Improve electrical and optical properties

During the ensuing decades, many fluoropolymers were developed. The entire sales volume for fluoropolymers is today more than 230,000 tons per year, for a total market value more than US$ 4 billion [1] and it is still growing.

The scope of this research was to apply different types of fluoropolymers: Ethylene-Chlorotrifluoroethylene with low melting point (Halar® LMP-ECTFE), poly(vinylidene fluoride) (PVDF grade 1015) and perfluoropolyether (PFPEs), for producing innovative membranes. Fluoropolymers were solubilized in a non-toxic solvents, according to the 5th principle of Green Chemistry (Safer solvents and auxiliaries: The use of auxiliary substances (e.g. solvents, separation agents, etc.) should be made unnecessary wherever possible and innocuous when used [2]. In this work, non-toxic solvents for humans and the environment have been selected and used for first time to solubilise the fluoropolymers of interest. Fluoropolymer membranes produced present numerous advantages making them very attractive for the application in water and organic solvent treatment. The approaches used for each type of membrane were reviewed and discussed in details in previous chapters:

- Halar® LMP ECTFE, a fluoropolymer developed by Solvay Specialty Polymers, has been employed in order to produce organic solvent filtration membranes, as reported in Chapter 1. This novel polymer was studied, and compared, with the standard Halar® 901. Thanks to its lower crystallinity and lower melting point, it was solubilized at 190°C (25wt% in Diethyl Adipate (DEA) as solvent). On the basis of their environmental impact, high boiling point and solubility, two solvents, DEA and Dibutyl Itaconate (DBI), less toxic that ones, were selected.

Membranes were prepared *via* thermally induced phase separation (TIPS) technique. Dense film was prepared in order to evaluate the membrane resistance to the most used solvents in chemical and pharmaceutical industries. Polar protic and aprotic solvents, and non-polar solvents were used for swelling tests carried out for 192h. Porous asymmetric membranes were tested for organic solvent filtration using pure Methanol, Ethanol and DMF. The results obtained from the characterization tests, show that LMP ECTFE membranes are promising candidates to be use in separation filtration processes under harsh conditions, such as nanofiltration (NF) and ultrafiltration (UF) [3].

- PVDF grade 1015, is a fluoropolymer commonly used for membranes preparation via TIPs or NIPs processes. Traditionally solvents used for solubilized this polymer are extremely toxic and have a negative effect on human health. In this work, a non-toxic family of plasticizers, the citric acid esters, commercially known as "Citroflex", was employed to produce flat sheet membranes. The use of ATEC and TEC as solvents, was studied for the first time. Membranes were produced via TIPs technique, the effect of the different solvents and the casting parameters were investigated, as reported in Chapter 2. The first part of this research examines how the polymer/solvent affinity influenced the membrane formation during the TIPs process. Sol-gel transitions were studied in details. The membranes produced were tested in microfiltration (MF), process that is widely applied to separate contaminants such as bacteria, algae, colloids, and macromolecules from the feed water and frequently used in the food industry, or for sterilisation and clarification of pharmaceuticals [4].
- Fluorolink®AD1700 and Fluorolink®MD700, are UV-curable PFPE-(meth)acrylate resins, developed by Solvay Specialty Polymers and specifically designed for the modification of surfaces (paper, textile, membranes) and as additives for various polymers. In particular, Fluorolink®AD1700 (Mw ~4000) is a PFPE-urethane acrylate and Fluorolink®MD700 (Mw ~1500) is a PFPE-urethane dimethacrylate. These materials combine the inner properties of PFPE-(meth)acrylates (low Refractive Index, a low degree of shrinkage upon UVcuring and a high level of cure) with a polar structure, which enhances its miscibility with hydrogenated acrylates; the hydrogen bonding of the urethane moieties also provides a higher mechanical strength in the cured coating strength in the cured coating. According to the other works, these materials could be solubilized in a non-toxic solvent, such as, butylacetate. The aim of this study was to coat several hydrophilic commercial membranes, with morphology and pore-size selected "a priori" for the application of interest, in order to produce hydrophobic/hydrophilic coated membranes. In fact due to their excellent properties, fluorinated polymers, have found a large application, as membrane materials, in different

fields, such as MF, UF, pervaporation (PV), membrane distillation (MD). The most important advantages of producing hydrophobic/hydrophilic coated membranes lies in the possibility of modifying the surface of cheaper hydrophilic commercial membranes. In this way two starting hydrophilic membrane materials, polyamide (PA) and polyethersulfone (PES) with a contact angle around 40°, were selected and coated with the PFPE resins. Membranes characterization confirmed that the coating did not affect the membranes morphology. The hydrophobic and oleophobic nature of the coated membranes were studied too. Coating stability was evaluated during time using salty solution NaCl 0.6M and with hard chemicals cleaning agents for potential application in desalination process. In fact, the membranes were tested in Direct Contact Membrane Distillation (DCMD) using deionized water and salty solution 0.6 M. Best flux was obtained for PA coated membrane at 0.45μm (about 22 Kg/m^2h at 60°C), and concerning the test carried out with salty solution as feed (0.6 M) at Tfeed=50°C, a high rejection of about 99.3% was obtained [5] [6]. Experiments demonstrated the stability of the coating in time and the good performance of the membranes. PFPE coated membranes can be used in DCMD applications for producing pure water, and thanks to its chemical resistance, also for the removal of contaminants (e.g. benzene) from surface water or fermentation products (e.g. ethanol, butanol) [7].

As further follow-up of this thesis, several are the possibilities concerning the use of fluoropolymers in membrane science. In fact, the results on the development of fluropolymeric membranes are really promising and they could be successfully applied also at industrial level. In this direction, the wastewater treatment, desalination, and recovery or organic solvents, represent an important opportunity within the logic of sustainable water management. Water is essential for the life and water purification by membranes is likely to continue with growing water scarcity and water rationalization. For doing it, we will need to further investigate and improve the stability of the fluoropolymeric membrane produced together with their performance. For example, LMP-ECTFE will be employed for MF membrane preparation, for wastewater treatment; Fluorolink® monomers will be tested also in different membrane process PV (VOCs removal from water) and gas separation processes.

This thesis may be considered as a basis study for further developments opening up interesting perspectives on the use of fluoropolymeric membranes in several fields.

References

[1] D.W.S. Jr., S.T. Iacono, S.S. Iyer, Handbook of Fluoropolymer Science and Technology, first edit, John Wiley & Sons, Inc., 2014.

[2] A. Figoli, T. Marino, S. Simone, E. Di Nicolò, X.-M. Li, T. He, S. Tornaghi, E. Drioli, Towards non-toxic solvents for membrane preparation: a review, Green Chemistry. 16 (2014) 4034. doi:10.1039/C4GC00613E.

[3] C. Ursino, S. Simone, L. Donato, S. Santoro, M.P. De Santo, E. Drioli, E. Di Nicol?, A. Figoli, ECTFE membranes produced by non-toxic diluents for organic solvent filtration separation, RSC Advances. 6 (2016). doi:10.1039/c6ra13343f.

[4] S.-I. Sawada, C. Ursino, F. Galiano, S. Simone, E. Drioli, A. Figoli, Effect of citrate-based non-toxic solvents on poly(vinylidene fluoride) membrane preparation via thermally induced phase separation, Journal of Membrane Science. 493 (2015). doi:10.1016/j.memsci.2015.07.003.

[5] A. Figoli, C. Ursino, F. Galiano, E. Di Nicolò, P. Campanelli, M.C. Carnevale, A. Criscuoli, Innovative hydrophobic coating of perfluoropolyether (PFPE) on commercial hydrophilic membranes for DCMD application, Journal of Membrane Science. 522 (2017) 192–201. doi:10.1016/j.memsci.2016.08.066.

[6] C.Ursino, E.DiNicolò, P.Campanelli, B.Gabriele, A.Criscuoli, A.Figoli, "Development of a novel perfluoropolyether (PFPE) hydrophobic/hydrophilic coated membranes, for water treatment application" TO BE SUBMITTED, 2017

[7] M. Mulder, Basic Principles of Membrane Technology. Kluwer Academic Publishers, (1997) 2003.